CRCLEME
Cooperative Research Centre for
Landscape Evolution & Mineral Exploration

CSIRO
EXPLORATION
AND MINING

AMIRA
Australian Mineral Industries Research Association Limited ACN 004 448 266

OPEN FILE
REPORT
SERIES

FURTHER GEOCHEMICAL STUDIES OF THE SOIL AT THE PANGLO GOLD PROSPECT, KALGOORLIE, WESTERN AUSTRALIA

M.J. Lintern

CRC LEME OPEN FILE REPORT 101

May 2001

(CSIRO Division of Exploration and Mining Report 251R, 1996.
2nd Impression 2001.)

AMIRA
Australian Mineral Industries Research Association Limited ACN 004 448 266

CRCLEME
Cooperative Research Centre for
Landscape Evolution & Mineral Exploration

CSIRO
EXPLORATION
AND MINING

FURTHER GEOCHEMICAL STUDIES OF THE SOIL AT THE PANGLO GOLD PROSPECT, KALGOORLIE, WESTERN AUSTRALIA

M.J. Lintern

CRC LEME OPEN FILE REPORT 101

May 2001

(CSIRO Division of Exploration and Mining Report 251R, 1996.
2nd Impression 2001.)

CRC LEME is an unincorporated joint venture between The Australian National University,
University of Canberra, Australian Geological Survey Organisation and CSIRO Exploration and Mining
Headquarters: CRC LEME c/o CSIRO Exploration and Mining, Private Bag No 5, PO Wembley, Western Australia, 6913.

RESEARCH ARISING FROM CSIRO/AMIRA YILGARN REGOLITH GEOCHEMISTRY PROJECTS 1987-1996

In 1987, CSIRO commenced a series of multi-client research projects in regolith geology and geochemistry which were sponsored by companies in the Australian mining industry, through the Australian Mineral Industries Research Association Limited (AMIRA). The initial research program, "Exploration for concealed gold deposits, Yilgarn Block, Western Australia" had the aim of developing improved geological, geochemical and geophysical methods for mineral exploration that would facilitate the location of blind, buried or deeply weathered gold deposits. The program commenced with the following projects:

P240: Laterite geochemistry for detecting concealed mineral deposits (1987-1991). Leader: Dr R.E. Smith.
Its scope was development of methods for sampling and interpretation of multi-element laterite geochemistry data and application of multi-element techniques to gold and polymetallic mineral exploration in weathered terrain. The project emphasised viewing laterite geochemical dispersion patterns in their regolith-landform context at local and district scales. It was supported by 30 companies.

P241: Gold and associated elements in the regolith - dispersion processes and implications for exploration (1987-1991). Leader: Dr C.R.M. Butt.
The project investigated the distribution of ore and indicator elements in the regolith. It included studies of the mineralogical and geochemical characteristics of weathered ore deposits and wall rocks, and the chemical controls on element dispersion and concentration during regolith evolution. This was to increase the effectiveness of geochemical exploration in weathered terrain through improved understanding of weathering processes. It was supported by 26 companies.

These projects represented 'an opportunity for the mineral industry to participate in a multi-disciplinary program of geoscience research aimed at developing new geological, geochemical and geophysical methods for exploration in deeply weathered Archaean terrains'. This initiative recognised the unique opportunities, created by exploration and open-cut mining, to conduct detailed studies of the weathered zone, with particular emphasis on the near-surface expression of gold mineralisation. The skills of existing and specially recruited research staff from the Floreat Park and North Ryde laboratories (of the then Divisions of Minerals and Geochemistry, and Mineral Physics and Mineralogy, subsequently Exploration Geoscience and later Exploration and Mining) were integrated to form a task force with expertise in geology, mineralogy, geochemistry and geophysics. Several staff participated in more than one project. Following completion of the original projects, two continuation projects were developed.

P240A: Geochemical exploration in complex lateritic environments of the Yilgarn Craton, Western Australia (1991-1993). Leaders: Drs R.E. Smith and R.R. Anand.
The approach of viewing geochemical dispersion within a well-controlled and well-understood regolith-landform and bedrock framework at detailed and district scales continued. In this extension, focus was particularly on areas of transported cover and on more complex lateritic environments typified by the Kalgoorlie regional study. This was supported by 17 companies.

P241A: Gold and associated elements in the regolith - dispersion processes and implications for exploration (1991-1993). Leader: Dr. C.R.M. Butt.
The significance of gold mobilisation under present-day conditions, particularly the important relationship with pedogenic carbonate, was investigated further. In addition, attention was focussed on the recognition of primary lithologies from their weathered equivalents. This project was supported by 14 companies.

Most reports related to the above research projects were published as CRC LEME Open File Reports Series (Nos 1-74), with an index (Report 75), by June 1999. Publication now continues with release of reports from further projects.

P252: Geochemical exploration for platinum group elements in weathered terrain. Leader: Dr C.R.M. Butt.
This project was designed to gather information on the geochemical behaviour of the platinum group elements under weathering conditions using both laboratory and field studies, to determine their dispersion in the regolith and to apply this to concepts for use in exploration. The research was commenced in 1988 by CSIRO Exploration Geoscience and the University of Wales (Cardiff). The Final Report was completed in December 1992. It was supported by 9 companies.

P409: Geochemical exploration in areas of transported overburden, Yilgarn Craton and environs, WA.
Leaders: Drs C.R.M. Butt and R.E. Smith.
About 50% or more of prospective terrain in the Yilgarn is obscured by substantial thicknesses of transported overburden that varies in age from Permian to Recent. Some of this cover has undergone substantial weathering. Exploration problems in these covered areas were the focus of Project 409. The research was commenced in June 1993 by CSIRO Exploration and Mining but was subsequently incorporated into the activities of CRC LEME in July 1995 and was concluded in July 1996. It was supported by 22 companies.

Although the confidentiality periods of Projects P252 and P409 expired in 1994 and 1998, respectively, the reports have not been released previously. CRC LEME acknowledges the Australian Mineral Industries Research Association and CSIRO Division of Exploration and Mining for authority to publish these reports. It is intended that publication of the reports will be a substantial additional factor in transferring technology to aid the Australian mineral industry.

This report (CRC LEME Open File Report 101) is a second impression (second printing) of CSIRO, Division of Exploration and Mining Restricted Report 251R, first issued in 1996, which formed part of the CSIRO/AMIRA Project P409.

Copies of this publication can be obtained from:
The Publication Officer, c/- CRC LEME, CSIRO Exploration and Mining, Private Bag 5, Wembley, WA 6913, Australia. Information on other publications in this series may be obtained from the above or from http://leme.anu.edu.au/

Cataloguing-in-Publication:
Lintern, M.J.
Further geochemical studies of the soil at the Panglo Gold Deposit, Kalgoorlie, Western Australia.
ISBN 0 643 06726 4
1. Geochemistry - Western Australia 2. Soils - Western Australia
I. Title
CRC LEME Open File Report 101.
ISSN 1329-4768

PREFACE

The CSIRO-AMIRA Project "Exploration in Areas of Transported Overburden, Yilgarn Craton and Environs" (Project 409) has, as its principal objective, development of geochemical methods for mineral exploration in areas with substantial transported overburden, through investigations of the processes of geochemical dispersion from concealed mineralization. The Project has two main themes. One of these, *'Surface and subsurface expression of* concealed *mineral deposits'* is addressed by this report, which focuses on the soil geochemistry of the Panglo Au deposit (Kalgoorlie Area).

This study is located in the northern part of the deposit where the thickness of transported material is less than 5 metres, and the depth to mineralization (beneath barren saprolite) is of the order of 30 to 40 metres. While the thickness of transported material is not substantial, the great thickness of barren saprolite provides an interesting contrast with other sites from the Kalgoorlie area which have similar thicknesses of barren transported overburden. It is considered that a detailed study of the nature of Au in surficial material from such an environment will enhance our understanding of the processes whereby Au may be enriched in the surficial environment in areas of substantially transported material.

C.R.M. Butt
R.E. Smith
Project Leaders
November 1996

TABLE OF CONTENTS

1. INTRODUCTION

In previous CSIRO-AMIRA Projects (240, 240A, 241, 241A) the geochemical expression of primary and supergene Au mineralization in the regolith was investigated. These studies demonstrated that in in regional- and prospect-scale exploration of relict and erosional landform regimes, carefully directed shallow sampling is usually more cost- and technically-effective than routine drilling to deep saprolite. In some locations, it was found that there was a surface expression even when mineralization is concealed by up to 40 m of leached saprolite. In this project (409 - Exploration in Areas of Transported Overburden), outcomes of the previous projects are being further tested to determine whether similar procedures can be routinely applied in depositional regimes. This report summarizes further studies undertaken at the Panglo Au deposit (Figure 1).

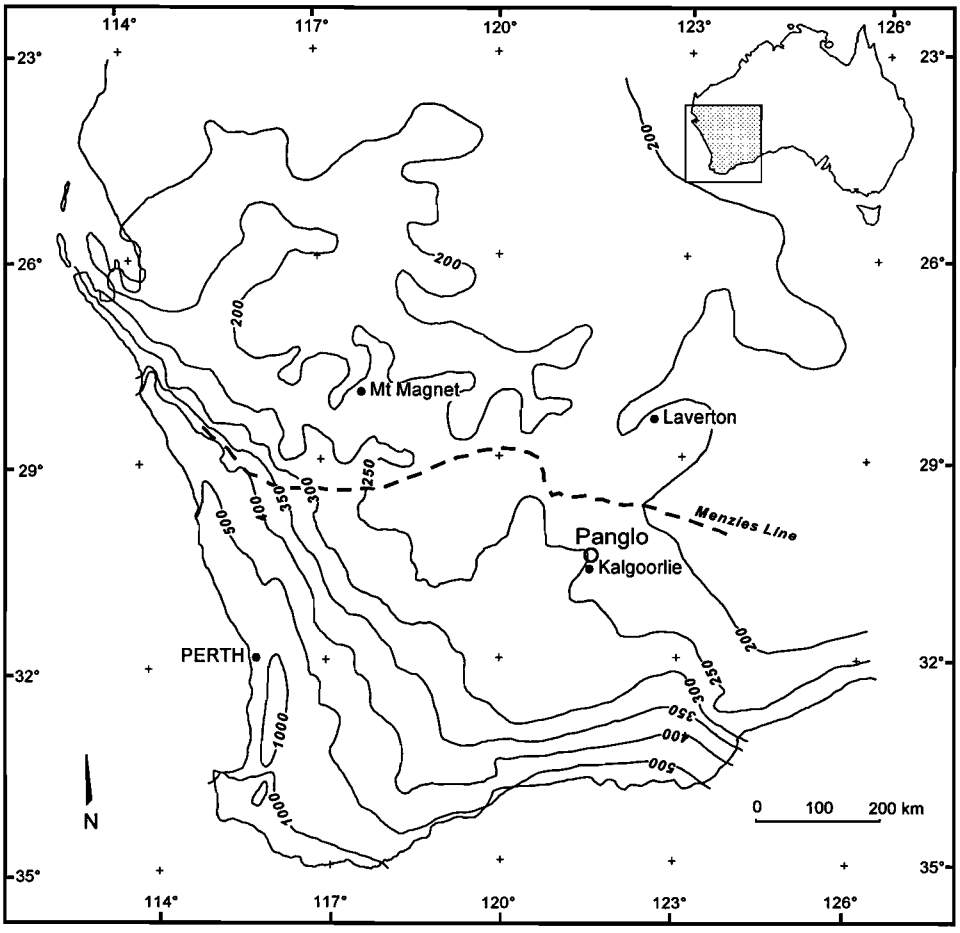

Figure 1: Location of the Panglo Au deposit. Contours show rainfall isohyets.

Two groups of sample media have particular value for Au exploration in the Yilgarn Craton:

(i) calcareous soil horizons, which are widespread in the semi-arid parts of the southern Yilgarn. Gold concentrations are often much greater in pedogenic carbonate, compared with immediately adjacent horizons. It has been shown in previous studies in relict and erosional areas that failure to sample this horizon in an exploration programme will result in ineffective soil surveys;

(ii) ferruginous materials, particularly lateritic residuum and lag.

In the Kalgoorlie area, the work programme has been to investigate potential sample media in the transported regolith above mineralization. Specifically the study analysed for:

(i) Au in surface horizons;

(ii) Au below surface in transported overburden;

(iii) pathfinder elements in transported and residual regolith and bedrock.

Several sites were offered by P409 sponsor companies for pilot studies (Table 1). All sites were visited and a preliminary set of samples was taken at most locations. Sites were assessed using various criteria (Table 1) and the most suitable sites were selected for more detailed investigations of the geochemistry of regolith materials, vegetation and groundwater.

Table 1: Advantages and disadvantages of study sites examined during the P409 pilot study and previous AMIRA projects.

Site	Type of mineralization	Advantages	Disadvantages
Sites chosen			
Apollo	*In saprolite , beneath 5-10 m of transported sediments and 10 m of saprolite.*	*Extensive drilling available. Strong mineralization. Distant from upslope Au deposit. Proximity to Argo deposit facilitates comparisons. Reported weak surficial anomaly.*	*Poor condition of drill material in top 10 m.*
Argo	*At interface and saprolite, beneath 20 m or more of lacustrine sediments.*	*Extensive drilling available. Strong mineralization. Exposed pit. Distant from upslope Au deposit.*	*Surficial sampling not completed, due to pit excavation. Poor condition of drill material in top 10 m.*
Mitchell Challenge Swordsman (Higginsville)	*At base of transported material beneath 35 m to 50 m of transported sediments.*	*Strong mineralization. Distant from upslope Au deposit. Reported surficial anomaly.*	*Ground partly disturbed before sampling took place.*
Kurnalpi	*At interface and saprolite, beneath 60 m of transported sediments.*	*Moderate drilling available. Distant from known Au mineralization.*	*Not scheduled to be mined. Weak mineralization.*
Mt Celia	*Beneath 5 to 15 m of transported deposits.*	*Extensive drilling available. Distant from upslope Au mineralization.*	*Not scheduled to be mined. Not typical of regolith in Kalgoorlie area.*
Panglo (I)	**In saprolite, beneath <1 m to 2 m of transported soil and 40 m of saprolite.**	**Reported strong surficial anomaly overlying strongly leached saprolite above mineralization. Distant from upslope Au deposit. Pit face available to sample.**	**Not deeply buried.**
Runway	*In saprolite, beneath 1m of possibly transported soil and 50 m of saprolite.*	*Reported strong surficial anomaly overlying strongly leached saprolite above mineralization. Distant from upslope Au deposit. Moderate drilling available.*	*Not scheduled to be mined. Not deeply buried.*

Table 1: (continued)

Site	Type of mineralization	Advantages	Disadvantages
Sites chosen			
Steinway	*In saprolite, 5 m beneath 30 m of transported sediments.*	*Known surficial anomaly. Extensive drilling available. Distant from known Au mineralization.*	*Not scheduled to be mined. Weak mineralization.*
Wollubar (Enigma)	*At interface and saprolite, beneath 55 m of transported sediments.*	*Moderate drilling available. Distant from upslope Au deposit.*	*Not scheduled to be mined. Weak mineralization.*
Sites not chosen			
Gindalbie	*With sulphides at interface, beneath 60 m of transported sediments.*	*Moderate drilling available. Distant from upslope Au deposit.*	*Poorly mineralized. Not scheduled to be mined.*
Kat Gap (Forrestania)	*Little information available.*	*Moderate drilling available. Distant from upslope Au mineralization.*	*Depth of transported material not determined - may be thin.*
Kurrawang	*Little information available.*	*Known surficial anomaly. Exposed pit (at a later stage).*	*Surface regolith mostly residual. Little drill spoil.*
Lady Bountiful Extended	*At interface beneath 25 m of transported deposits, and also in underlying quartz veins.*	*Moderate drilling available. Distant from upslope Au deposit. Exposed pit (at a later stage). Strong mineralization.*	*Severe surficial disturbance.*
Lake Cowan	*Various deposits associated with palaeochannel and underlying saprolite.*	*Known surficial anomaly. Extensive drilling available.*	*Known upslope mineralization.*
Samphire	*Little information available.*	*Exposed pit.*	*Surface regolith mostly residual.*
Previous studies			
Baseline	*Beneath 20 m of transported sediments.*	*Exposed pit. Known surficial anomaly.*	*Samples not available.*
Matt Dam	*At interface and saprolite, 15 m beneath 10 m of transported sediments.*	*Extensively studied in earlier project. Known surficial anomaly.*	*This part of deposit not scheduled to be mined.*
Panglo (II)	*Located in saprolite 20 m beneath base of 15 m of transported sediments.*	*Extensively studied in earlier project. Known surficial anomaly.*	*This part of deposit not scheduled to be mined.*
Zuleika	*At interface and saprolite, beneath 20 m of transported sediments.*	*Exposed pit. Extensively investigated in earlier project.*	*Known upslope mineralization. No further surface samples available.*

Table 2: Gold, Ca and Fe concentrations from selected coarse material from the surficial environment at Panglo; extract from Appendix 2, Lintern and Scott, 1990.

Sample	N	E	Fe (%)	Ca (%)	Au (ppb)
108092B	6621956	345202	0.8	0.08	110
108103	6621903	345149	48.5	0.06	160
108098A	6621925	345171	36.2	0.01	340
108105B	6621892	345138	6.9	0.06	350
108105A	6621892	345138	38.1	0.10	950

The Panglo Gold deposit has been the subject of several CSIRO/AMIRA research reports in recent years (Scott 1989a, b; Scott and Dickson, 1989; Scott and Davis, 1990; Gray, 1990; Lintern and Scott, 1990; Scott, 1990a, b; Cudahy *et al.*, 1992). The presence of Au in surficial material has been noted in many of these reports and is the subject of further investigation here. Anomalously high concentrations of Au occur in the soil directly overly mineralization and appear to be separated from it by many tens of metres of barren saprolite. In Lintern and Scott (1990), it was demonstrated that there is a strong link between Au and pedogenic carbonate in surficial material at Panglo, and, indeed, this relationship has been successfully exploited to find new deposits in the area (Figure 2).

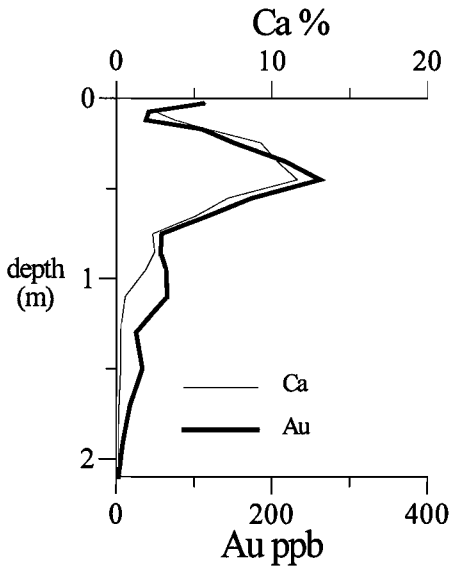

Figure 2: Relationship between Au and pedogenic carbonate in a soil profile at Panglo (Lintern and Scott, 1990).

However, in some *non-calcareous* surficial material (e.g. sample 108105A in Table 2; from Lintern and Scott, 1990), there also appears to be anomalous concentrations of Au. The nature of this material requires more investigation since it may have significant implications in understanding the development and evolution of Au anomalies in the soil. Further sampling was undertaken to supplement material already collected from earlier studies.

Although much of the Panglo Au deposit lies beneath less than *1 or 2 m* of transported soil, with respect to the distribution Au in the regolith, it shares characteristics with other study sites from the Kalgoorlie Area which have *many tens of metres* of transported overburden; these include (i) a relatively rich zone of surficial Au enrichment in a calcareous red clay compared with non-calcareous material immediately beneath, (ii) several metres to tens of metres of barren material between the surface and mineralization and (iii) a quasi-horizontal zone of supergene mineralization. However, at Panglo, one important difference is that the concentrations of Au in selected material from near the surface are significantly greater than equivalent material from the sites having thick transported cover. Hypotheses to explain the Au at the surface include:

(i) vertical upwards concentration of Au at the surface (by aqueous or vapour modes); the especially high concentrations of Au at the surface at Panglo (Table 2) require that the mechanism of transportation, regolith characteristics and/or environmental conditions prevailing were/are substantially more favourable for accumulation than has been observed at other study sites (e.g., Kurnalpi, Steinway, Wollubar-Enigma and Argo, Lintern and Gray, 1995a, b, c, d);

(ii) vertical downwards concentration of Au through weathering, erosion and deflation; this Au may have been chemically re-mobilised or merely be a mechanically re-located relic e.g., primary Au.

(iii) horizontal transport of Au by a mechanical/chemical mechanism from upslope; e.g., the Paddington Au deposit is located a few kilometres to the north.

For areas with substantial transported overburden, the above hypotheses have important implications for exploration: vertical upwards migration of Au provides the most optimistic scenario for detecting buried mineralization, whereas horizontally re-located Au is the most pessimistic.

2. SITE DESCRIPTION

The Panglo Au deposit is 30 km NNW of Kalgoorlie and 5 km south-east of the Paddington Mine, within a 200 m wide sequence of steeply west-dipping carbonaceous shales and mafic to ultramafic volcanic rocks, within a major shear zone (Figure 3). Mineralization occurs as a relatively flat-lying, supergene deposit, up to 16 m thick between 30 and 55 m depth, over a 1 km long, N-trending zone. Underlying primary mineralization is associated with disseminated pyrite and arsenopyrite within strongly sheared and carbonated shales and mafic volcanic rocks. Panglo was discovered in 1987, but mining did not commence until late 1994. The mineable reserves are 1.5 Mt at 2.7 g/t Au.

Most of the Panglo deposit has a thin (<1 m), weakly ferruginous-calcareous soil, commonly with a transported component and 35-40 m of leached kaolinitic saprolite, locally containing alunite, overlying mineralization. Potassic (muscovite-rich) rocks occur with primary mineralization. Laterally, the wall-rocks have paragonite (Na-mica) and muscovite, instead of muscovite alone. At the southern end of the deposit, the saprolite is partly overlain by a palaeochannel containing up to 10 m of sediments.

The soils near the Panglo deposit may be divided into two main groups:-

(i) Gravelly soils. These occur in high areas of the landscape and include those overlying the known southern limits of mineralization, which are developed on sediments in a palaeochannel, of presumed Tertiary age. The soils consist of an organic surface horizon containing Fe-rich gravels in a sandy matrix. Beneath this, the soil is characterized by unconsolidated, Fe-rich, rounded to sub-rounded ferruginous nodules, varying in size from a few millimetres to several centimetres in diameter, in a sandy to loamy matrix. In certain areas, saprolite limits soil depth to a few centimetres.

(ii) Clay-rich soils. These are dominant in the axis of the present broad drainage that covers the northern and central sections of the deposit. They consist of a veneer of sandy loam overlying pale grey to yellow, homogeneous clays. Blocks of weathered rock are common within the soil profile and are either pale (clay-rich) or red (Fe-rich). Towards the south, the soils become increasingly saline as the drainage nears a playa.

Pedogenic carbonates are present near the surface and continue down to 1 to 1.5 m depth. They are disseminated through clay-rich soils, as friable fragments and thin veneers on the ferruginous nodules in unconsolidated Fe-rich material, and as coatings, up to several millimetres thick, on indurated, shallow subcrops of saprolite.

The diversity and abundance of the vegetation is largely determined by the characteristics of the soil. Salt- and drought-tolerant species *e.g. Maeriana* spp. and *Atriplex* spp. (<0.5 m in height) with minor *Eremophila* spp. (up to 2 m) dominate the clay-rich soils of the broad valley floor to form an open

heathland. Where soils are thin, the vegetation is sporadic and the total biomass is low. Tall *Eucalyptus* spp. trees (up to 20 m) with an under-storey of *Eremophila* spp. (1-2 m) form a medium dense woodland over the gravelly soils but are absent in the broad valley floor. There is a sharp transition between these two vegetation communities reflecting the different soil types, although individual examples of plant species occur sporadically in both communities.

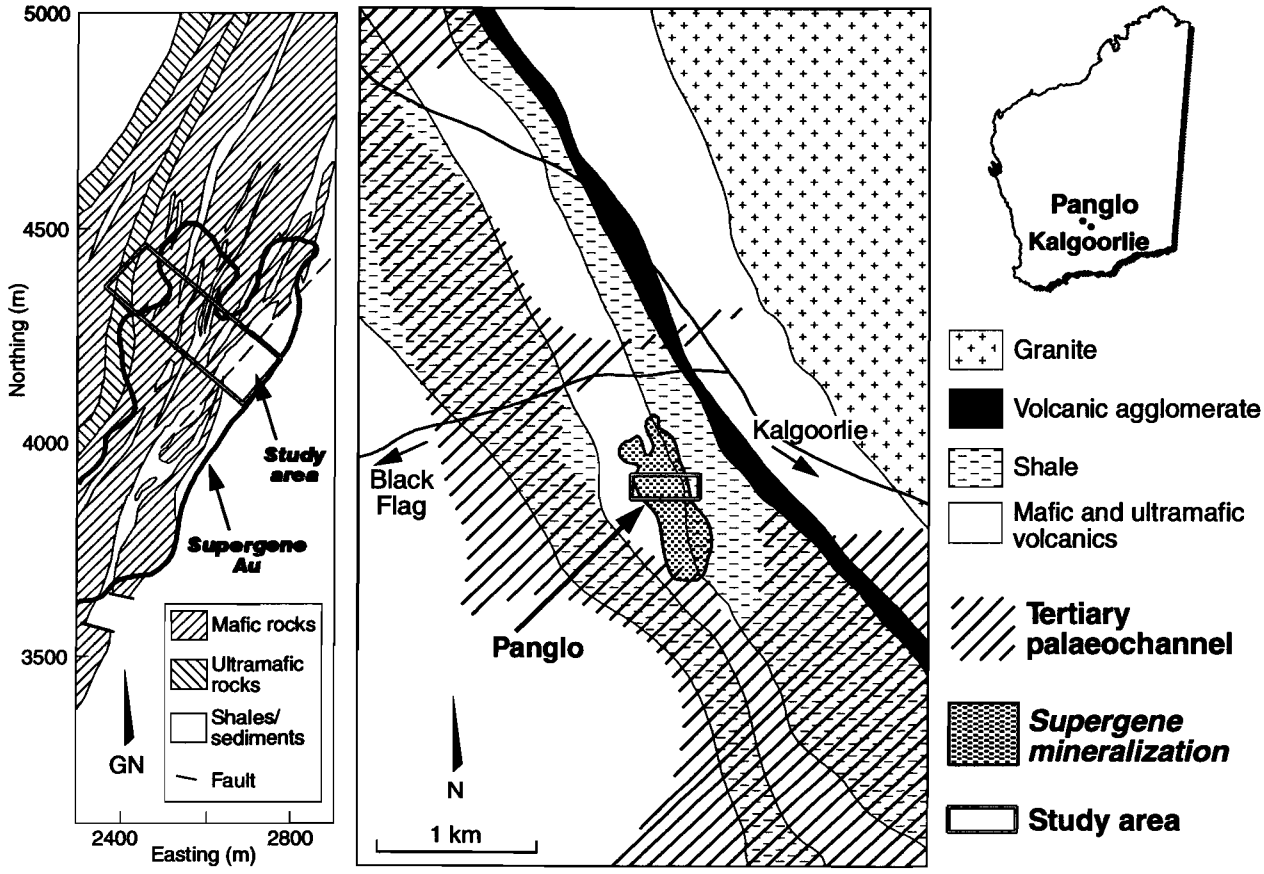

Figure 3: Detailed geology and location of the Panglo area (from company data).

3. METHODS

The methods used in this study were primarily aimed at (i) identifying regolith material containing high Au concentrations from soil composites and (ii) isolating Au grains contained therein. In addition, further information on geochemical relationships between elements, and appropriate sampling media for exploration in superficially transported terrains would be gained.

3.1 Sample collection

Thirty composite 1-2 kg soil samples (09-3651 to 09-3680) were collected along a traverse from the top 3 m close to the edge of the pit with a vehicle-mounted power auger. The surface had been cleared of vegetation in preparation for mining and so some contamination may be expected of near surface material. Sample location was determined using real-time differential GPS with a maximum estimated error of 10 m (Figure 4).

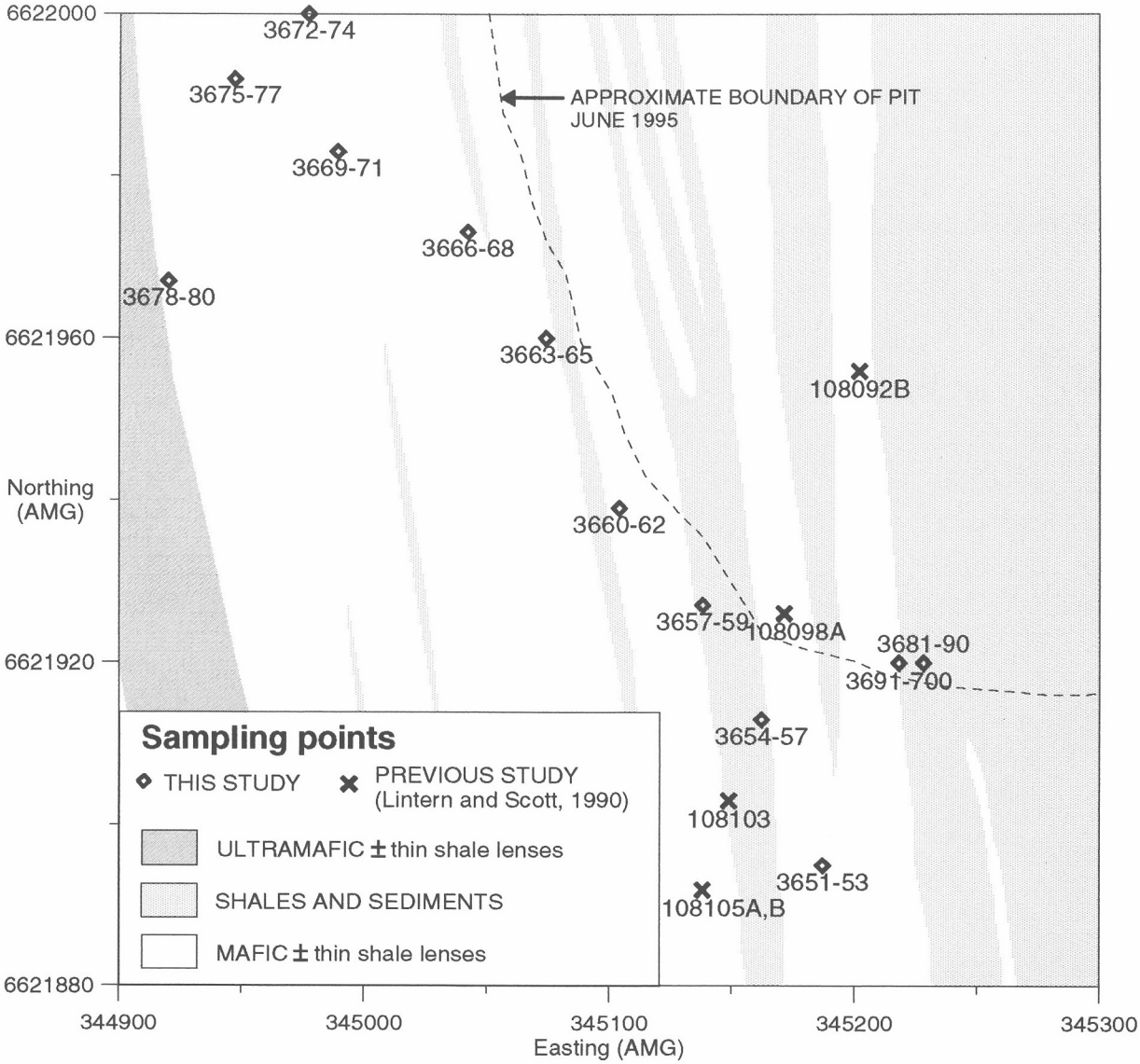

Figure 4: Location map showing sampling points and geology at Panglo. See Table 2 for geochemical data for samples collected in previous study. See Figures 1 and 2 for study location. Note that almost entire study area is underlain by supergene mineralization. Prefix 09- has been omitted for clarity. Geology from company data.

Nineteen 1-2 kg channel samples (09-3681 to 09-3700) were collected from the top 12 m of two profiles located on the pit wall. Near surface material may have been contaminated.

3.2 Sample preparation and analysis

One to two kilograms of sample were collected using a vehicle-mounted power auger. These were dried at 70°C, split and jaw-crushed (as required) before a 100-200 g sub-sample was pulverized in a K1045 steel ring mill to nominal <75 μm.

(i) Gold, Sb, As, Ba, Br, Ce, Cs, Cr, Co, Eu, Hf, Ir, Fe, Au, La, Lu, Mo, K, Rb, Sm, Sc, Se, Ag, Na, Ta, Th, W, U, Yb and Zn were analysed using a 10 g sub-sample by Instrumental Neutron Activation Analysis (INAA) at Becquerel Laboratories, Lucas Heights;

(ii) Calcium and Mg were analysed using a 1 g sub-sample by atomic absorption spectrophotometry (AAS) after first digesting in 5M HCl for 15 minutes and then diluting to 1M HCl; this procedure dissolves the carbonate present.

3.3 Size fraction study

Twelve samples with high Au contents (determined from earlier analyses) were dry sieved into 4 different size fractions (>1000 μm, 1000 - 250 μm, 250 - 63 μm and <63 μm) using a ROTAP testing sieve shaker (International Combustion Australia Ltd). Samples were analysed as for the bulk samples (see above). The plus 1000 μm material was wet sieved and the finer material discarded.

3.4 Gold grain investigation

Samples of coarse material (>1000 μm) with high Au content were mounted in epoxy and examined by petrological and scanning electron microscopy. Fabrics are more likely to be observed in coarse material.

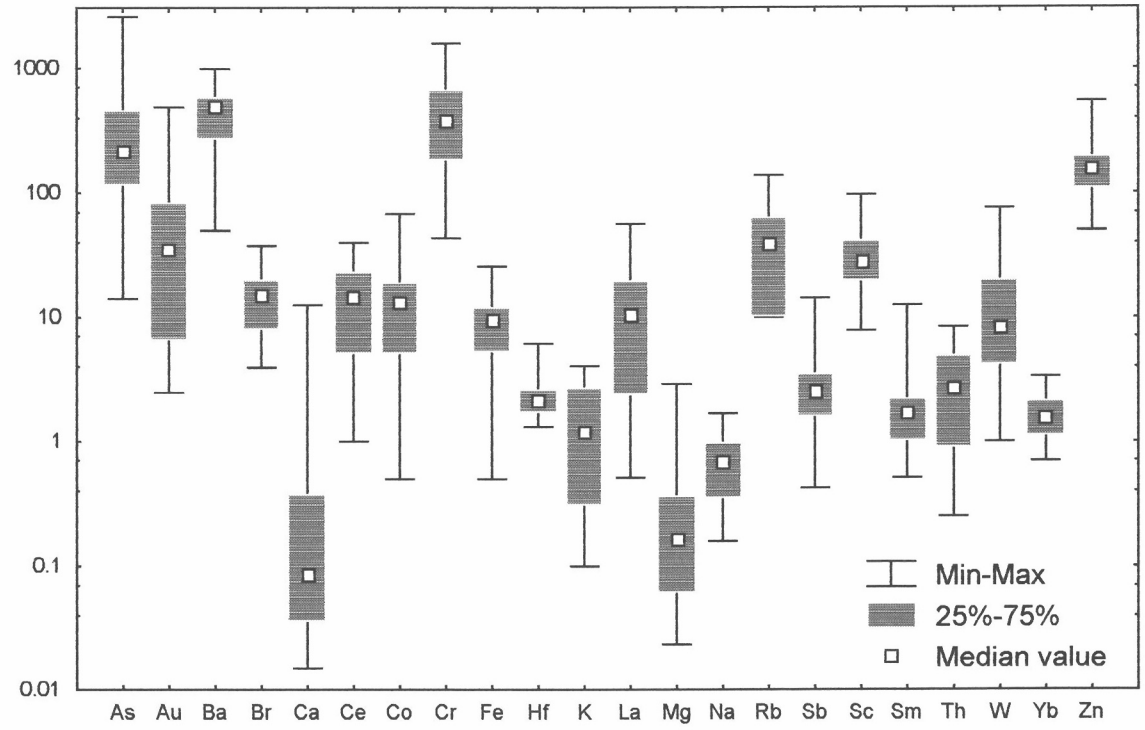

Figure 5: Summary statistics of geochemical data for the soils. Majors elements (Ca, Fe, Mg, K and Na) in %; trace elements in ppm; Au in ppb.

4. RESULTS

4.1 Soils

Summary statistics for the composition of the bulk samples (soils and deeper profile) indicate high variability for Ca and Au (Figure 5).

The results indicate that 12 out of 52 samples contain over 100 ppb Au. These samples were selected for the size fraction analysis. For the soil and profile bulk samples, highly significant elemental

associations exist between several elements (correlation coefficient r>0.6, significance $\alpha<0.001$) (Figure 6).

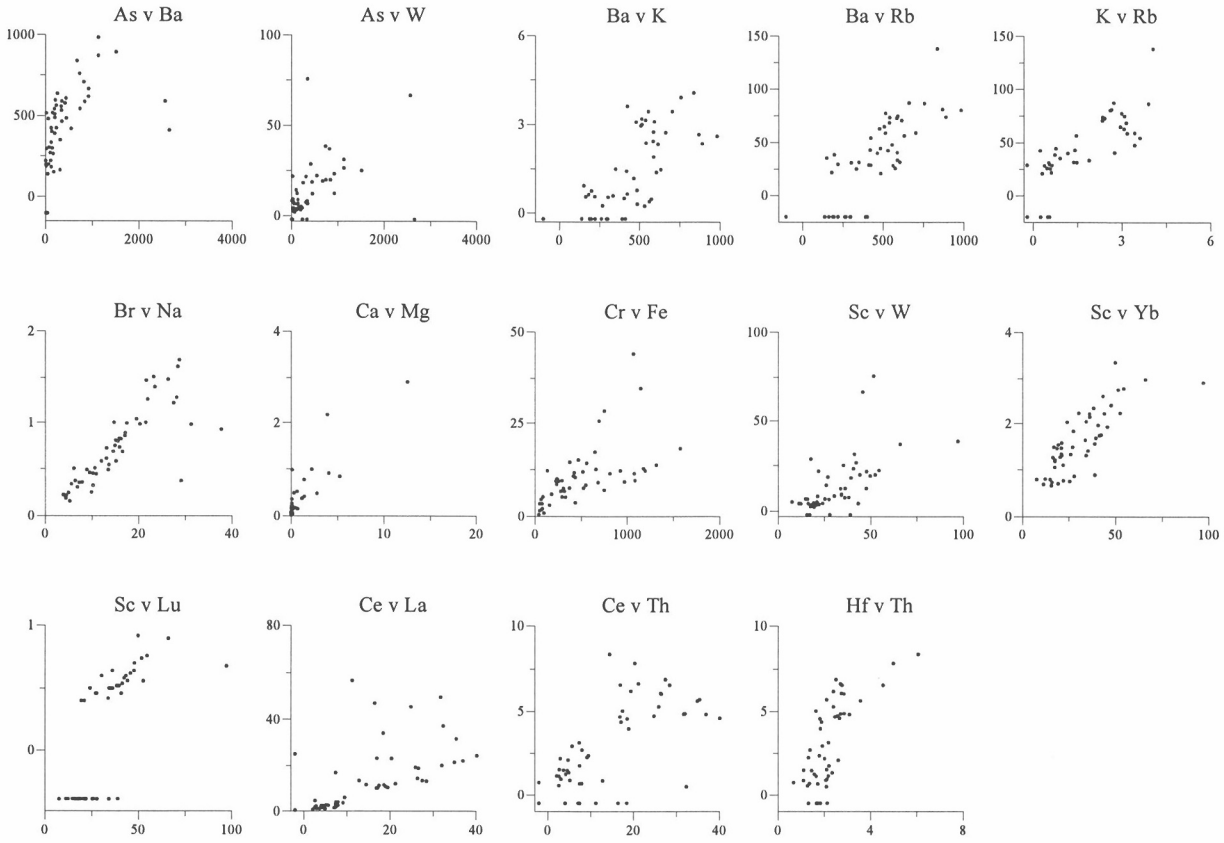

Figure 6: Scatter plots of selected elements for soil and profile bulk samples from Panglo. First element in header is the X axis. Major elements (Ca, Fe, K, Mg and Na) in %, trace elements in ppb.

Earlier studies at Panglo (Table 3) are used to interpret lithology using the geochemical data. The reports (Scott 1990a, b) indicate that weathered rock types can be distinguished by their chemical and mineralogical components.

A rudimentary differentiation can be inferred using Cr and K alone. Although muscovite is present in some mafic and ultramafic rocks (Scott and Dickson, 1989), K contents are useful in distinguishing mafics (low) from the shales (high) (Table 3). The present results (Figure 6, Appendix Figure A1.1.2) indicate that samples with higher K concentrations also tend to be richer in Ba, REE, Rb, Hf and Th. Scott and Dotter (1990) found that lower Cr contents of weathered shales could distinguish them from weathered ultramafics (Table 3). Chromium concentrations from this study appear to be more directly related to Fe (Figure 6) and are probably related to the ferruginization of mafic materials, but Fe oxides as indicated by Fe do not appear to be hosts for As, Sb and Zn.

Table 3: Geochemical indicators of lithology at Panglo (after Scott 1990a, b)

Lithology	Soil Cr (ppm)	Soil K (%)	Leached saprolite Cr (ppm)	Leached saprolite K (%)
Shale	400	0.7	330	3
Mafic volcanics	300-700	0.3-0.5	250-500	0.7-1.7
Ultramafic rocks	1100	0.3-0.6	2100-2400	<0.1

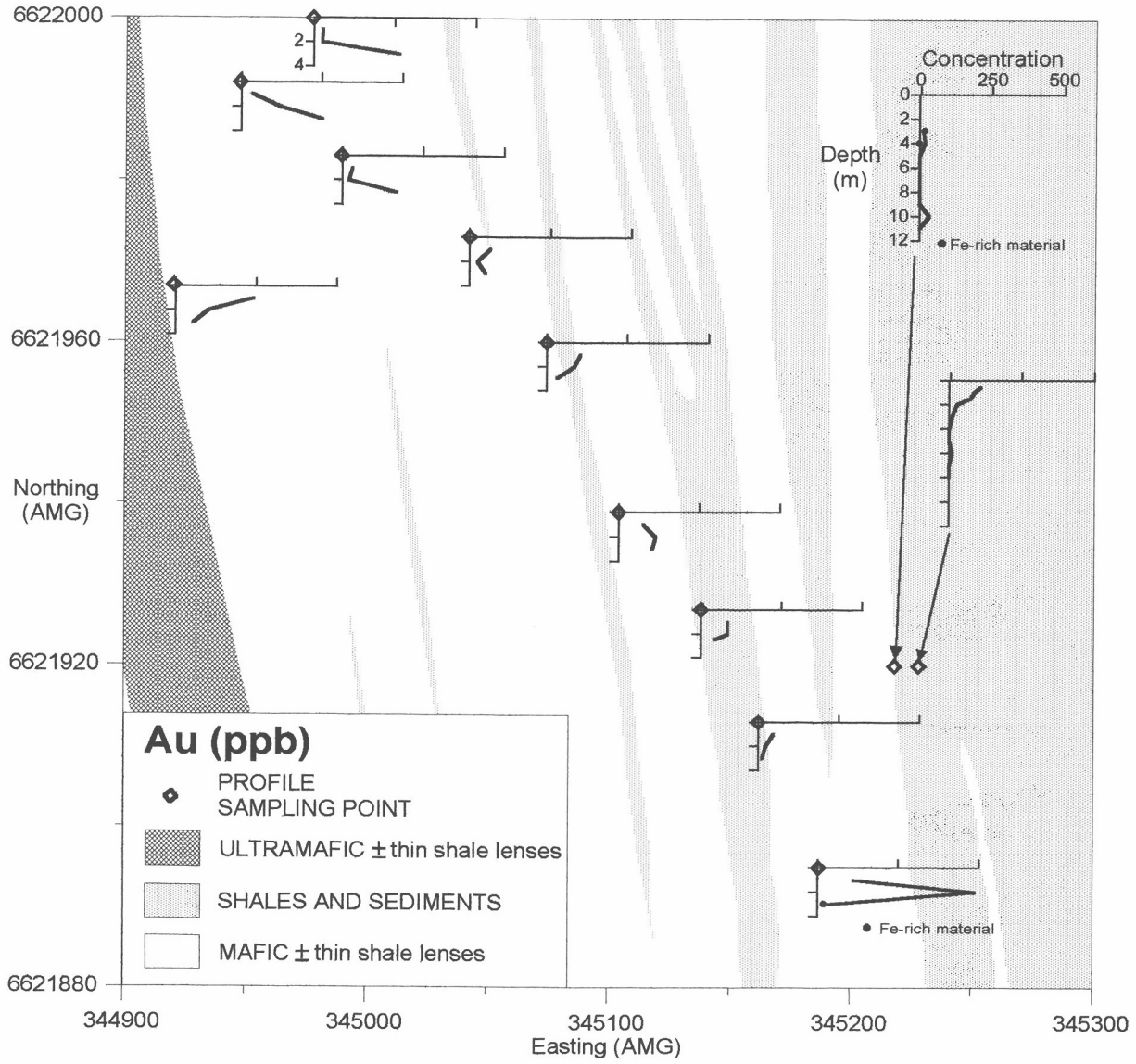

Figure 7: Gold distributions in soils and the upper regolith, Panglo.

Gold is inconsistently distributed in the soil and upper regolith. In some profiles, Au concentration increases sharply below 1 - 2 m, although this is not obviously associated with either Cr-rich (mafic) or K-rich (shale) lithologies. In other profiles, Au (and W) enrichment is associated with Ca and Mg, presumably in pedogenic carbonates. Previously, Scott (1989b) reported that elevated Au, As and, in places, Mo, Sn and W contents were related to the occurrence of muscovite in volcanic rocks - presumably representing a relict primary alteration zone (Figure 7).

4.2 Size fractions

Gold. The samples with the highest Au content (>100 ppb) were selected for the size fraction analysis. Most of these samples are from below 1 m depth. In these samples, Au is not consistently associated with either Fe (ferruginous) or Ca (calcareous) components (Table 4); other elements are tabulated and graphed in Appendix A2.1. Size fraction analysis (>1000 μm, 250-1000 μm, 63-250 μm and <63 μm) indicates that the distribution of Au is bimodal, with the highest concentration

occurring in either the finest or coarsest fraction (Figure 11). Five of the six samples with the highest Au concentrations in the coarse fraction were selected for petrological study.

Iron. Iron is always richer (mean of 28%) in the coarse material (>1000 μm); for the finer fractions (e.g., <63 μm, mean of 6% Fe) there is a weak correlation between Fe and As, Cr, Sb (Figure 8). The components of the coarse material are presumably cemented by Fe oxides, and less likely to fracture during weathering. The finer fractions are dominated by Fe - poor silts, clays and sands.

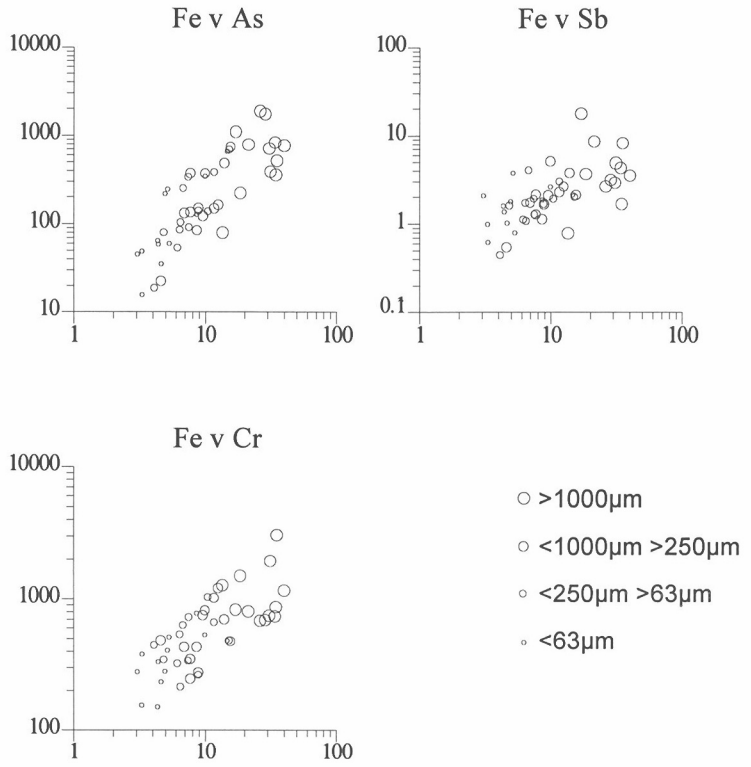

Figure 8: Scatter plots for Fe (%) v As, Sb and Cr (ppm) in different size fractions. X axis is for Fe concentrations.

Sodium and Br. Sodium and Br are strongly correlated if the size fraction samples are considered as separate sub-sets (Figure 9). The coarsest size fraction has a lower Na content, probably an artefact of wet sieving. Alternatively, it may reflect the poorer penetration of groundwater into interstitial pores and the domination of rock lithology on chemical composition. The correlation of these elements is discussed further below.

Calcium and Mg. Calcium and Mg contents are highly variable (Figure 9, and Appendix A2.1). Most of the Ca present in near surface samples at Panglo has previously been reported to be in calcite, although the strong relationship between Ca and Mg here for some samples (Figure 9) suggests that some dolomite may be present. In an earlier report (Lintern and Scott, 1990), a very strong relationship between Ca, Sr, Mg and Au was noted in surficial soils from this area (Figure 10); in these samples, no dolomite was recorded and some of the Mg present was assigned to vermiculite-chlorite and talc, which were present in considerable quantities.

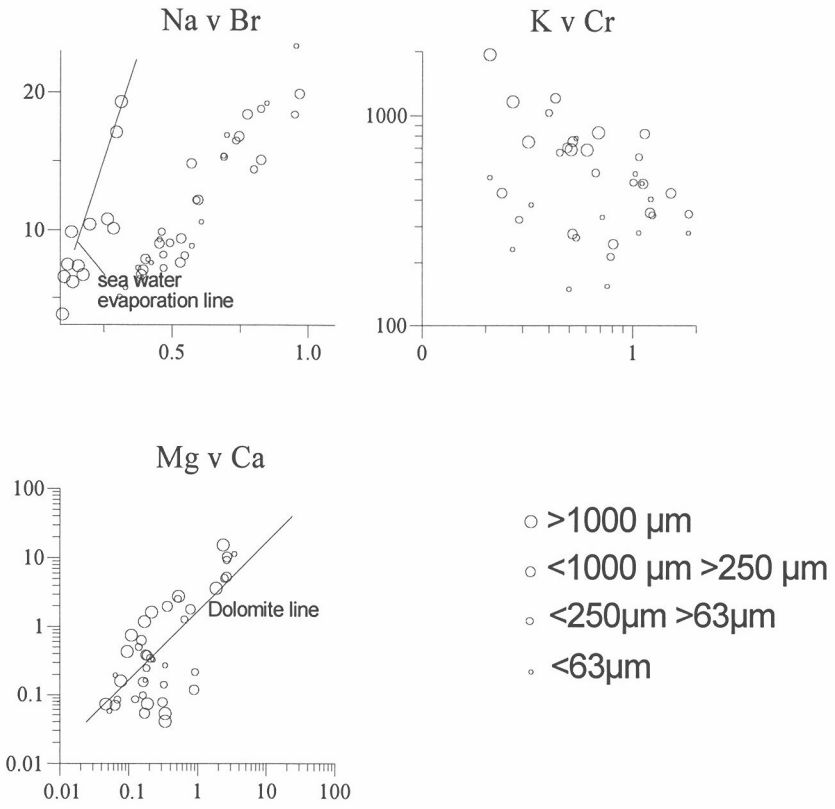

Figure 9: Scatter plots of Na v Br, K v Cr and Mg v Ca for the size fractions at Panglo. Calcium, K, Mg and Na in %; Cr and Br in ppm. X axis is for first element in header.

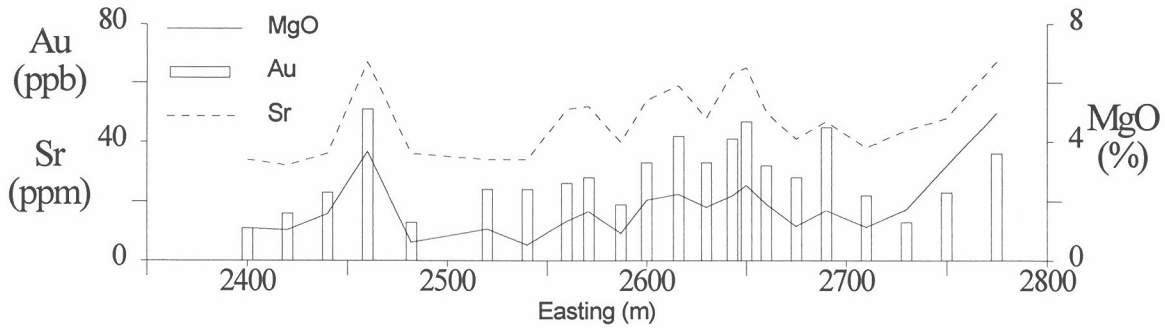

Figure 10: Au, Sr and MgO concentrations in topsoils (0 - 0.1 m) from Panglo section 3700N (company grid); after Lintern and Scott, 1990.

Table 4: Gold, Ca and Fe concentrations in the coarse fraction (plus 1000 μm) of selected surface samples, Panglo. Coarse fraction of samples in bold italics selected for petrological studies.

Sample	Number	N	E	Depth (m)	Fe (%)	Ca (%)	Au (ppb) bulk	Au (ppb) +1000 μm
09-3679	1	6621967	344920	1.5	11.4	12.58	102	75
09-3662	***2***	***6621939***	***345104***	***2.5***	***9.47***	***0.06***	***103***	***309***
09-3663	3	6621960	345074	0.5	9	1.47	105	96
09-3681	4	6621920	345228	0.3	12.6	0.14	106	14
09-3651	5	6621895	345187	0.5	10.7	0.11	110	113
09-3661	6	6621939	345104	1.5	14.5	0.72	115	260
09-3676	7	6621992	344947	1.5	13.7	2.25	123	42
09-3671	***8***	***6621983***	***344989***	***2.5***	***11.4***	***0.43***	***166***	***349***
09-3680	9	6621967	344920	2.5	3.72	3.96	241	93
09-3677	***10***	***6621992***	***344947***	***2.5***	***14.2***	***0.17***	***253***	***376***
09-3674	***11***	***6622000***	***344977***	***2.5***	***11.6***	***0.30***	***264***	***369***
09-3652	***12***	***6621895***	***345187***	***1.5***	***6.73***	***0.05***	***485***	***742***

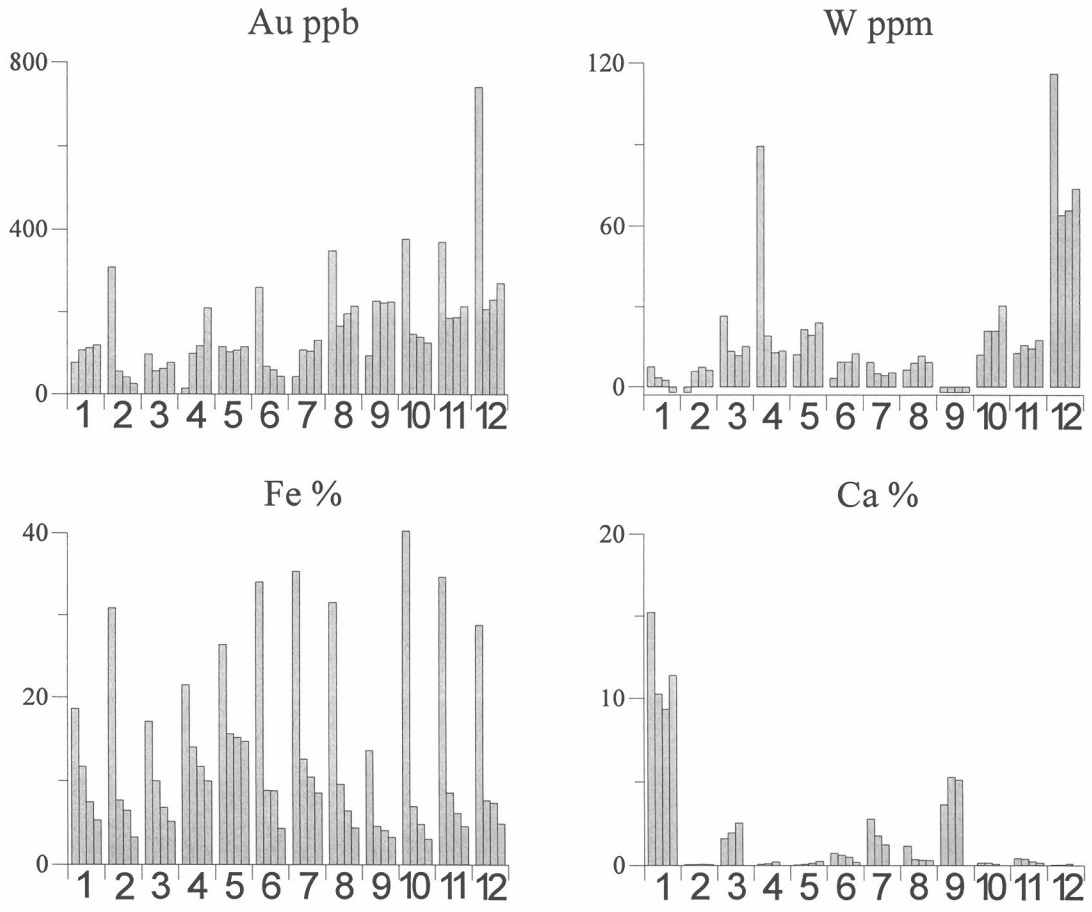

Figure 11: Gold, Ca, Fe and W concentrations from 4 size fractions for the 12 highest Au concentration samples from the surficial environment at Panglo. For each sample (1-12), the size fractions (from left to right) are >1000 μm, 1000-250 μm, 250-63 μm and <63 μm. See Table 4 for sample numbers. The samples are ranked (from left to right) according to highest Au concentration in the bulk sample.

4.3 Microscopy

Petrological investigations were undertaken of the coarse fraction of selected Au-rich samples (samples in bold italics Table 4). In addition, sample 108105A (950 ppb, Table 2), collected during the earlier study (Lintern and Scott, 1990), was also examined. Brief descriptions are given in Appendix 2.6.

The surficial material has undergone one or more episodes of pervasive ferruginization, but in several samples, relict primary fabrics are identifiable (Appendix 2.6; Figure 12). Gold grains up to 10 μm in size were observed by SEM, although no Ag was detected.

5. DISCUSSION

The purpose of this study was to compare the distribution of Au from a site with superficially-transported overburden with studies at sites being undertaken in areas of deep transported overburden. Gold has been reported to be in high concentrations (>100 ppb) in surficial material over the Panglo deposit (Lintern and Scott, 1990) despite the presence of many metres of barren residual overburden; Steinway is the only P409 study site above barren transported overburden where similar high concentrations of Au have been found (150 ppb, Gardiner, 1993; Lintern and Gray, 1995a). Are the processes that result in Au anomalies in soil over these two different regolith types, transported and residual, similar?

The weathering profile at Panglo is probably truncated; any pre-existing lateritic residuum, assuming that it was originally present, has been eroded, and the depleted zone is exposed as either outcrops or subcrops beneath a shallow soil cover (Figure 13a). Consequently, the presence of Au grains in sub-cropping, leached saprolite is unexpected. The grains have low Ag contents (<1%), which indicates that they may be secondary; however, because of their small size (<10 μm), they may have been 'refined' in situ, by the same processes that produce Ag-poor rims on larger grains (Gray *et al.*, 1992). Beneath these surface zones with preserved particulate Au, the regolith is leached and Au-poor to 40-50 m, the depth of the supergene Au mineralisation.

The origin of the surficial Au enrichment is uncertain. A possible explanation is that the strong leaching that has led to the development of the depletion zone occurred predominantly after the truncation of the pre-existing profile. Irrespective of whether any lateritic residuum was preserved, the material that currently forms the land surface was originally deeper in the regolith profile. This pre-existing profile was probably formed under more humid climates (Figure 13a). Some chemical and physical mobility of Au is characteristic of surface horizons, but little dissolution or mobility of Au would be expected in the saprolite (Figure 13a). Following truncation, therefore, high concentrations of Au would be present in the 'new' surface horizons developed directly in saprolite (Figure 13b).

During the subsequent trend to aridity and the extreme salinization in lower parts of the landscape, as at Panglo, Au in the saprolite, particularly that close to and below the water-table, is dissolved and leached. However, the upper horizons above the water-table are less saline and less strongly leached, and here Au is preserved (Figure 13c). Preservation may also be aided through armouring by secondary precipitation by Fe oxides and silica. This 'relict' Au, hosted by saprolite or ferruginous mottles, acts as a reserve that allows the soil Au anomaly to persist. The Au in carbonate probably represents relatively recently mobilization from these relict grains. It is highly mobile and is probably being leached, but is continuously supplemented by slow dissolution of the relict grains.

Figure 12 (overleaf): Photomicrographs of Au - rich samples from Panglo. Arrows indicate Au grains

Photo	Description	Photo	Description
A	Sample 108105A - talc schist fabric.	E	Sample 09-3677 - fine grained mica; probably amphibolite fabric.
B	Sample 108105A - tourmaline crystals (some split) and irregular channel veinlet showing alteration selvedge and solution goethite.	F	Sample 09-3652 - accordion structures of kaolinite, largely destroying primary mafic fabrics.
C	Sample 108105A - channel filled with mixture of goethite and clay.	G	Sample 09-3662Fe - 2 Au grains in Fe (pale) and Si-Al-rich matrix. Mafic - ultramafic fabric.
D	Sample 108105A - Au grain in Fe-rich matrix.	H	Sample 09-3662Fe - as for G but high contrast showing 2 Au grains.

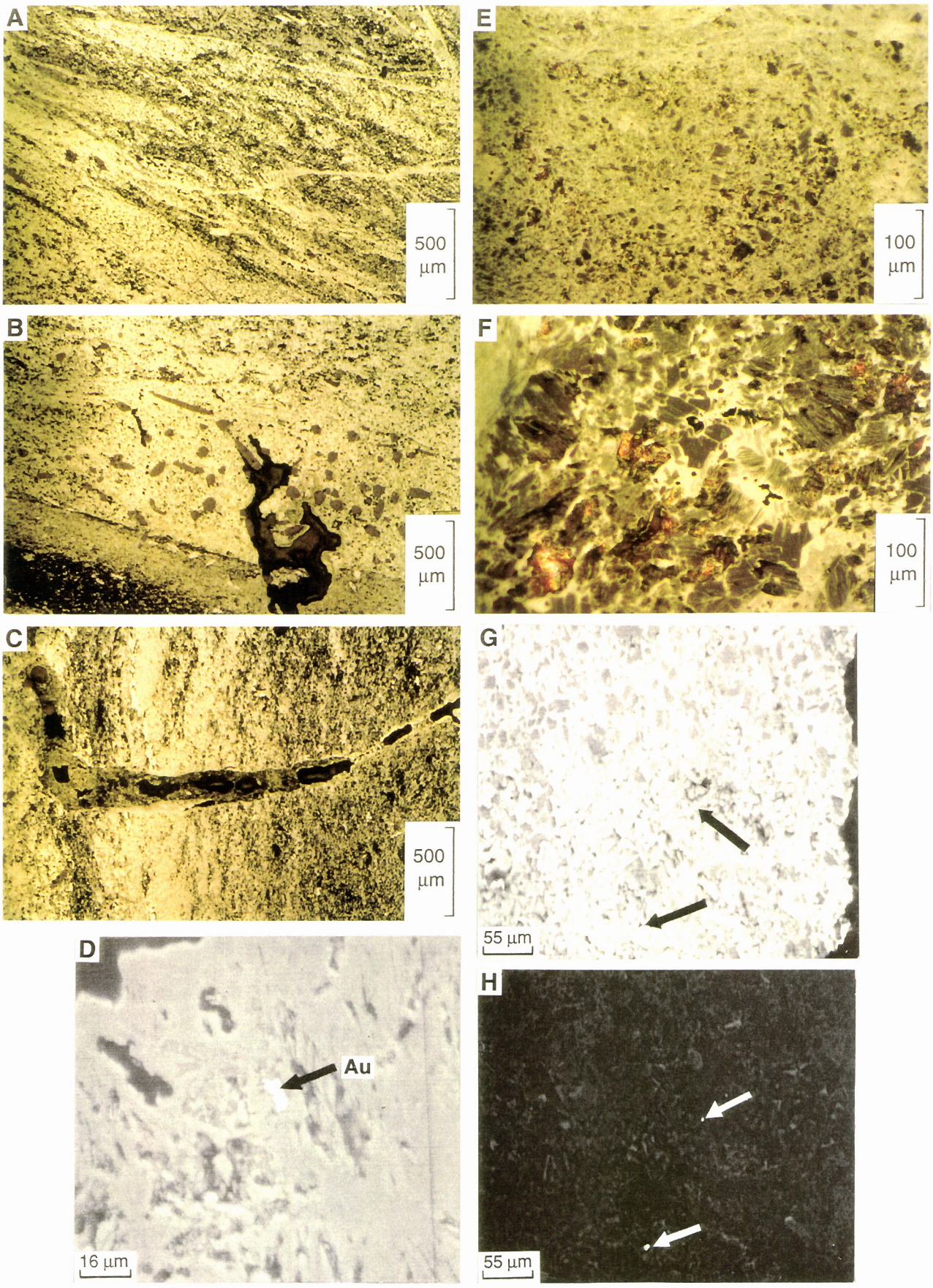

Figure 12: Photomicrographs of Au - rich samples from Panglo. Arrows indicate Au grains

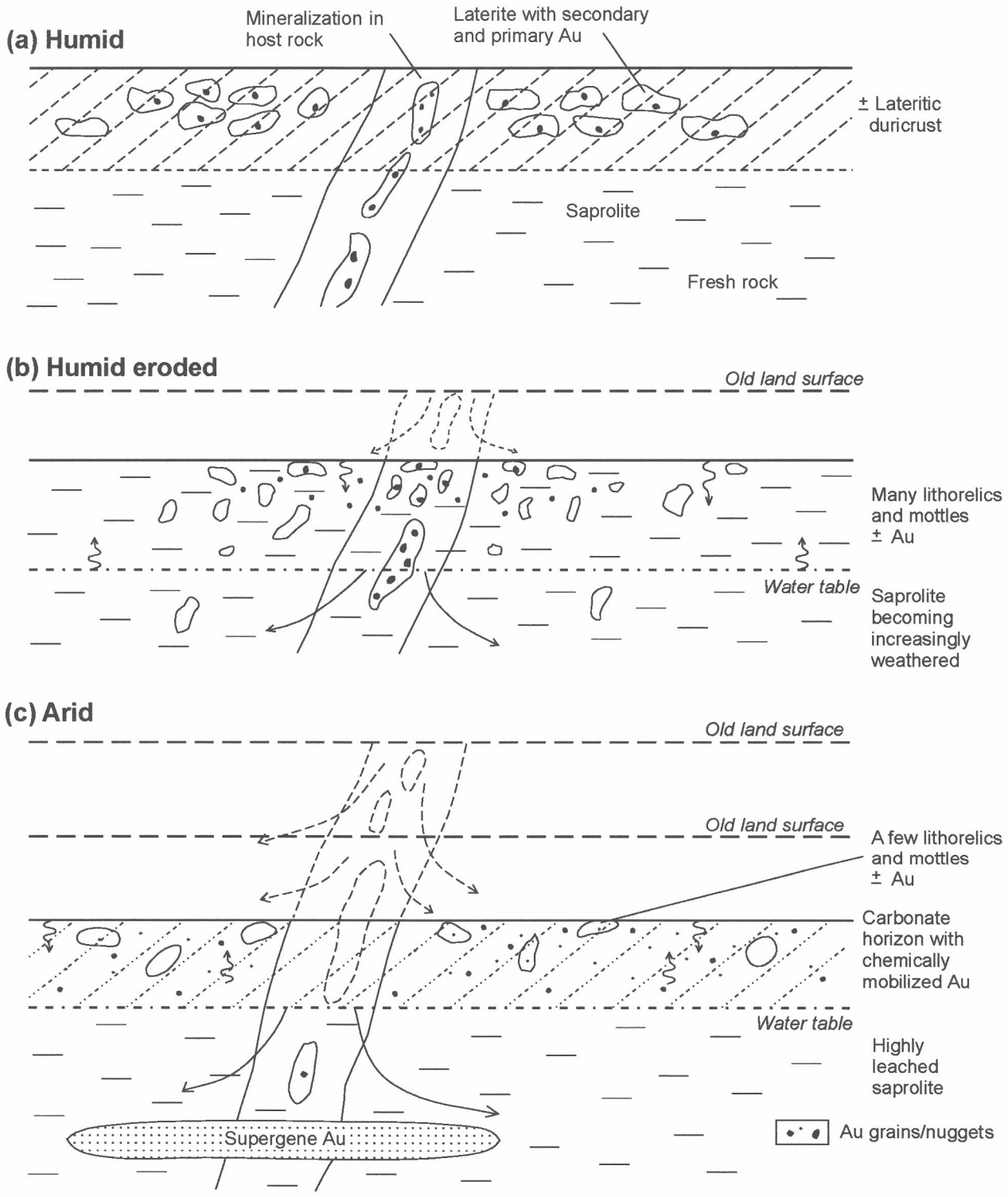

Figure 13: Diagrammatic representation of the formation of Au anomalies in surficial material at Panglo.

The presence of talc and, particularly, muscovite in the near-surface horizons may provide supplementary evidence for this process. These minerals are generally resistant to weathering, being only partially weathered, even in lateritic residuum (Butt, 1991, 1993; Robertson *et al.*, 1990). Consequently, their distribution, particularly in saprolite, tends to reflect that originally present in the fresh rocks. However, at Panglo, it is possible that the same processes that have leached Au from the saprolite have also destroyed muscovite and talc. At the surface, the Au-muscovite-talc association represents the primary distribution, and confirm the relationship between the surface anomaly formation of the underlying supergene zone.

Another possible explanation for some of the surficial Au at Panglo comes from the distribution and ratios of highly soluble elements. The data indicate that there may be evidence for a "geochemical fingerprint" by groundwater on the near surface. Sodium and Br ratios in regolith materials appear to be related to (i) groundwater, (ii) evaporating meteoric (sea)water and/or (iii) a mixing of groundwater and meteoric waters and (iv) the depth of sampling (Figure 14).

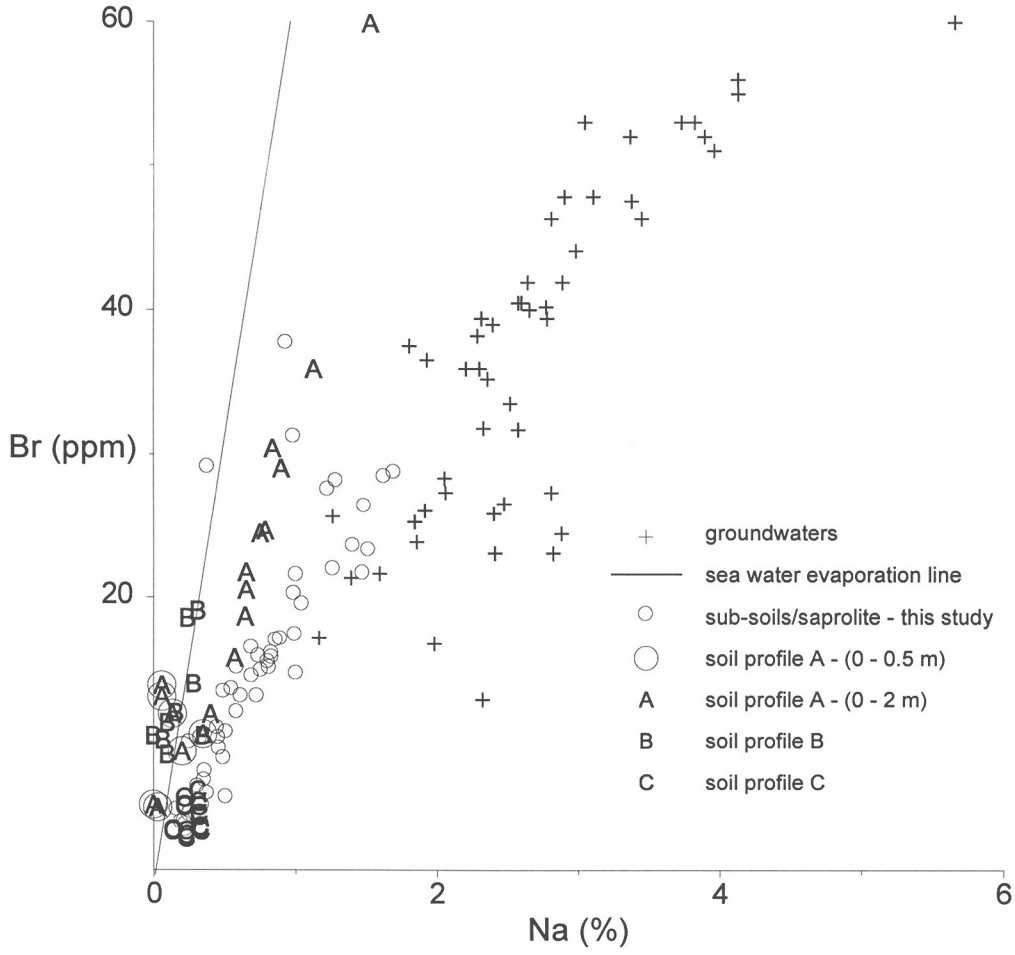

Figure 14: Sodium v Br scatter plot for regolith material and groundwater from Panglo. In caption, sub-soils are the bulk soils from this study; soil profiles are from an earlier study (Lintern and Scott, 1990).

These data suggest that groundwater levels were either (i) higher than at present or (ii) that the Na-Br signature of the current groundwater is being currently imprinted on sub-surface materials presumably by capillarity. Rainfall would be expected to penetrate the sub-soils and dilute the groundwater ratio (decrease the Na:Br ratio) with time and so (ii) is probably the more likely explanation. The argument for groundwater influence on sub-surface regolith materials can be extended from Na and Br ratios to other elements of the surficial environment including Au; but,

whereas Au may accumulate in regolith materials such as ferruginous saprolite, elements such as Na and Br will be more mobile. Redox, salinity and pH conditions are favourable at Panglo for Au dissolution. The water table is about 5 - 10 m below the present land surface. Gold has been reported in groundwater at Panglo (up to 3.7 ppb, Gray, 1990), hence it is possible that Au in the surficial materials has been precipitated from the groundwater. In comparison, groundwaters at Steinway are saline and acid but generally reducing and therefore not favourable to Au dissolution (Lintern and Gray, 1995a). Most groundwater samples are below detection (<0.03 ppb) with respect to dissolved Au, and the water table is at about 20 m which is too deep for capillarity to be invoked as a prevailing surficial process.

In summary, two explanations for the source of the Au in the near surface material have been suggested: relict grains and precipitation from groundwater. It is possible that both processes are occurring or have occurred in the past. However, it seems unlikely that the Au has been horizontally (laterally) dispersed into the area (as suspected at Steinway) since appreciable concentrations have been found within mottled (ferruginous) clays after saprolite.

Exploration procedures in terrain such as Panglo can be assisted by being aware of the presence of high concentrations of Au in ferruginous (and other) sample media present close to the surface. Simple soil or auger surveys may indicate the presence of Au associated with calcareous material. However, unusually high concentrations of Au may be found in non-calcareous material by drilling slightly deeper. Such material may be collected by carefully hand picking coarse material from drill cuttings; this will ensure that the danger of cross-hole contamination from finer material will be minimized. Generally, however, sampling Au in carbonate is the most effective procedure in erosional terrains despite the possible presence of high concentrations in other media.

6. ACKNOWLEDGEMENTS

The following people and company are thanked for their support and expertise in preparation of this report: Goldfields Pty. Ltd. for providing the resources required for the auger survey; I.D.M. Robertson for petrological investigations and descriptions of the polished mounts; B.W. Robinson for assistance with photomicrographs; J.F. Crabb and R. Bilz for sample and polished section preparation; K. Lim for sample preparation and selected analyses; A. Vartesi and C. Steel for the preparation of Figures 12 and 13. Finally, C.R.M. Butt and D.J. Gray gave advice in the preparation of this report.

7. REFERENCES

Butt, C.R.M., 1991. Geochemical dispersion in the regolith, Mystery Zone, Mt Percy mine, Kalgoorlie, Western Australia. (CSIRO/AMIRA Project 241: Weathering Processes). CSIRO Division of Exploration Geoscience Restricted Report 156R. Volumes I and II. 226 pp.

Butt, C.R.M., 1993. Geochemical background, Mt Percy, Kalgoorlie, Western Australia. (CSIRO/AMIRA Project 241A: Weathering Processes). CSIRO Division of Exploration Geoscience Restricted Report 389R. 110 pp.

Cudahy, T.J., Scott, K.M. and A.R. Gabell, A.R., 1992. Spectral properties of muscovite- and paragonite-bearing rocks and soils from the Panglo Gold Deposit, Ora Banda region, Western Australia. (CSIRO/AMIRA Project 241: Weathering Processes). CSIRO Division of Exploration Geoscience Restricted Report 234R. 53 pp.

Gardiner, N., 1993. Regolith geology and geochemistry of the Steinway gold prospect, Kalgoorlie, Western Australia. University of Western Australia, unpublished thesis. 165 pp.

Gray, D.J., 1990. Hydrogeochemistry of the Panglo gold deposit. (CSIRO/AMIRA Project 241: Weathering Processes). CSIRO Division of Exploration Geoscience Restricted Report 125R. 74 pp.

Lintern, M.J. and Scott, K.M., 1990. The distribution of gold and other elements in soils and vegetation at Panglo, Western Australia. (CSIRO/AMIRA Project 241: Weathering Processes). CSIRO Division of Exploration Geoscience Restricted Report 129R. 96 pp.

Lintern, M.J., and Gray, D.J., 1995a. Progress Statement for the Kalgoorlie Study Area - Steinway Prospect, Western Australia. (CSIRO/AMIRA Project 409). CSIRO Division of Exploration and Mining Report 95R. 121 pp.

Lintern, M.J., and Gray, D.J., 1995b. Progress Statement for the Kalgoorlie Study Area - Argo Deposit, Western Australia. (CSIRO/AMIRA Project 409: Yilgarn Transported Overburden). CSIRO Division of Exploration and Mining Report 96R. 153 pp.

Lintern, M.J., and Gray, D.J., 1995c. Progress Statement for the Kalgoorlie Study Area - Kurnalpi Prospect, Western Australia. (CSIRO/AMIRA Project 409: Yilgarn Transported Overburden). CSIRO Division of Exploration and Mining Report 97R. 41 pp.

Lintern, M.J., and Gray, D.J., 1995d. Progress Statement for the Kalgoorlie Study Area - Enigma Prospect (Wollubar), Western Australia. (CSIRO/AMIRA Project 409: Yilgarn Transported Overburden). CSIRO Division of Exploration and Mining Report 98R. 36 pp.

Lintern, M.J., Gray, D.J., Scott, K.M. AND Butt, C.R.M., 1995e. The Panglo gold deposit. In: 17th International Geochemical Exploration Symposium Excursion 3, Regolith geology and exploration geochemistry in the Yilgarn Craton, Western Australia. CSIRO Exploration and Mining Report 134F. 134 pp

Robertson, I.D.M., Taylor, G.F., and Chaffee, M.A., 1990. The petrography, mineralogy and geochemistry of weathering profiles developed on felsic, mafic, ultramafic and sedimentary rocks, Rand Pit, Reedy Mine, Western Australia. (CSIRO/AMIRA Project 241: Weathering Processes). CSIRO Division of Exploration Geoscience Report 102. Volumes I and II. 205 pp.

Scott, K.M., 1989a. Mineralogy and Geochemistry of weathered shale profiles at the Panglo Gold Deposit, Eastern Goldfields, W.A. (CSIRO/AMIRA Project 241: Weathering Processes). CSIRO Division of Exploration Geoscience Restricted Report 32R. 21 pp.

Scott, K.M., 1989b. Mineralogy and geochemistry of weathered mafic/ultramafic volcanics from section 4200N at Panglo, Eastern Goldfields, W.A. (CSIRO/AMIRA Project 241: Weathering Processes). CSIRO Division of Exploration Geoscience Report 42R. 22 pp.

Scott, K.M., 1990a. The mineralogical and geochemical effects of weathering on volcanics from the Panglo deposit, Eastern Goldfields, WA. (CSIRO/AMIRA Project 241: Weathering Processes). CSIRO Division of Exploration Geoscience Restricted Report 143R. 47 pp.

Scott, K.M., 1990b. The mineralogical and geochemical effects of weathering on shales at the Panglo deposit, Eastern Goldfields, WA. (CSIRO/AMIRA Project 241: Weathering Processes). CSIRO Division of Exploration Geoscience Restricted Report 171R. 35 pp.

Scott, K.M. and Davis, J.J., 1990. Gold morphology and composition at Panglo, Eastern Goldfields W.A. (CSIRO/AMIRA Project 241: Weathering Processes). CSIRO Division of Exploration Geoscience Restricted Report 110R. 9 pp.

Scott, K.M. and Dickson, B.L., 1989. Radioelements in weathered shales and mafic volcanics, Panglo gold deposit, Eastern Goldfields, W.A. (CSIRO/AMIRA Project 241: Weathering Processes). CSIRO Division of Exploration Geoscience Restricted Report 41R. (Joint report with Project P263). 31 pp.

Scott, K.M. and Dotter, L.E., 1990. The mineralogical and geochemical effects of weathering on shales at the Panglo Deposit, Eastern Goldfields, WA.. (CSIRO/AMIRA Project 241: Weathering Processes). CSIRO Division of Exploration Geoscience Restricted Report 171R. 35 pp.

APPENDICES

Index

APPENDIX 1: BULK SAMPLES

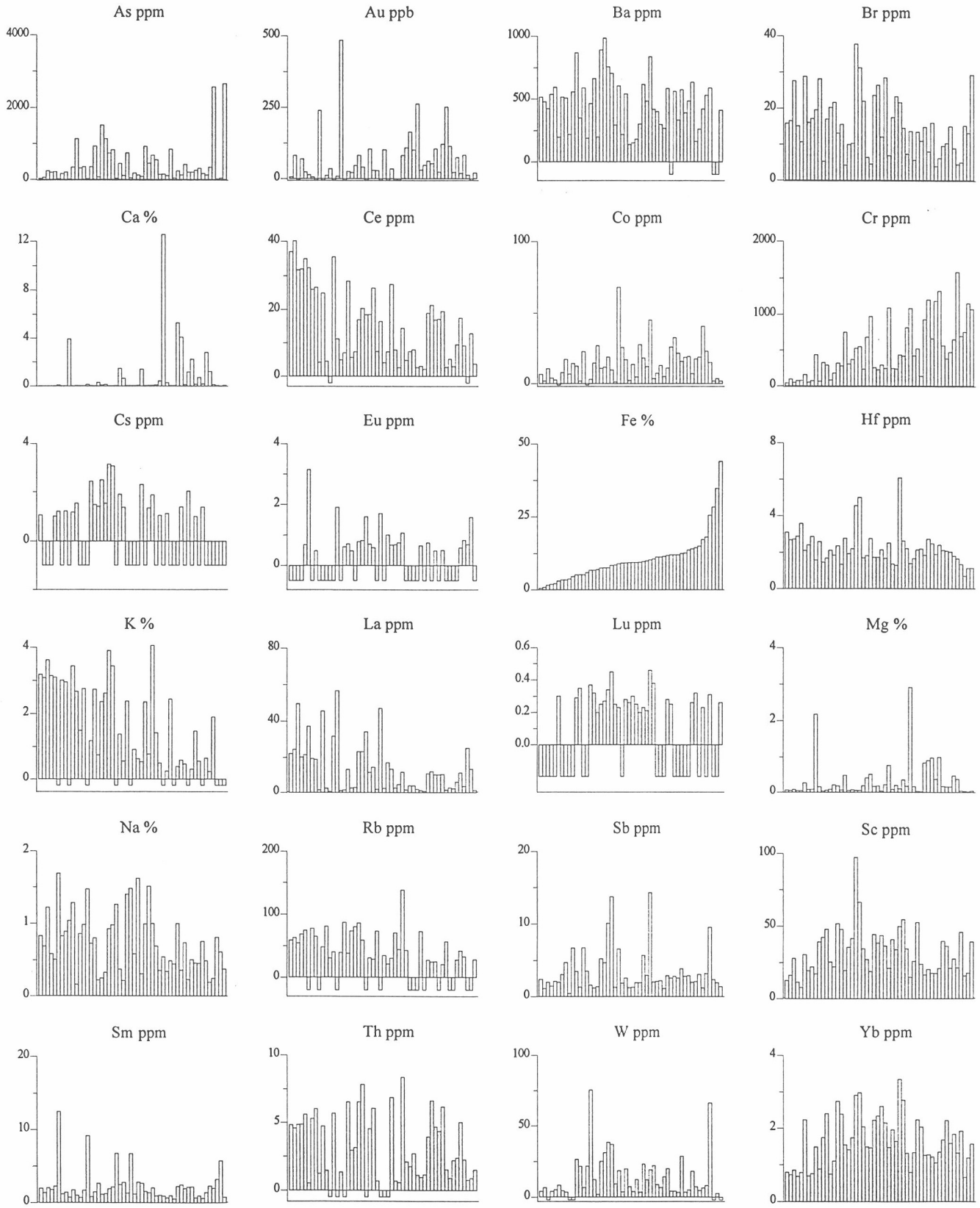

Figure A1.1.1: Elemental abundances for bulk samples from Panglo sorted on Fe contents.
Increasing Fe contents from left to right. Negative data below detection.
For all samples Ag (5), Ir (0.02), Se (5), Ta (1) and U (2) below detection (ppm) indicated in parentheses.

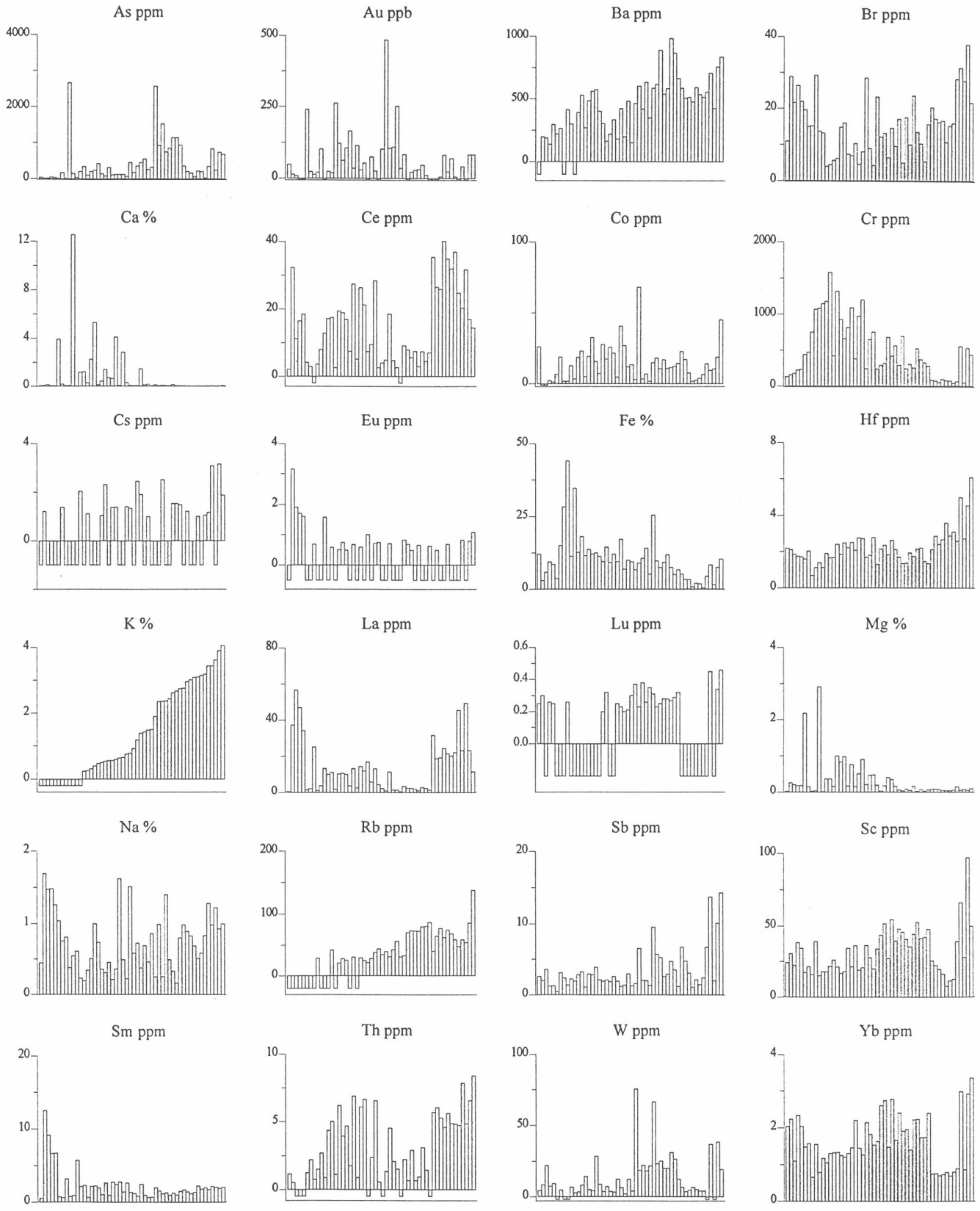

Figure A1.1.2: Elemental abundances for bulk samples from Panglo sorted on K contents.
Increasing K contents from left to right. Negative data below detection.
For all samples Ag (5), Ir (0.02), Se (5), Ta (1), and U (2) below detection (ppm) indicated in parentheses.

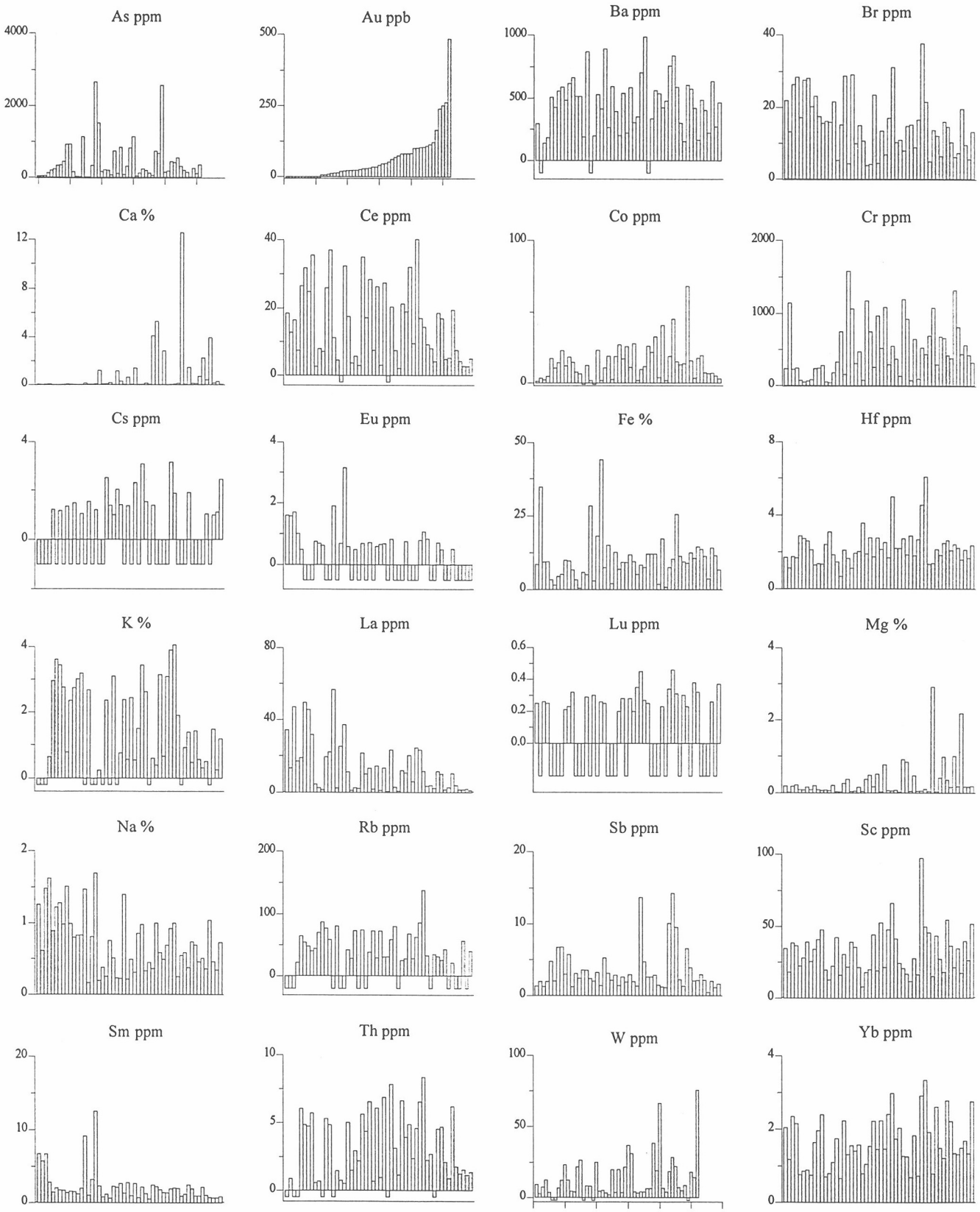

Figure A1.1.3: Elemental abundances for bulk samples from Panglo sorted on Au contents.
Increasing Au contents from left to right. Negative data below detection.
For all samples Ag (5), Ir (0.02), Se (5), Ta (1) and U (2) below detection (ppm) indicated in parentheses.

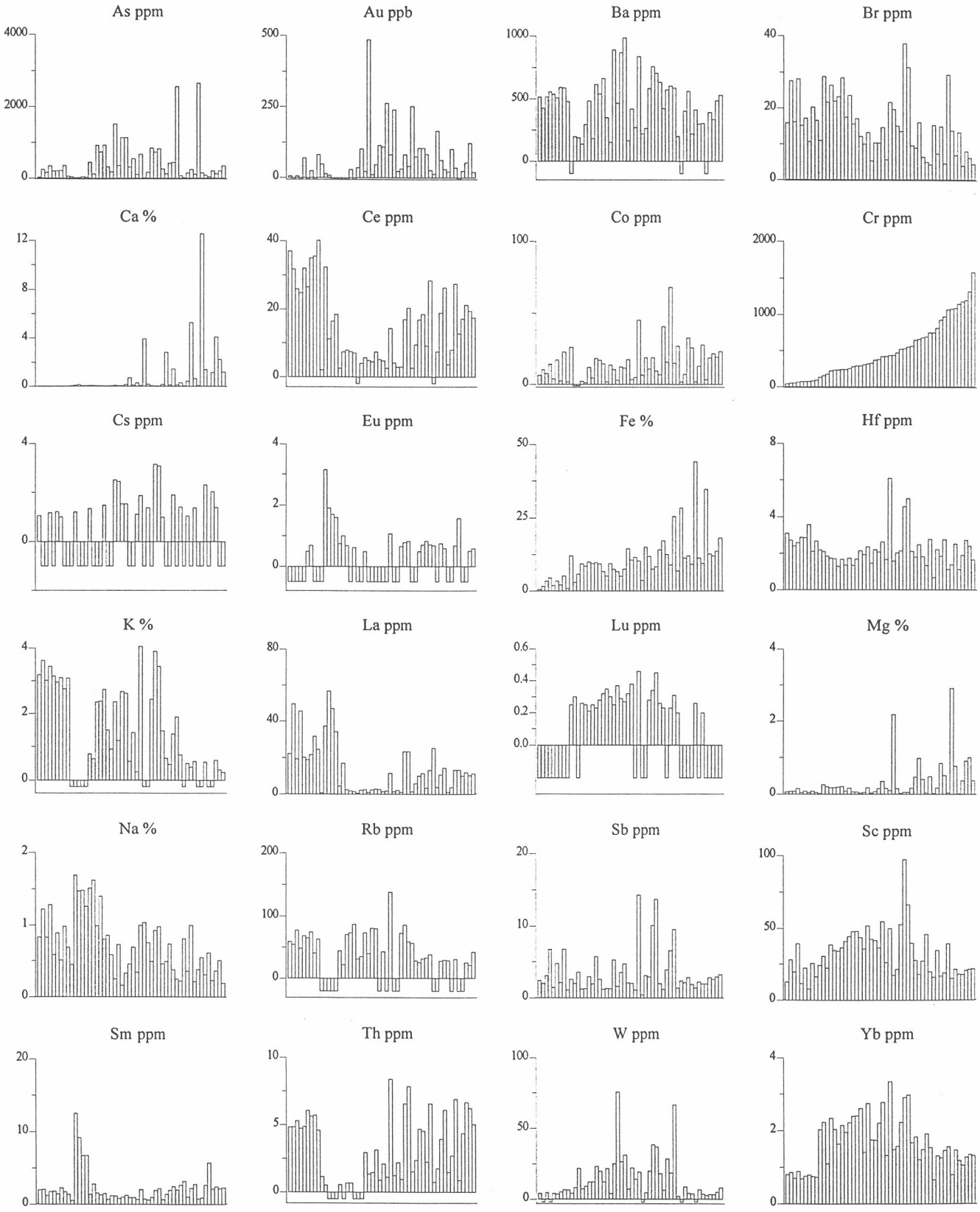

Figure A1.1.4: Elemental abundances for bulk samples from Panglo sorted on Cr contents.
Increasing Cr contents from left to right. Negative data below detection.
For all samples Ag (5), Ir (0.02), Se (5), Ta (1) and U (2) below detection (ppm) indicated in parentheses.

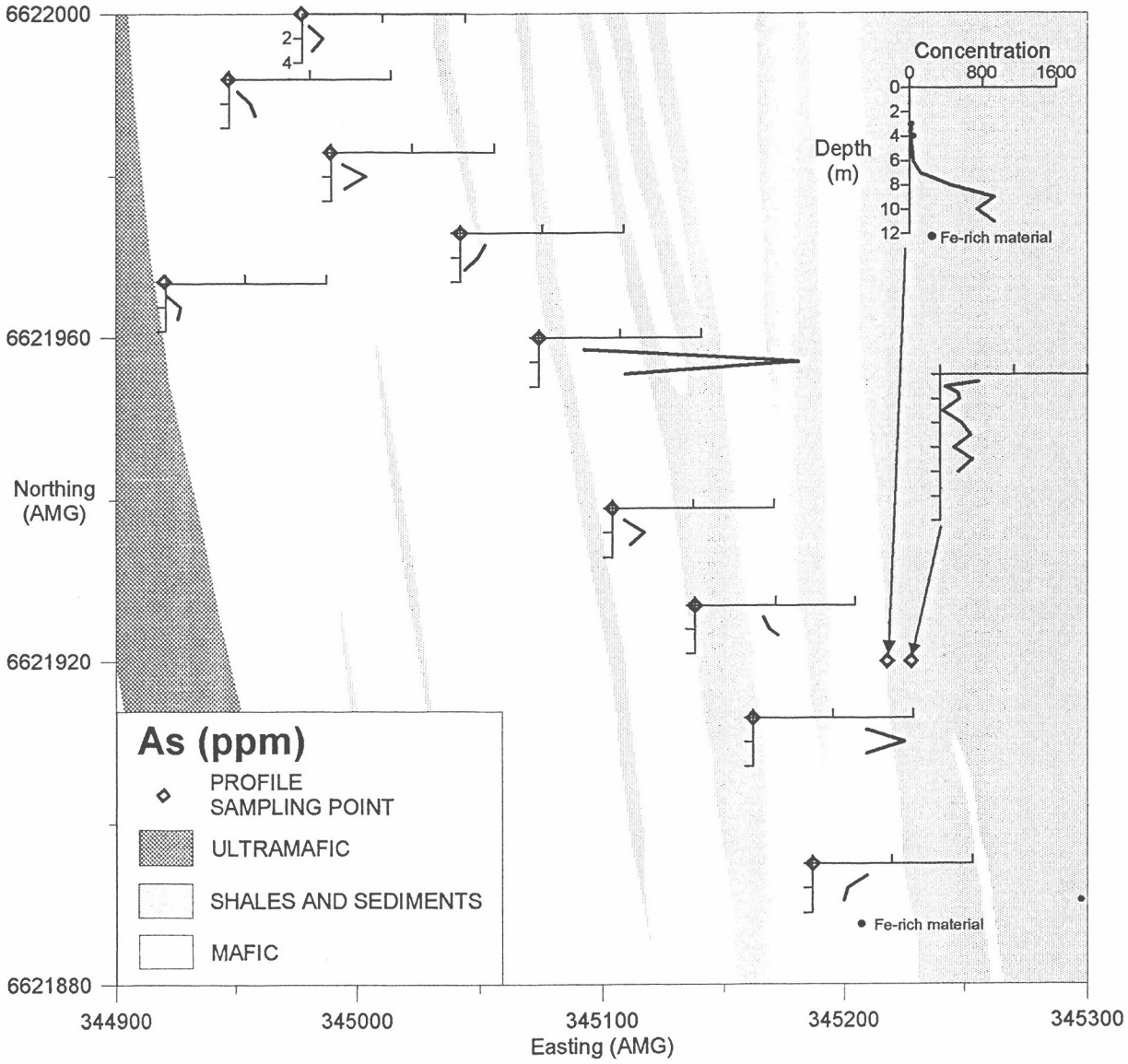

Figure A1.2: Plan showing spatial distribution of As concentrations.

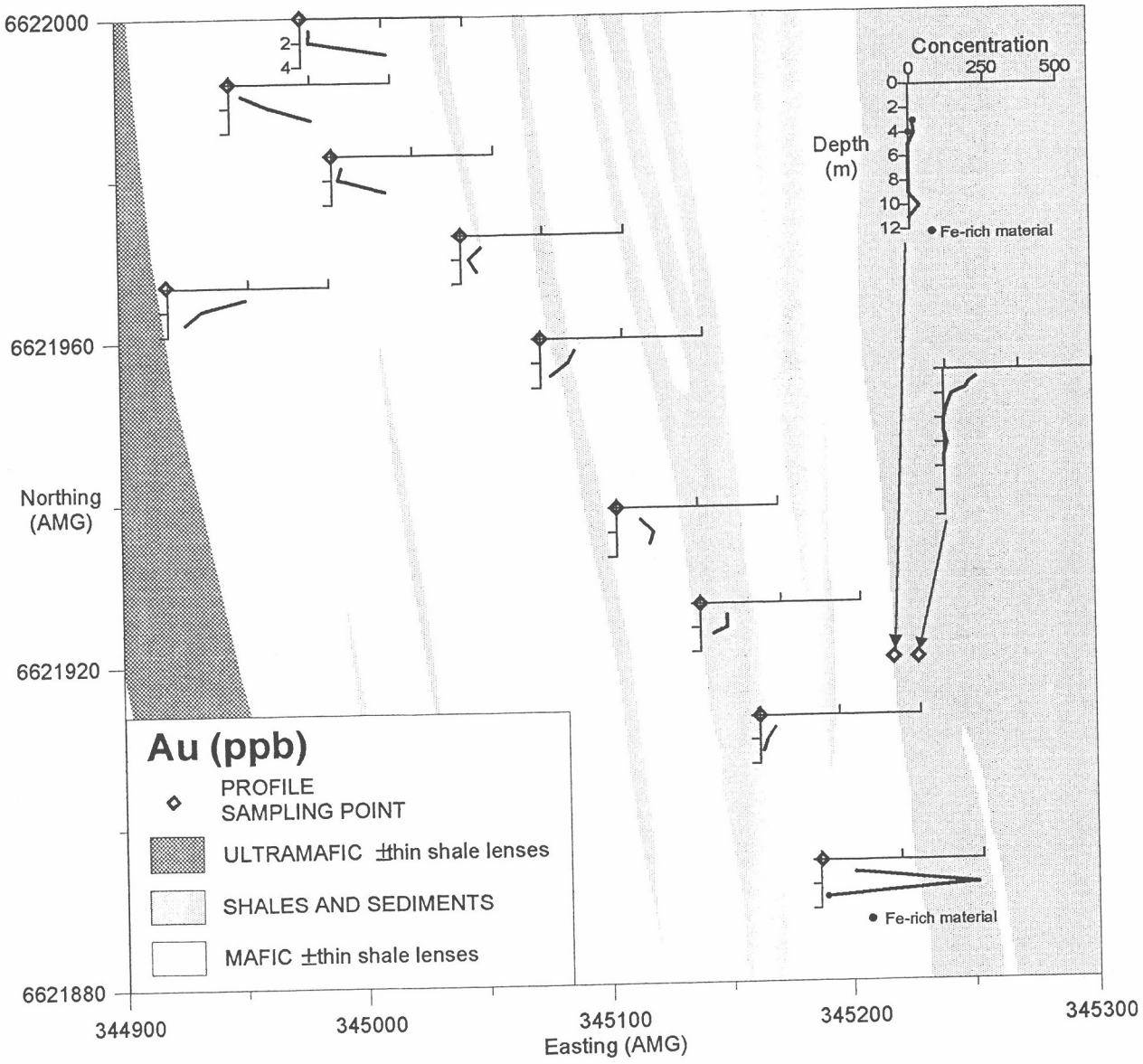

Figure A1.2 :Plan showing spatial distribution of Au concentrations

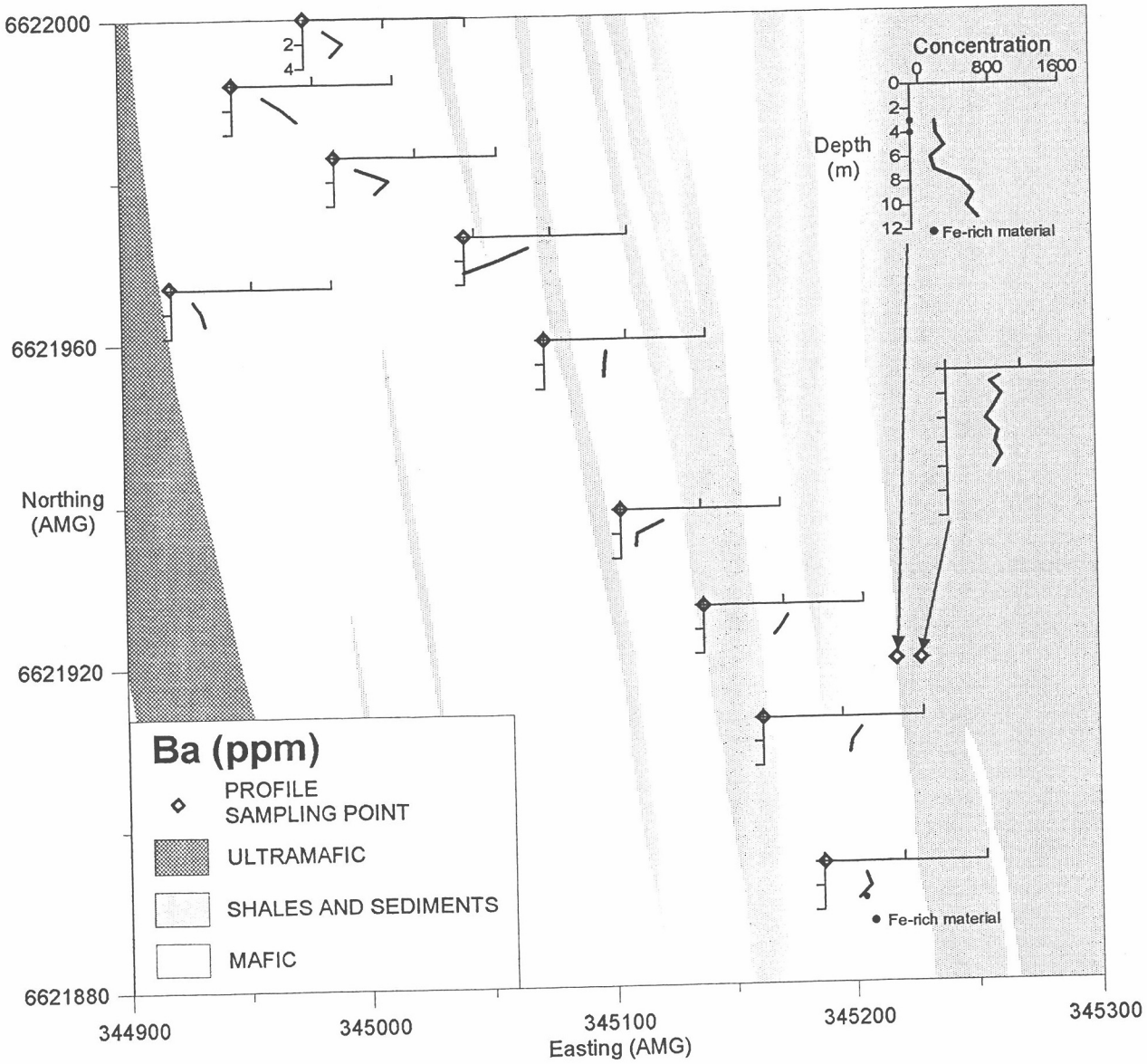

Figure A1.2 (continued): Plan showing spatial distribution of Ba concentrations.

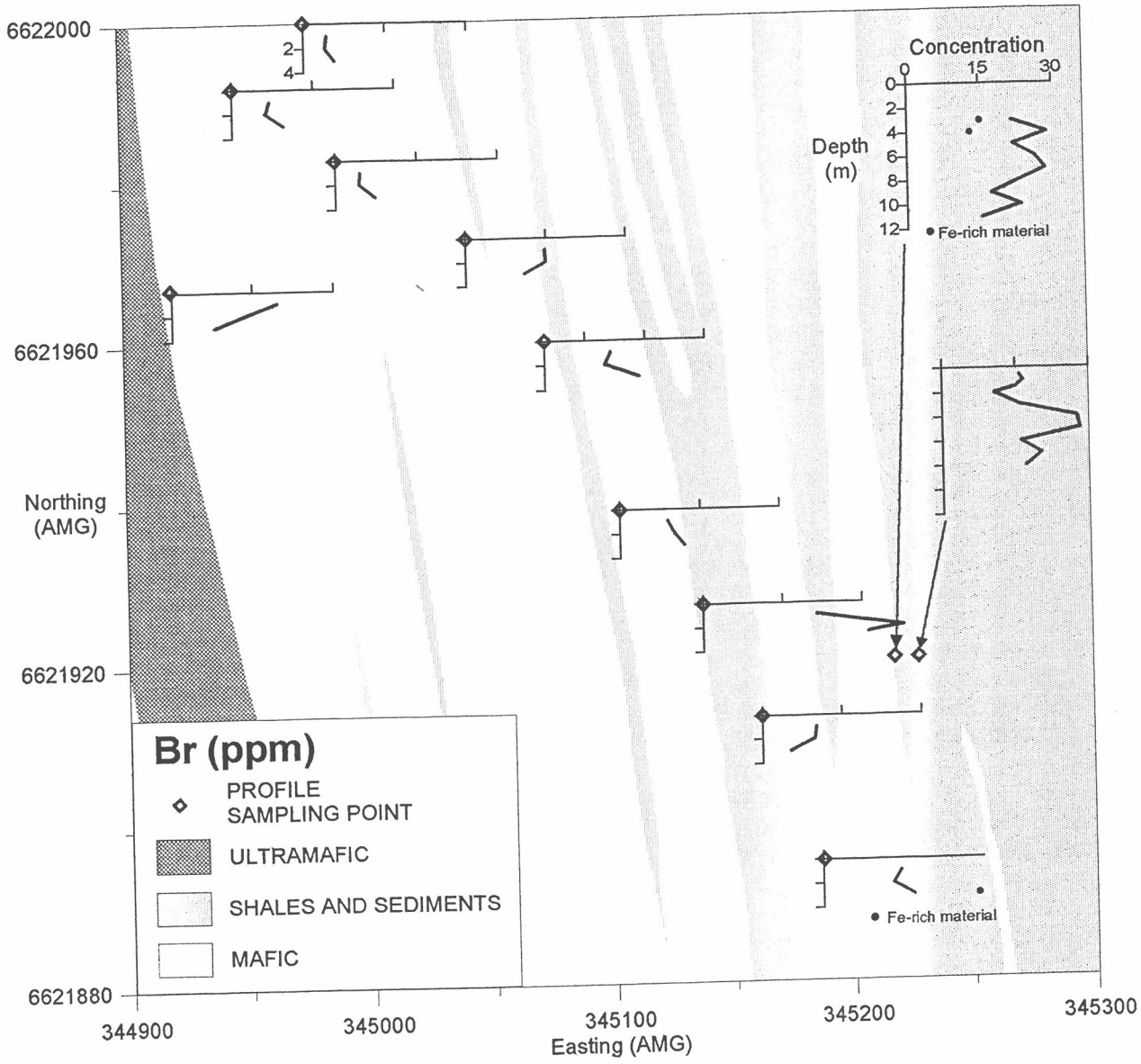

Figure A1.2. (continued): Plan showing spatial distribution of Br concentrations.

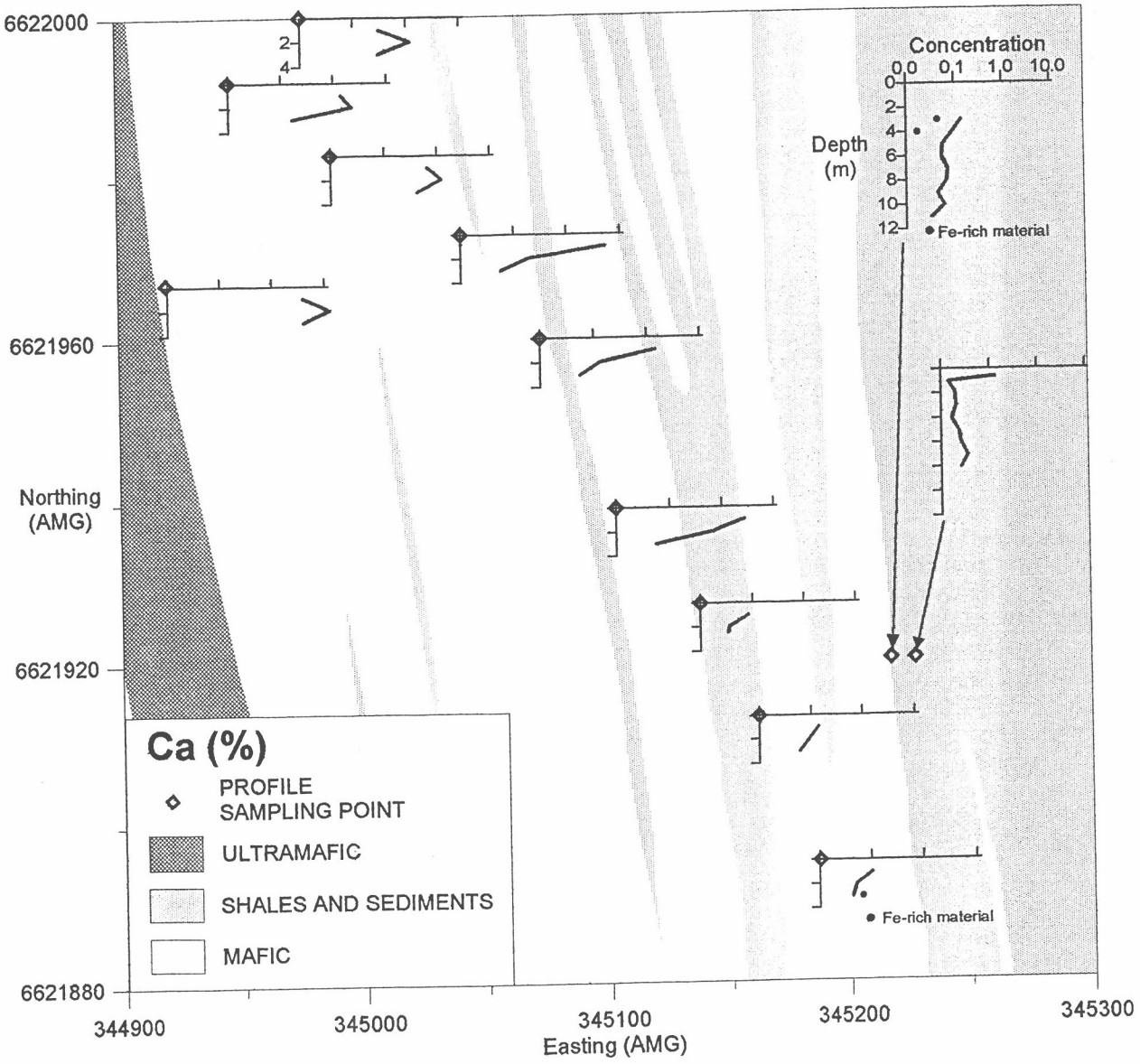

Figure A1.2 (continued): Plan showing spatial distribution of Ca concentrations.

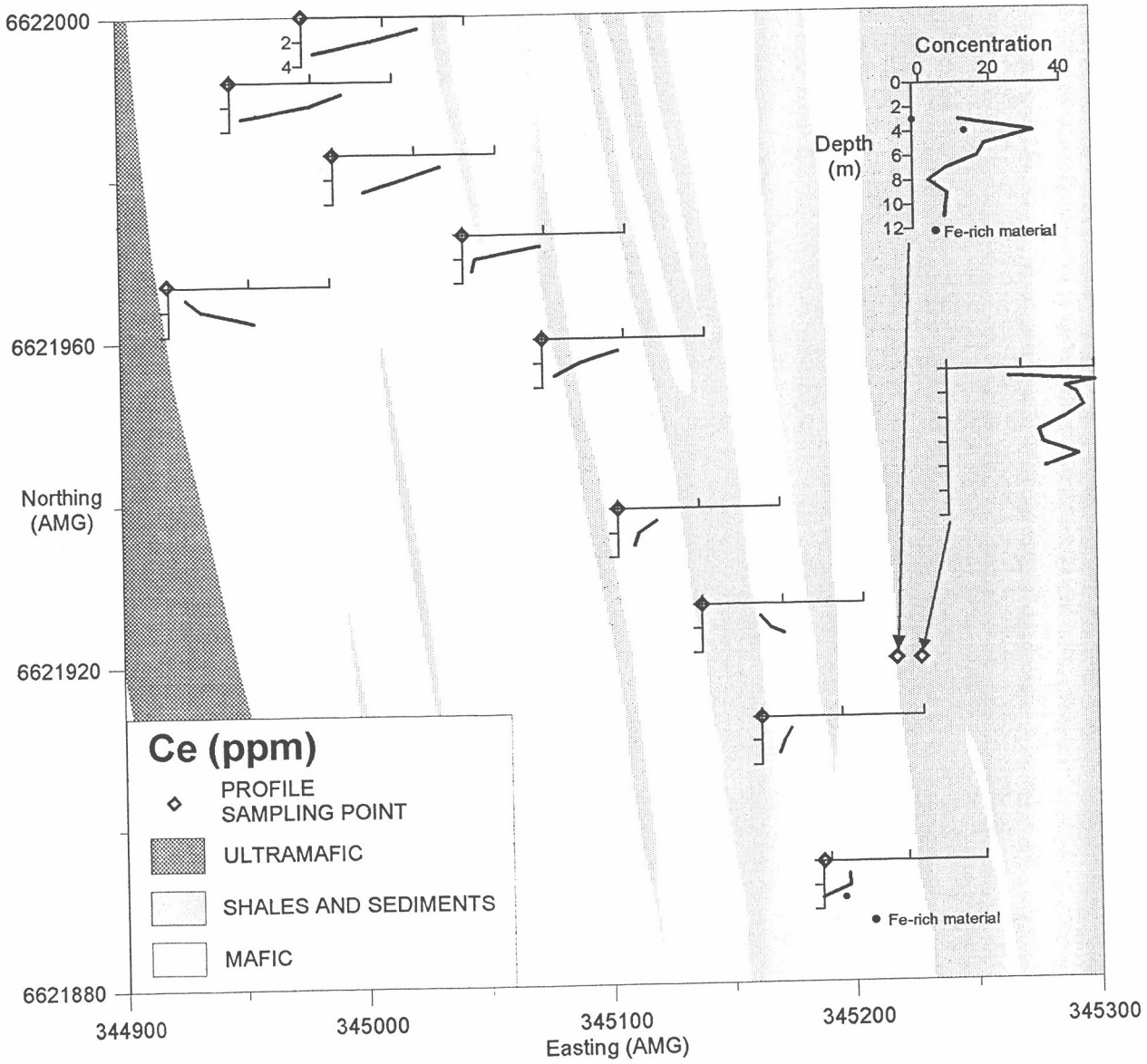

Figure A1.2 (continued): Plan showing spatial distribution of Ce concentrations.

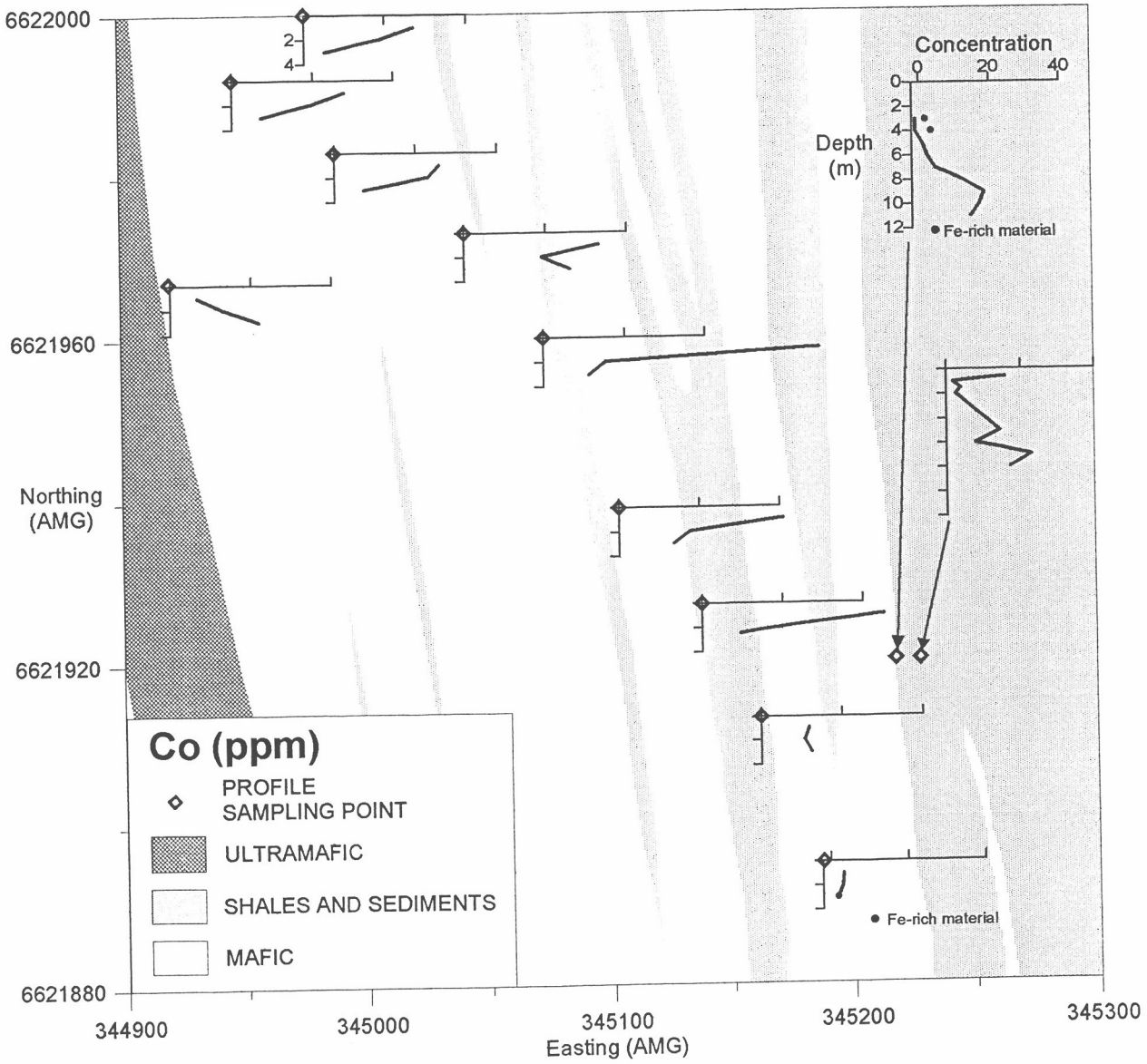

Figure A1.2 (continued): Plan showing spatial distribution of Co concentrations.

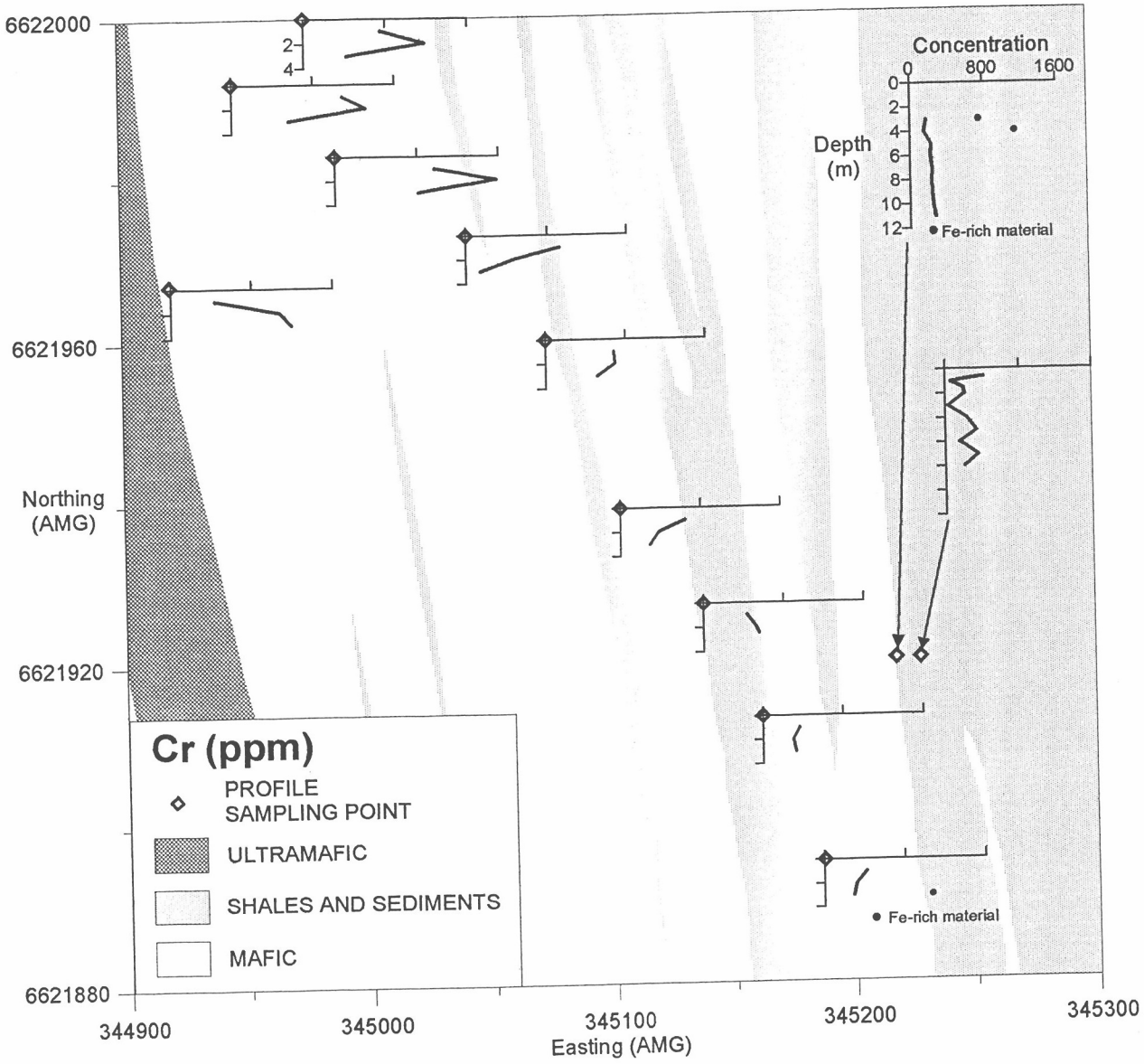

Figure A1.2 (continued): Plan showing spatial distribution of Cr concentrations.

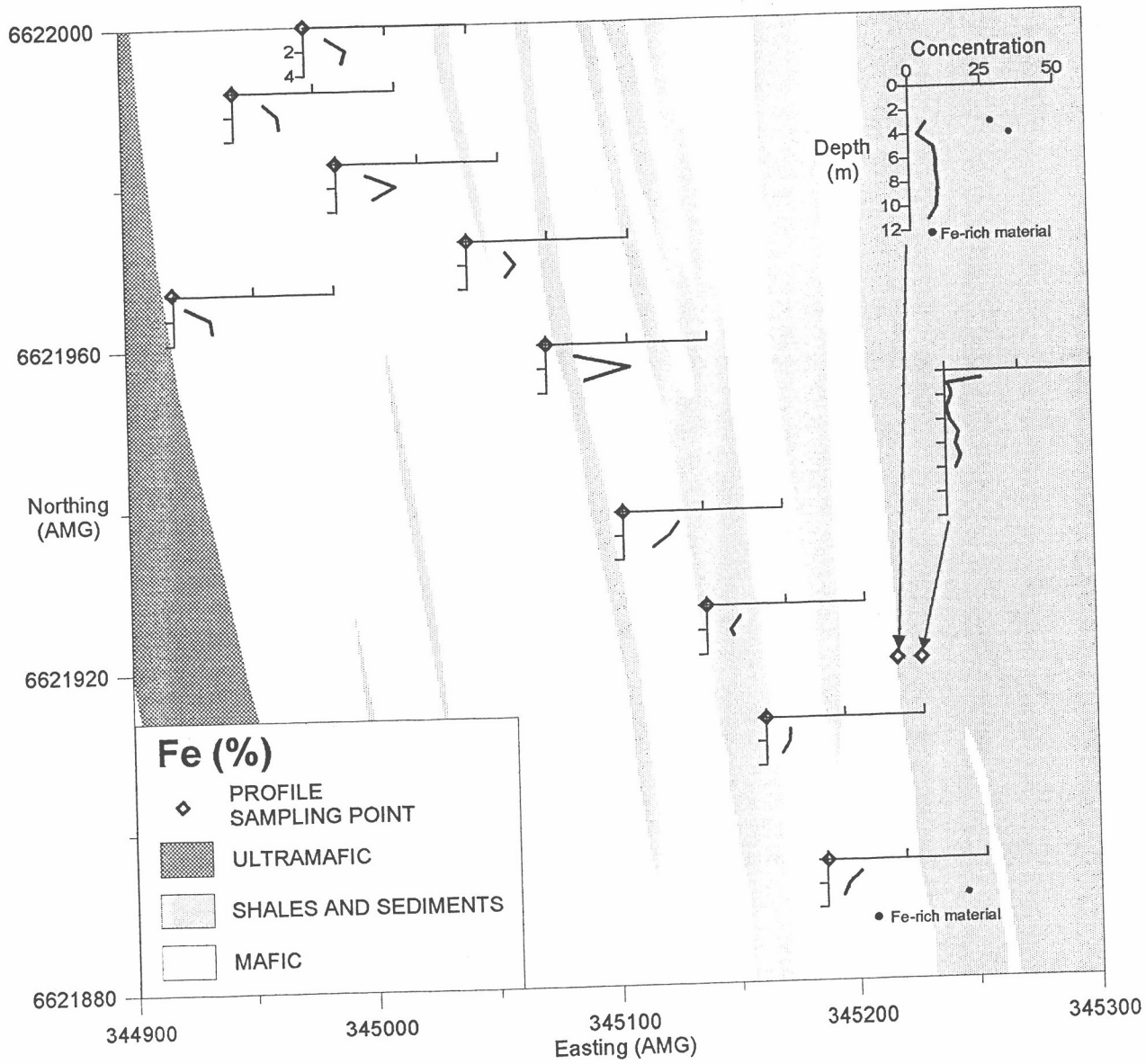

Figure A1.2 (continued): Plan showing spatial distribution of Fe concentrations.

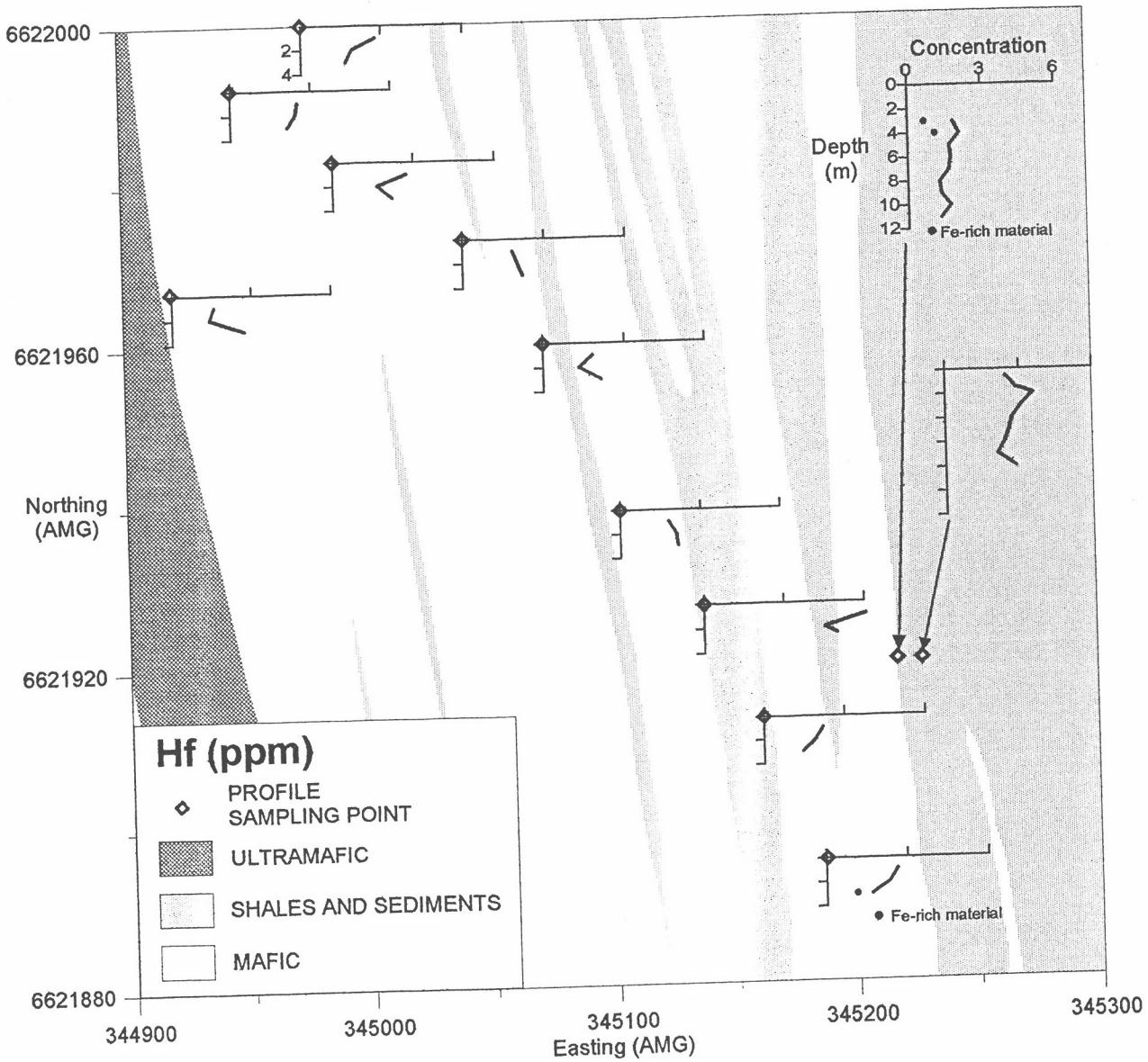

Figure A1.2 (continued): Plan showing spatial distribution of Hf concentrations.

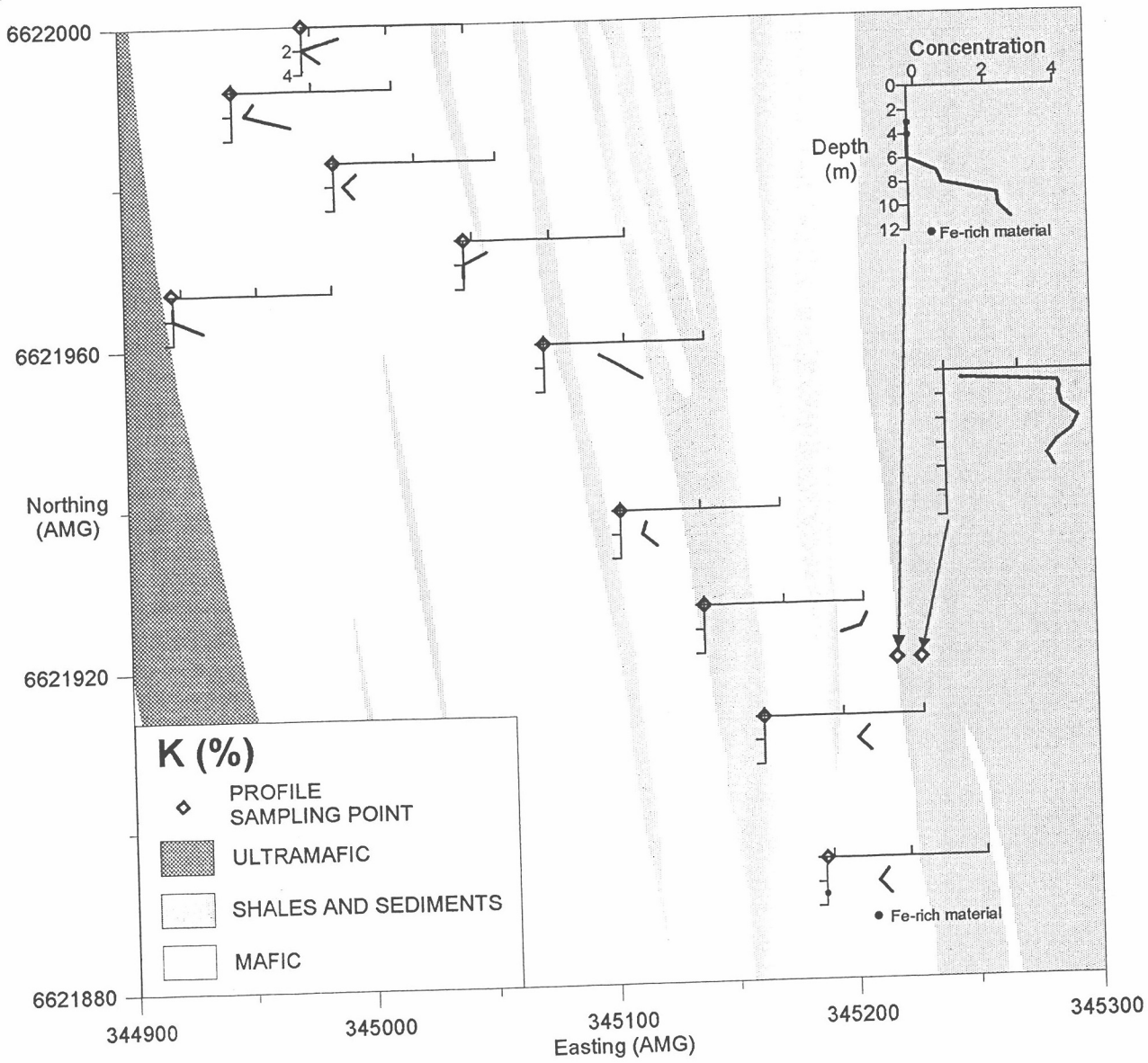

Figure A1.2 (continued): Plan showing spatial distribution of K concentrations.

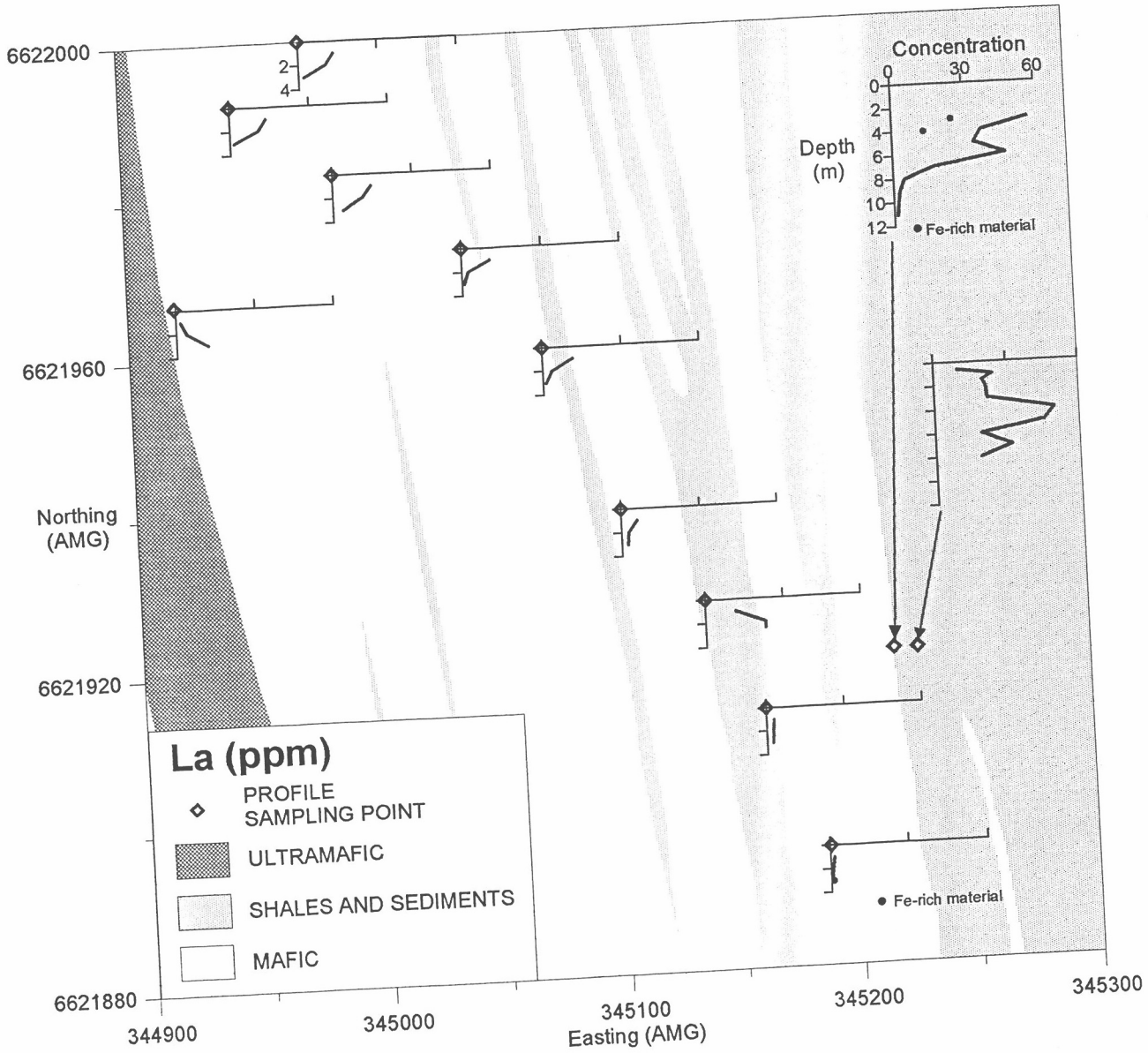

Figure A1.2 (continued): Plan showing spatial distribution of La concentrations.

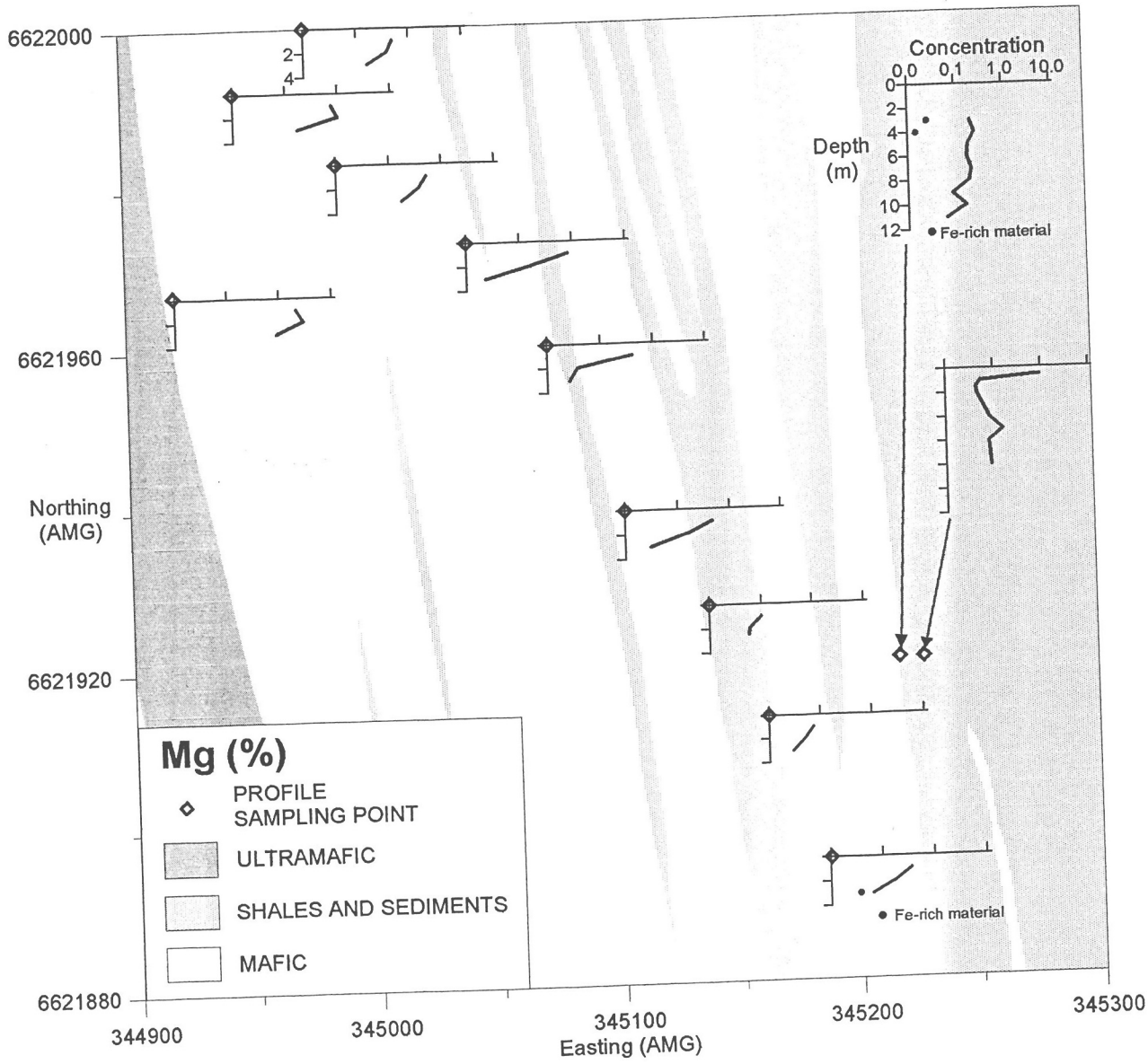

Figure A1.2 (continued): Plan showing spatial distribution of Mg concentrations.

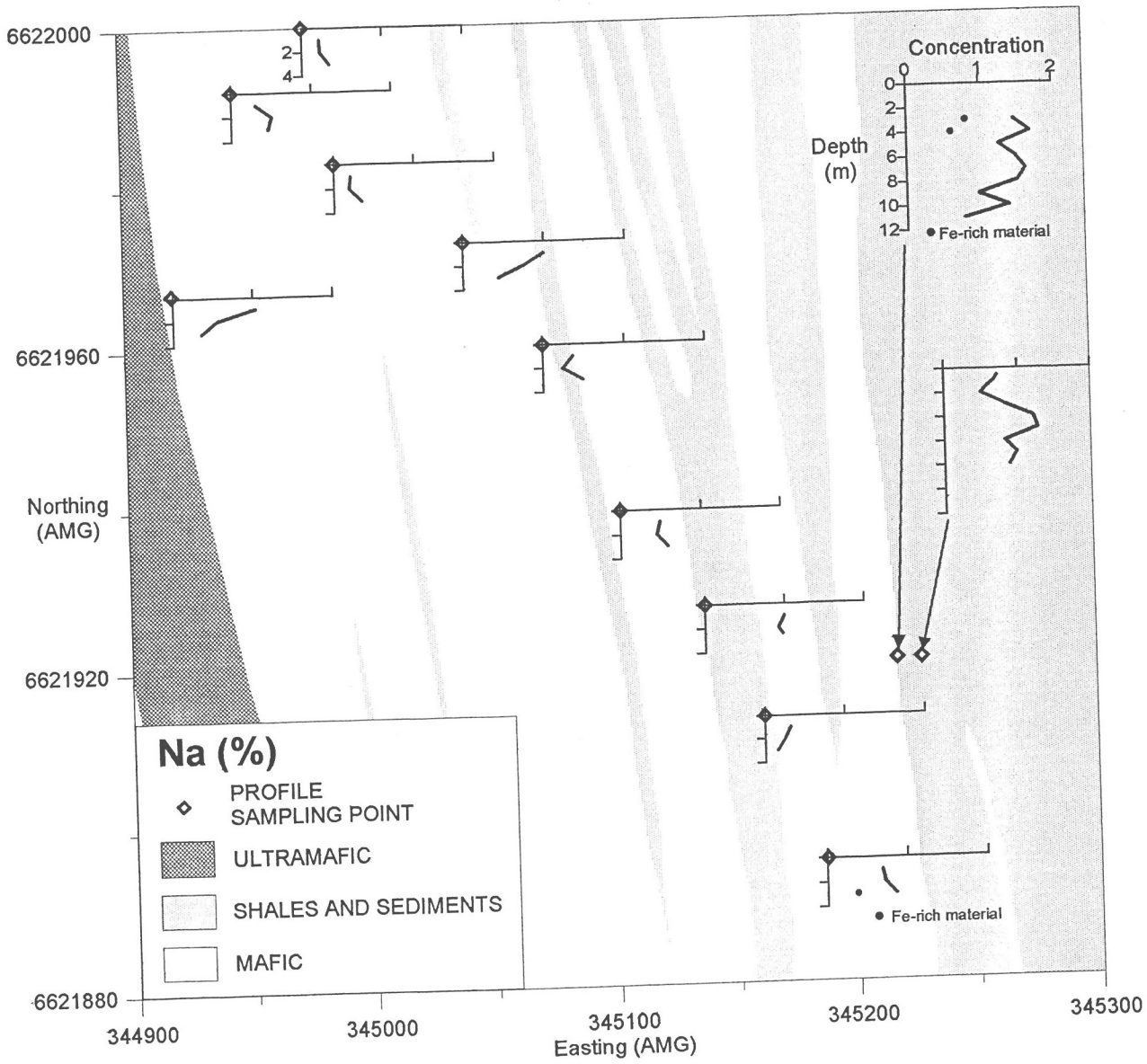

Figure A1.2 (continued): Plan showing spatial distribution of Na concentrations.

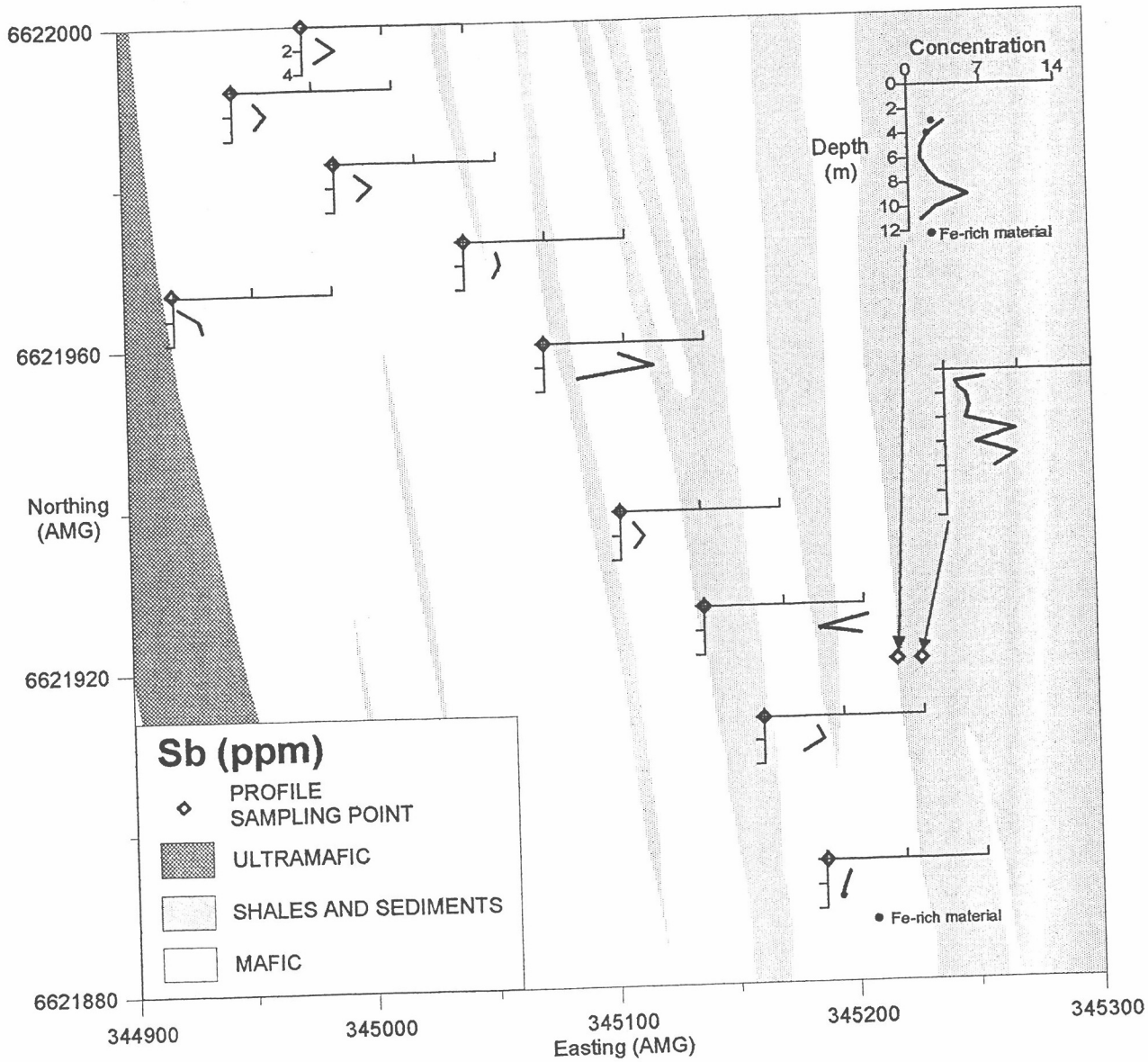

Figure A1.2 (continued): Plan showing spatial distribution of Sb concentrations.

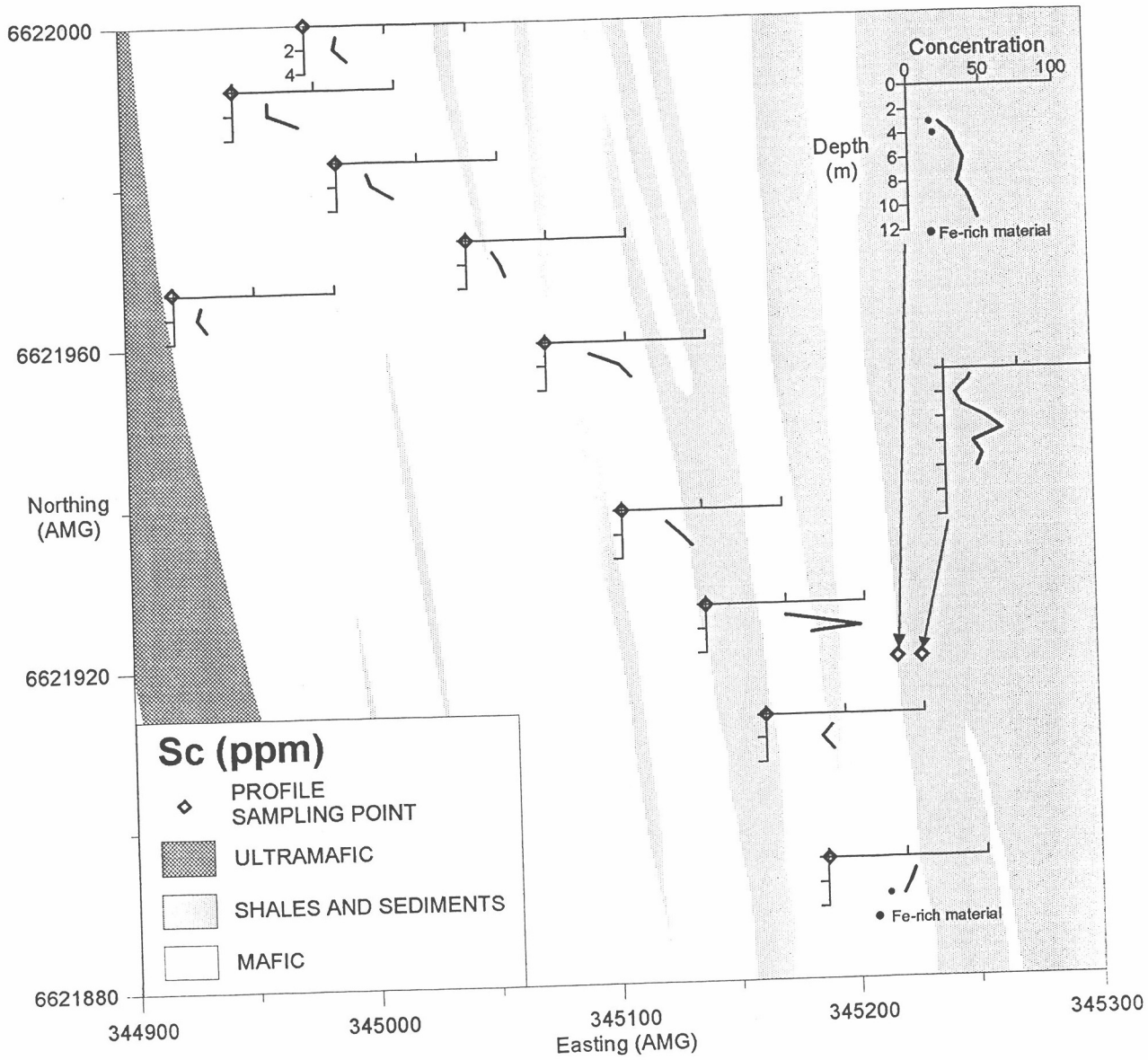

Figure A1.2 (continued): Plan showing spatial distribution of Sc concentrations.

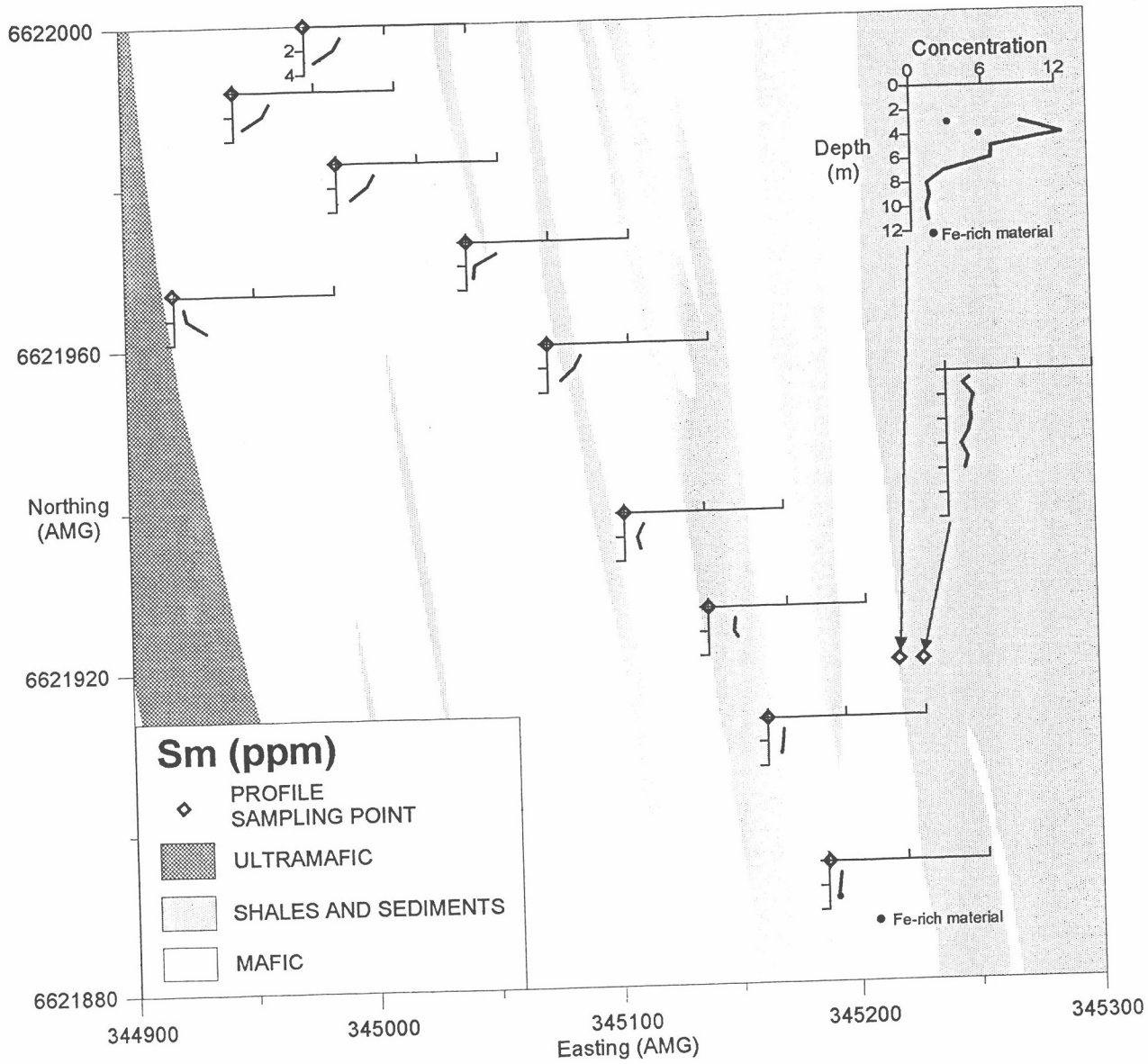

Figure A1.2 (continued): Plan showing spatial distribution of Sm concentrations.

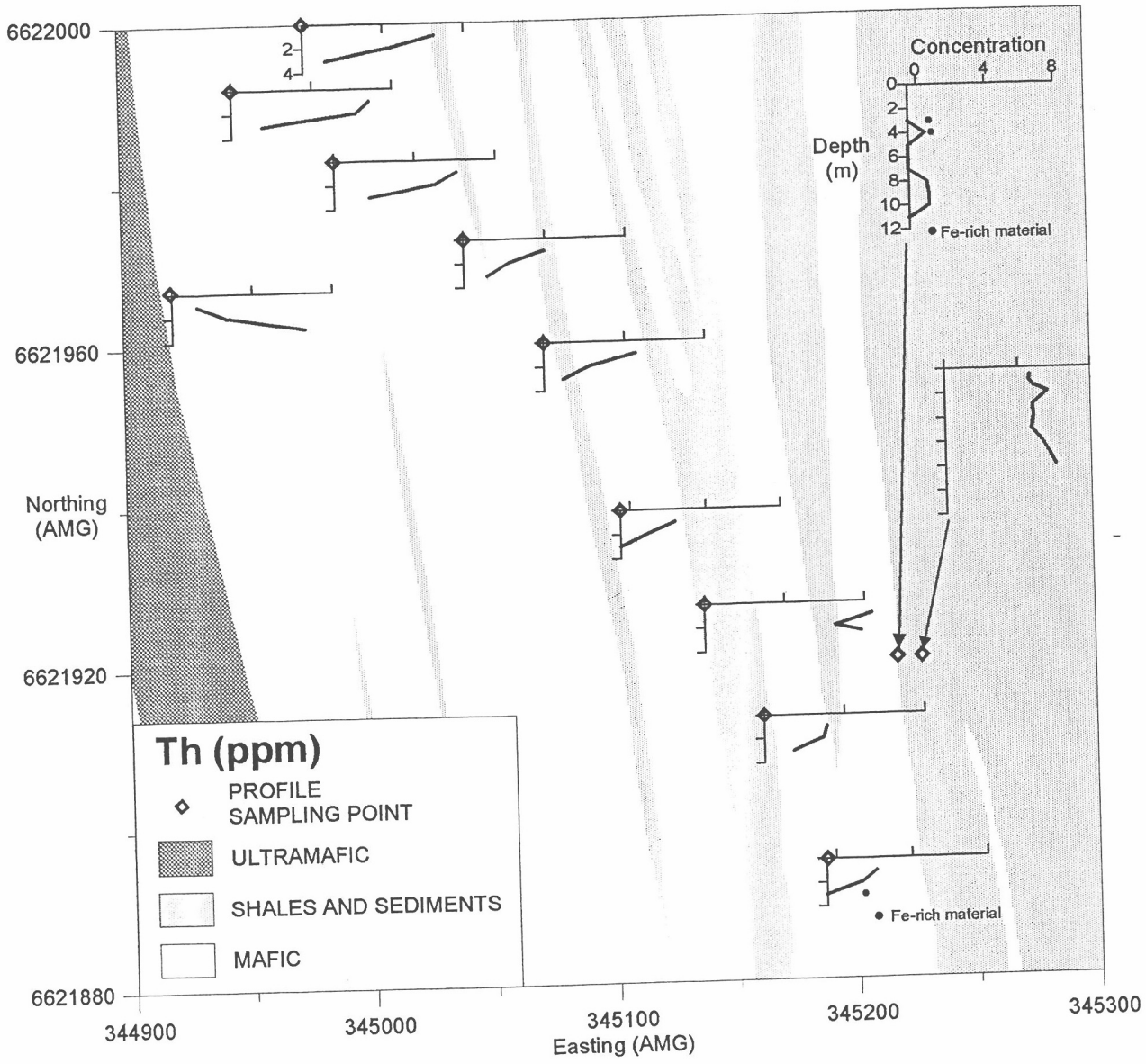

Figure A1.2 (continued): Plan showing spatial distribution of Th concentrations.

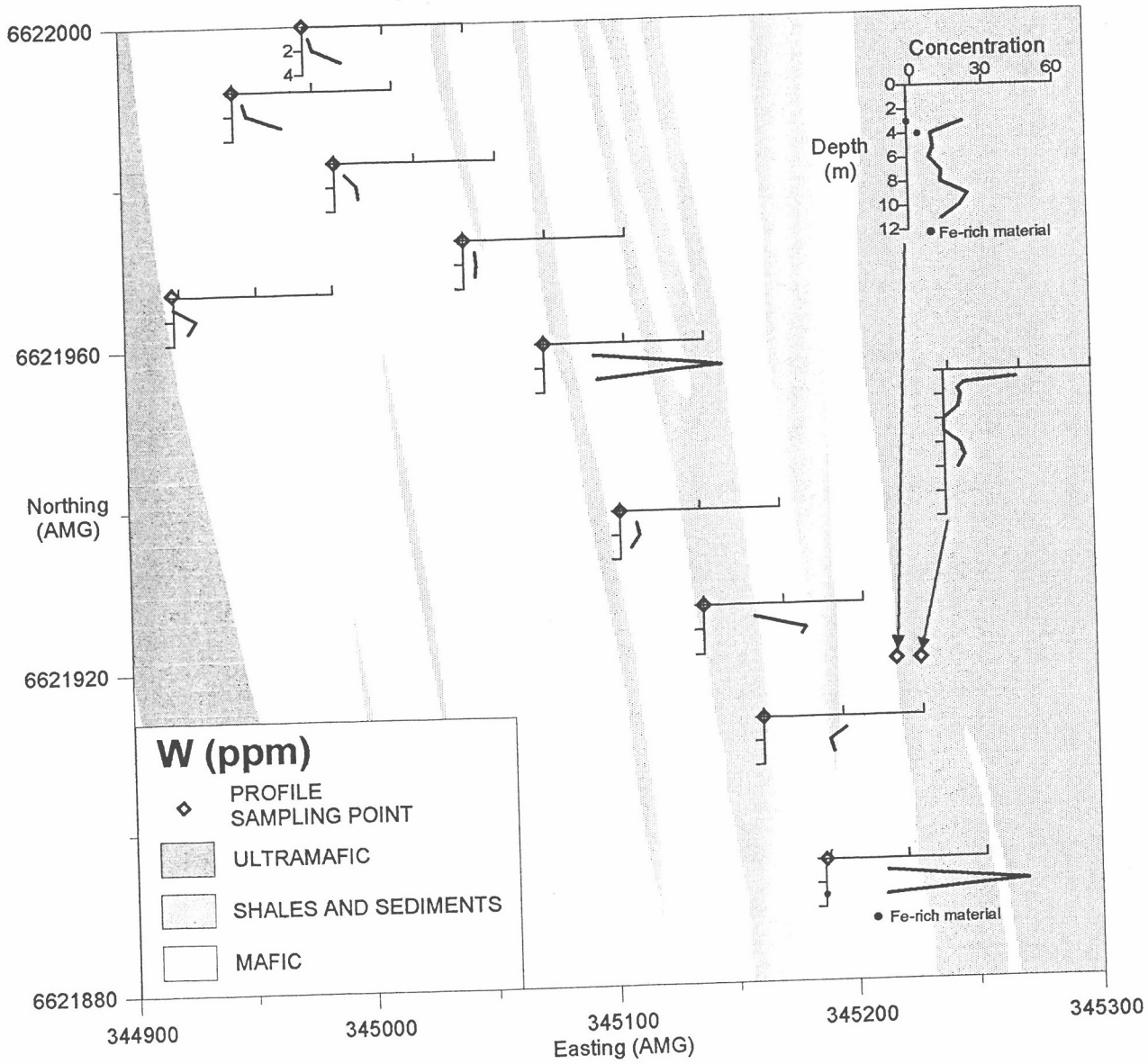

Figure A1.2 (continued): Plan showing spatial distribution of W concentrations.

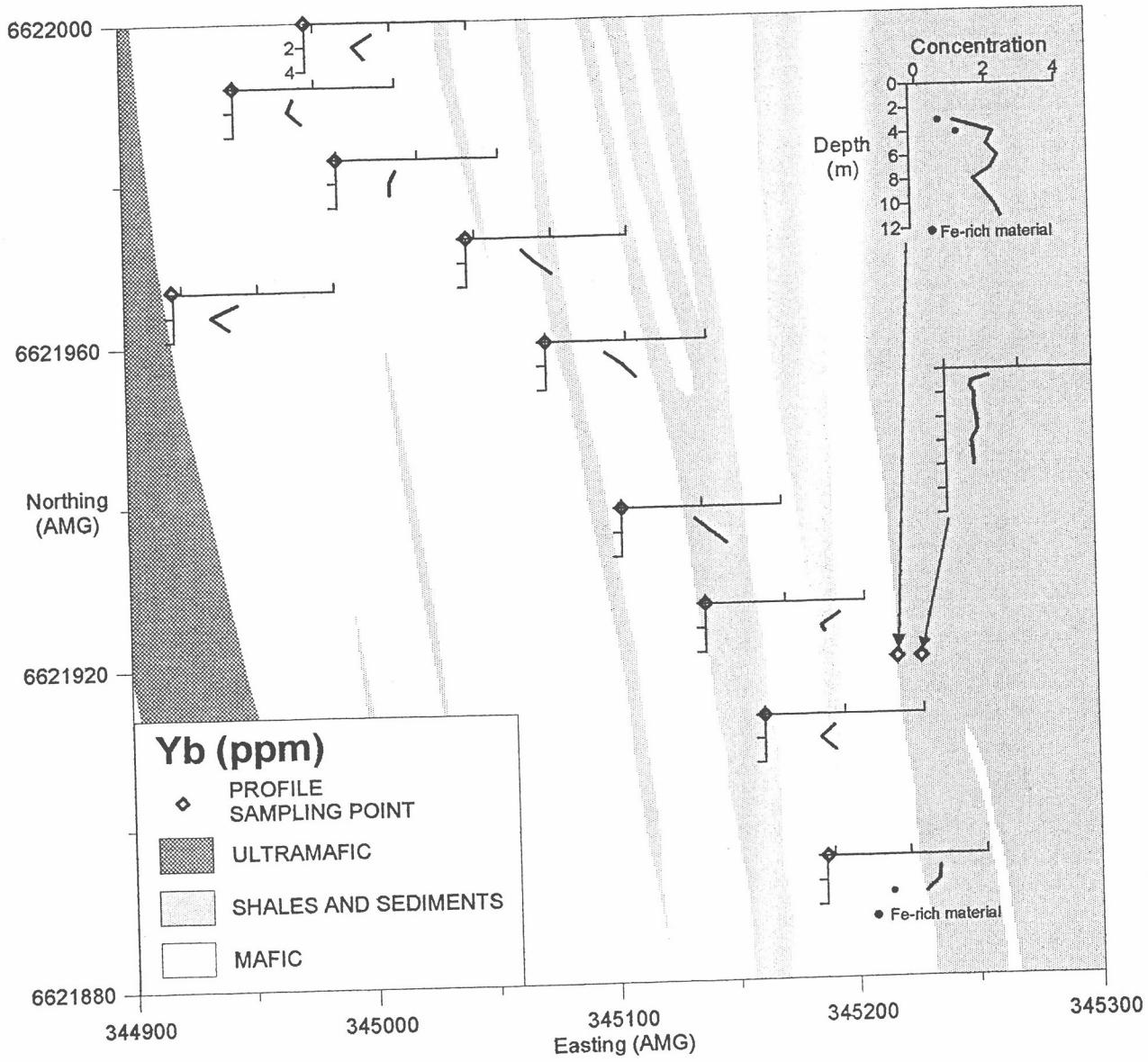

Figure A1.2 (continued): Plan showing spatial distribution of Yb concentrations.

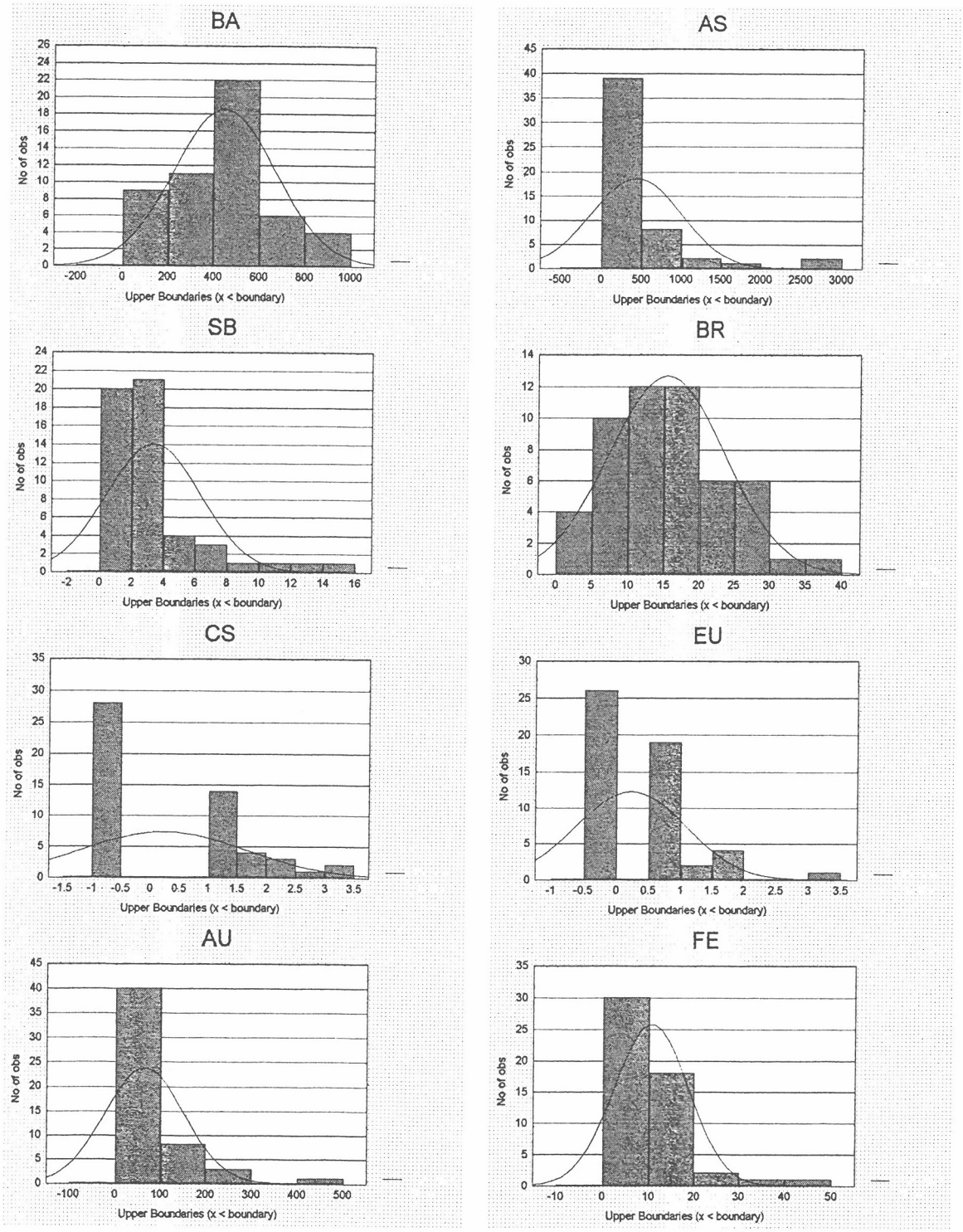

Figure A1.3: Histograms showing concentration distributions

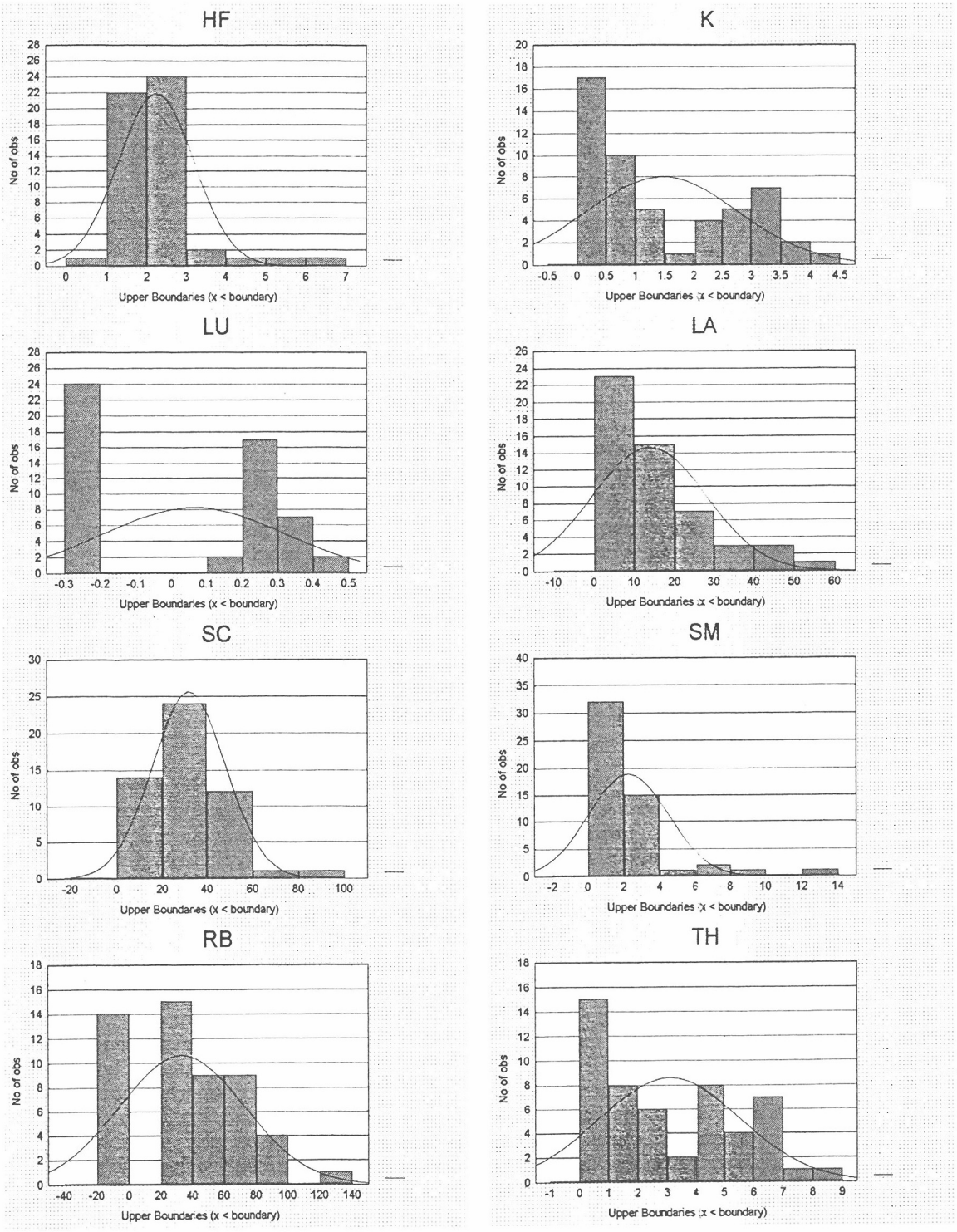

Figure A1.3: Histograms showing concentration distributions (continued).

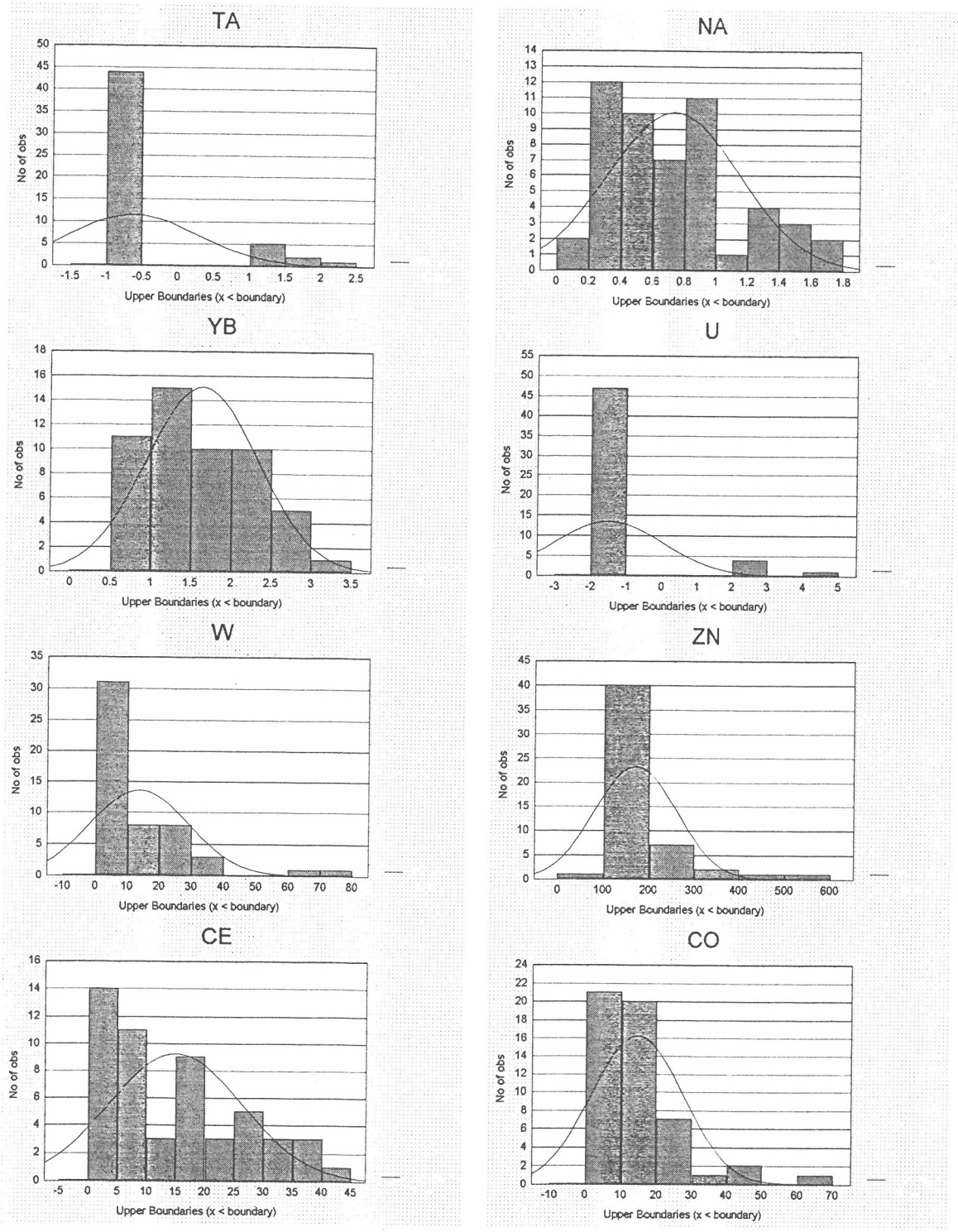

Figure A1.3: Histograms showing concentration distributions (continued).

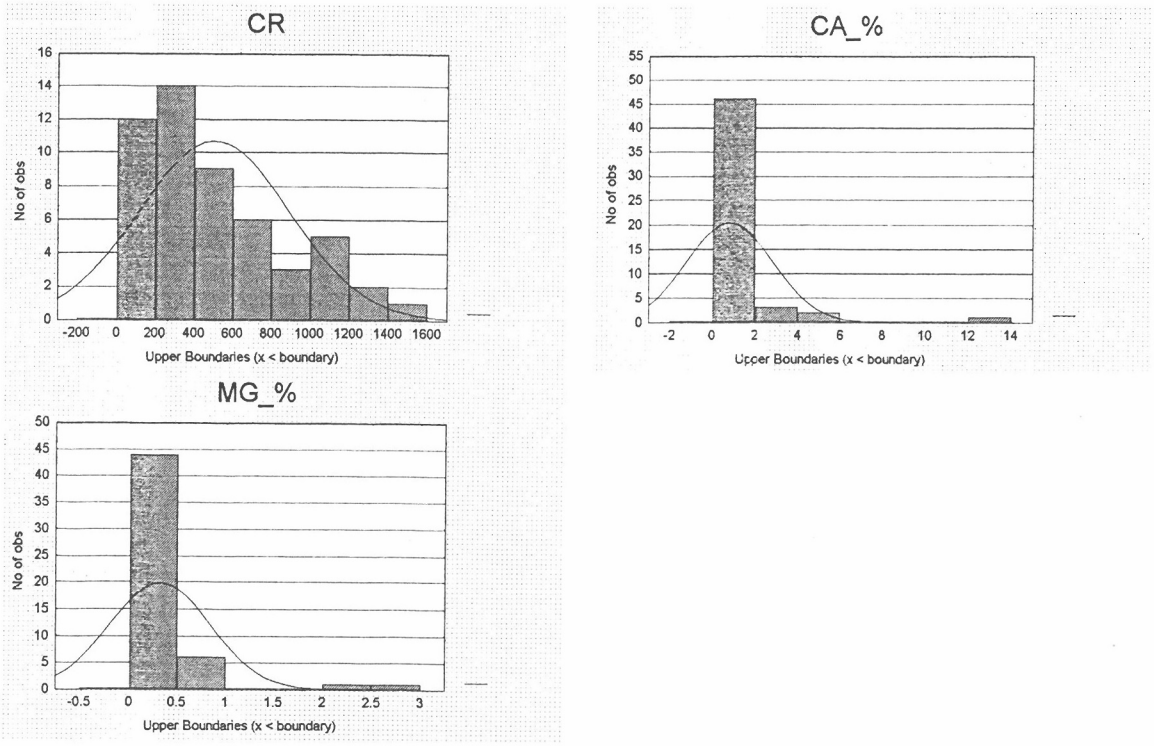

Figure A1.3: Histograms showing concentration distributions (continued).

Table A1.4: Compiled analytical data for bulk samples.

Concentrations for trace elements in ppm, and ppb for Au. Majors in %. Negative data below detection.

SAMPLE	E (AMG)	N (AMG)	from (m)	to (m)	Sb	As	Ba	Br	Ca	Ce	Cs	Cr	Co	Eu	Au
09-3651	345187	6621895	0	1	2.02	555	421	14.6	0.11	4.79	-1	420	3.49	-0.5	110
09-3652	345187	6621895	1	2	1.6	359	466	13.2	0.05	4.97	2.44	320	3.09	-0.5	485
09-3652Fe	345187	6621895	2	3	1.38	2660	414	29.2	0.07	3.74	-1	1070	1.82	-0.5	20.9
09-3653	345187	6621895	2	3	1.31	322	352	17.1	0.04	-2	-1	293	1.86	-0.5	35.4
09-3654	345162	6621913	0	1	4.7	1140	986	10.3	0.14	7.42	1.54	373	11.8	-0.5	47.2
09-3655	345162	6621913	1	2	5.24	1520	893	10	0.10	5.75	2.51	310	10.8	0.5	22.2
09-3656	345162	6621913	2	3	3.5	1140	871	5.33	0.06	4.55	1.54	332	12.5	-0.5	11.6
09-3657	345138	6621927	0	1	14.3	682	840	21.6	0.09	14.5	1.88	437	45.2	1.08	83.1
09-3658	345138	6621927	1	2	10.1	740	760	37.8	0.04	17	3.15	526	19.1	0.79	83
09-3659	345138	6621927	2	2.5	13.7	831	707	31.3	0.03	20.4	3.08	552	9.74	0.83	41.7
09-3660	345104	6621939	0	1	1.2	124	426	8.91	2.83	9.51	-1	651	40.9	-0.5	75
09-3661	345104	6621939	1	2	2.08	317	165	10.3	0.72	5.23	-1	380	17.7	-0.5	115
09-3662	345104	6621939	2	3	1.3	182	153	12.1	0.06	4.1	-1	293	13.7	-0.5	103
09-3663	345074	6621960	0	1	6.57	450	606	6.44	1.47	18.6	1.91	684	68.3	0.71	105
09-3664	345074	6621960	1	2	9.56	2570	591	5	0.13	9.18	-1	697	15.2	0.84	84.1
09-3665	345074	6621960	2	3	2.9	850	587	13.5	0.06	3.06	-1	520	11.1	0.66	31.9
09-3666	345042	6621973	0	1	2.81	241	564	14.8	5.28	19	-1	926	33	0.76	62.9
09-3667	345042	6621973	1	2	3.09	173	265	15	0.19	3	1.39	471	19.1	-0.5	23.2
09-3668	345042	6621973	2	3	2.55	45.1	-100	11	0.06	2.13	-1	138	26.1	-0.5	48.4
09-3669	344989	6621983	0	1	1.87	117	222	4.54	0.66	26.4	1.38	974	25.8	0.6	30.3
09-3670	344989	6621983	1	2	3.2	349	533	4.44	1.23	17.5	-1	1580	23.2	0.59	19.4
09-3671	344989	6621983	2	3	2.1	143	405	7.37	0.43	7.48	1.05	815	7.42	-0.5	166
09-3672	344977	6622000	0	1	1.4	69.4	200	4.29	0.31	28.5	1.42	754	27.1	0.72	26.3
09-3673	344977	6622000	1	2	2.81	205	393	3.94	1.19	17.2	2.04	1180	18.9	-0.5	24.1
09-3674	344977	6622000	2	3	1.11	107	271	5.64	0.30	2.69	1.13	424	5.07	-0.5	264
09-3675	344947	6621992	0	1	1.92	86	305	6.93	1.42	27.5	2.31	1090	27.8	0.68	35.2
09-3676	344947	6621992	1	2	2.9	209	488	6.19	2.25	19.5	-1	1320	19.5	0.51	123
09-3677	344947	6621992	2	3	1.97	262	636	9.57	0.17	2.72	1.01	563	7.14	-0.5	253
09-3678	344920	6621967	0	1	2.56	128	337	8	4.11	21.3	1.4	1200	21.9	-0.5	53.5
09-3679	344920	6621967	1	2	2.19	150	301	13.7	12.58	8.02	-1	1080	13.1	-0.5	102
09-3680	344920	6621967	2	3	0.42	14.1	222	19.6	3.96	4.25	-1	440	6.75	-0.5	241
09-3681	345228	6621920	0	0.6	3.87	424	577	16	0.14	16.9	-1	662	15.9	0.5	106
09-3682	345228	6621920	0.6	1	1.1	64.5	481	16.6	0.01	40.2	-1	96.6	1.87	-0.5	82.7
09-3683	345228	6621920	1	1.5	1.42	198	540	15.2	0.02	32.1	-1	75.1	4	-0.5	69.8
09-3684	345228	6621920	1.5	2	2.1	219	595	10.7	0.02	35	1.02	78.8	2.55	0.69	23.5
09-3685	345228	6621920	2	3	2.39	32.3	516	15.9	0.02	37	1.06	43.6	6.7	-0.5	6.5
09-3686	345228	6621920	3	4	1.98	241	427	27.6	0.02	31.8	-1	52.2	10.7	-0.5	-5
09-3687	345228	6621920	4	5	6.72	343	558	28.2	0.02	24.9	1.18	67.5	14.5	-0.5	-5
09-3688	345228	6621920	5	6	3.05	160	518	16.2	0.03	26	-1	53.1	7.94	-0.5	6
09-3689	345228	6621920	6	7	6.73	359	590	20.3	0.04	35.5	-1	85.9	22.9	-0.5	-5
09-3690	345228	6621920	7	8	4.76	208	510	17.2	0.03	26.6	1.23	77.6	17.3	0.5	-5
09-3691	345218	6621920	2	3	3.51	26.8	189	21.7	0.14	11.3	-1	181	-1	1.91	9
09-3691Fe	345218	6621920	2	3	2.36	19.8	-100	15.2	0.05	-2	-1	755	1.86	0.69	13.2
09-3692	345218	6621920	3	4	1.97	18	198	28.8	0.10	32.4	1.22	160	-1	3.16	14.1
09-3692Fe	345218	6621920	3	4	1.92	46.1	-100	13.2	0.02	12.9	-1	1150	3.58	1.59	-5
09-3693	345218	6621920	4	5	1.29	35	296	22	0.06	18.5	-1	237	1.31	1.61	-5
09-3694	345218	6621920	5	6	1.23	47.5	139	26.4	0.06	16.5	-1	228	2.44	1.71	-5
09-3695	345218	6621920	6	7	1.94	129	183	28.5	0.08	7.47	-1	244	4.81	1.01	-5
09-3696	345218	6621920	7	8	2.93	456	486	23.3	0.07	2.63	1.35	240	12.2	0.76	-5
09-3697	345218	6621920	8	9	5.7	928	618	17.5	0.05	7.96	-1	247	18.4	0.69	-5
09-3699	345218	6621920	9	10	2.57	747	543	23.6	0.06	7.5	-1	259	17.2	-0.5	29.5
09-3700	345218	6621920	10	11	1.21	933	665	15.6	0.03	7.09	1.49	281	14.7	0.63	-5

Table A1.4: Compiled analytical data for bulk samples (continued).

SAMPLE	Hf	Fe	La	Lu	Mg	K	Rb	Sm	Sc	Na	Ta	Th	W	U	Yb	Zn
09-3651	2.63	10.7	1.57	0.38	0.36	1.42	42.9	0.96	54.7	0.688	-1	2.11	22.2	-2	2.78	176
09-3652	2.36	6.73	0.95	0.37	0.18	1.18	39.8	0.84	51.8	0.724	1	1.35	75.6	-2	2.75	188
09-3652Fe	1.13	44.1	1.13	0.26	0.04	-0.2	28.9	0.78	39.1	0.374	-1	1.49	-2	-2	1.56	124
09-3653	1.7	5.21	0.51	0.35	0.07	1.49	31.1	0.71	48	0.858	-1	-0.5	21.7	-2	2.41	161
09-3654	2.21	7.57	2.96	0.27	0.08	2.62	80.3	1.24	41.5	0.325	-1	3.14	31.2	-2	1.74	213
09-3655	1.94	7.51	2.61	0.25	0.05	2.36	73.8	1.15	35.5	0.248	-1	2.95	25.1	-2	1.41	201
09-3656	1.47	5.17	2.42	0.29	0.03	2.67	81.1	1.01	42.4	0.159	-1	1.47	26.5	-2	1.75	185
09-3657	6.08	10.4	11.7	0.46	0.10	4.06	138	2.04	50	1	2.36	8.37	19.2	4.71	3.35	201
09-3658	4.56	7.59	23.2	0.34	0.06	3.91	86.4	1.93	97.3	0.927	1.53	6.56	38.6	-2	2.91	298
09-3659	5	8.39	23.2	0.45	0.06	3.44	59.2	2.18	66.2	0.981	1.45	7.83	37	-2	2.98	215
09-3660	1.81	17.3	6.09	0.23	0.48	0.65	28.5	1.41	27.7	0.489	-1	2.38	6.41	-2	1.83	-100
09-3661	2.09	14.5	2.73	0.32	0.16	0.56	-20	0.95	36.2	0.452	-1	0.89	7.3	-2	2.21	133
09-3662	2.15	9.47	2.4	0.3	0.03	0.92	35.2	1.21	43.5	0.582	-1	-0.5	4.2	-2	2.61	155
09-3663	1.83	9	11.5	0.23	0.41	1.38	31.4	2.47	27.1	0.372	-1	4.55	18.7	2.49	1.49	152
09-3664	1.34	25.6	3.62	0.31	0.04	1.9	33.3	1.97	45.9	0.243	-1	2.26	66.5	-2	1.92	543
09-3665	2.14	11.9	1.21	0.28	0.03	2.44	72.9	1	52.7	0.488	-1	0.96	20	2.95	2.23	437
09-3666	1.85	12.1	10.8	-0.2	0.84	0.39	28.1	2.23	16.6	1	1.04	3.96	4.25	-2	1.26	119
09-3667	2.03	15.1	2.25	-0.2	0.16	-0.2	-20	0.62	21.3	0.754	-1	2.2	4.72	2.73	1.58	120
09-3668	2.2	12.1	0.68	0.25	0.02	-0.2	-20	0.51	24.2	0.444	-1	1.15	4.25	-2	2.03	101
09-3669	2.76	9.23	14.5	-0.2	0.52	0.56	29.4	2.78	18.9	0.212	-1	6.08	3.83	-2	1.46	112
09-3670	1.66	18.2	11.3	-0.2	0.38	0.24	42.5	2.29	21.6	0.188	-1	5.02	8.22	-2	1.31	100
09-3671	2.22	11.4	3.91	-0.2	0.18	0.5	-20	1.04	34.4	0.351	-1	1.77	8.84	-2	1.31	107
09-3672	2.78	6.97	13.3	0.2	0.48	0.75	38.5	2.66	19.6	0.219	-1	6.55	2.07	-2	1.54	141
09-3673	1.91	12.7	10.3	-0.2	0.38	-0.2	-20	2.13	17.7	0.225	-1	4.37	3.41	-2	1.05	-100
09-3674	1.67	11.6	1.82	-0.2	0.17	0.25	-20	0.68	26.1	0.337	-1	1.13	14.2	-2	1.33	-100
09-3675	2.52	9.53	13.4	0.2	0.77	0.54	30.9	2.66	21.2	0.305	-1	6.88	3.66	-2	1.47	124
09-3676	2.42	13.7	10.5	-0.2	0.99	0.31	20.9	2.16	21.1	0.505	-1	6.2	5.13	-2	1.34	-100
09-3677	2.13	14.2	1.52	0.26	0.17	1.47	56.7	0.69	39.7	0.458	-1	1.53	18.2	-2	1.68	129
09-3678	2.72	12.1	12.1	-0.2	0.91	0.59	25.2	2.42	20.6	0.356	-1	6.64	3.35	-2	1.27	107
09-3679	1.4	11.4	3.95	-0.2	2.91	-0.2	-20	0.94	15	0.545	-1	2.71	6.66	2.68	0.79	-100
09-3680	1.59	3.72	1.58	-0.2	2.18	-0.2	-20	0.74	17.1	1.04	-1	1.24	-2	-2	1.49	108
09-3681	2.48	12.6	10.2	-0.2	0.98	0.47	25.6	1.95	17.9	0.735	-1	4.68	28.6	-2	1.21	140
09-3682	2.68	0.87	24.4	-0.2	0.05	3.09	63	1.4	16.1	0.686	-1	4.6	6.59	-2	0.73	-100
09-3683	2.88	1.93	20.2	-0.2	0.04	3.15	68.6	1.79	11.5	0.583	-1	4.87	4.12	-2	0.69	111
09-3684	3.59	2.12	21.5	-0.2	0.05	3.1	74.9	2.27	7.81	0.506	-1	5.63	5.18	-2	0.79	105
09-3685	3.11	0.5	22.1	-0.2	0.06	3.19	59	1.98	12.5	0.828	1.17	4.83	4.07	-2	0.8	-100
09-3686	2.73	1.59	49.6	-0.2	0.08	3.62	54.6	2.05	28	1.22	-1	4.85	-2	-2	0.86	168
09-3687	2.59	4.57	45.5	-0.2	0.16	3.44	48	1.75	39.1	1.28	1.6	4.73	-2	-2	0.89	286
09-3688	2.42	3.43	19.3	-0.2	0.08	3.01	77.4	1.2	19.4	0.825	-1	5.29	4.53	-2	0.7	334
09-3689	2.13	5.22	31.6	-0.2	0.09	2.76	40.5	1.72	25.6	0.984	-1	5.7	6.74	-2	0.75	303
09-3690	2.87	3.45	18.9	-0.2	0.09	2.96	65.1	1.43	22.2	0.888	-1	6.05	3.68	-2	0.76	276
09-3691	1.85	5.95	56.7	-0.2	0.21	-0.2	-20	9.17	22.1	1.47	-1	-0.5	21.9	-2	1.1	139
09-3691Fe	0.69	28.4	25.1	-0.2	0.03	-0.2	-20	3.19	15.8	0.809	-1	0.75	-2	-2	0.66	139
09-3692	2.11	3.04	37.2	0.3	0.27	-0.2	-20	12.5	30.5	1.69	-1	0.51	8.26	-2	2.23	162
09-3692Fe	1.12	34.7	13.4	-0.2	0.02	-0.2	-20	5.76	17.8	0.611	-1	0.87	2.7	-2	1.18	-100
09-3693	1.71	8.59	34.1	0.25	0.19	-0.2	-20	6.73	34.5	1.26	-1	-0.5	9.18	-2	2.04	161
09-3694	1.75	9.44	47	0.26	0.18	-0.2	-20	6.71	38.4	1.48	-1	-0.5	7.42	-2	2.34	170
09-3695	1.68	9.49	17	0.25	0.22	0.63	21.7	2.8	36.4	1.62	1.43	-0.5	12.4	-2	2.15	194
09-3696	1.3	10	4.6	0.21	0.21	0.78	44.4	1.39	34	1.51	-1	0.57	12.2	-2	1.64	164
09-3697	1.37	9.81	2.57	0.23	0.09	2.35	70.7	1.58	40.9	0.991	-1	0.69	23.3	-2	1.96	192
09-3699	1.74	9.34	1.87	0.28	0.17	2.38	73.5	1.31	44.3	1.4	-1	0.68	19.9	-2	2.22	188
09-3700	1.34	6.77	1.51	0.32	0.07	2.74	87.2	1.5	47.8	0.8	-1	-0.5	12.4	-2	2.4	196

APPENDIX 2: SIZE FRACTION STUDY

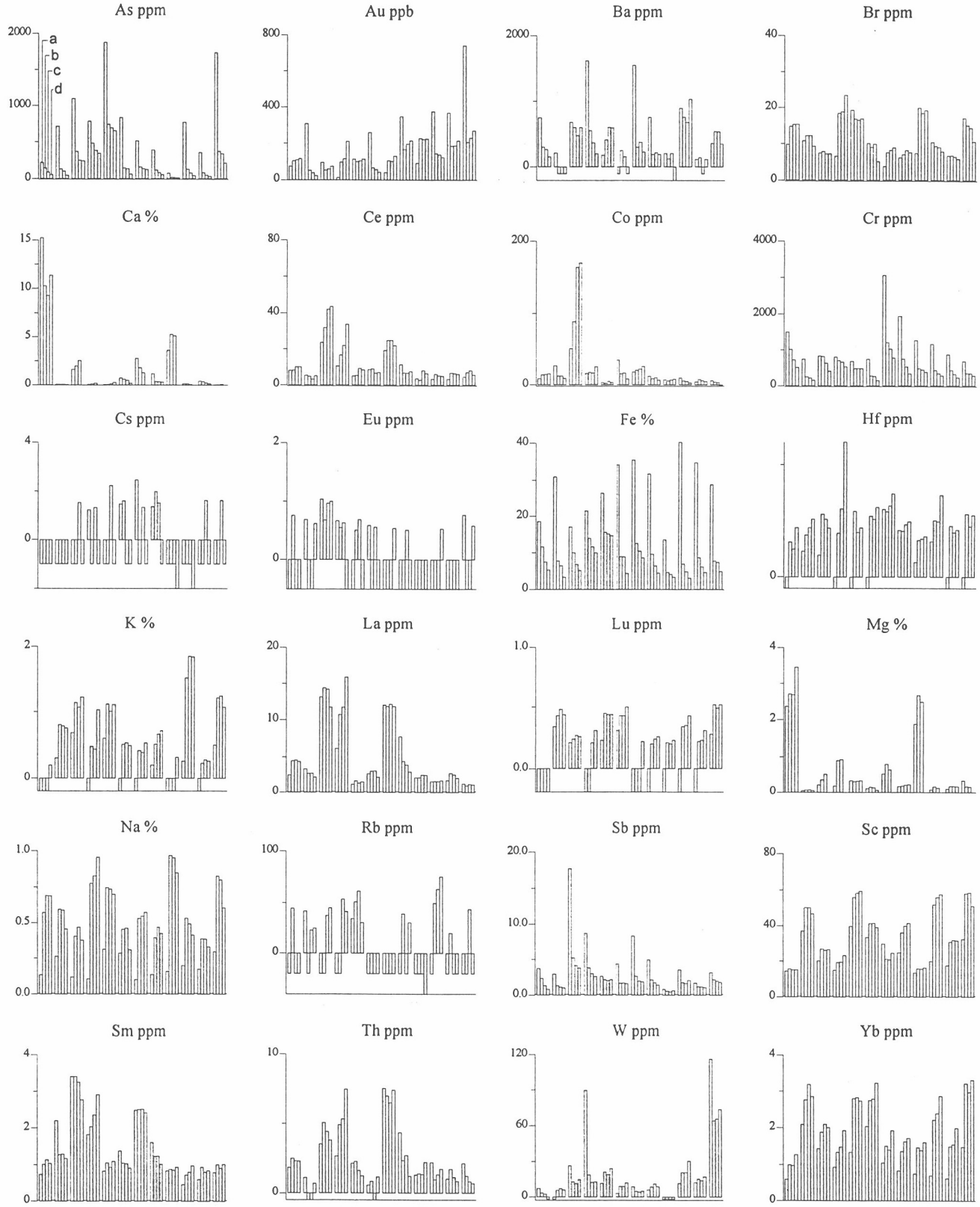

Figure A2.1: Elemental abundances for four size fractions from 12 Panglo samples with the highest Au contents.
Samples grouped into 4 size fractions and ranked according to bulk Au contents, highest Au content on right hand side.
a:+1000 µm; b: + 250 µm -1000 µm; c: - 250 µm +63 µm; d: -63 µm
For all samples Ag (5), Bi (1), Ir (0.02), Se (5), Ta (1) and U (2) were at or below detection (ppm) indicated in parentheses.
Insufficient -63µm fraction for some Ca and Mg analyses.

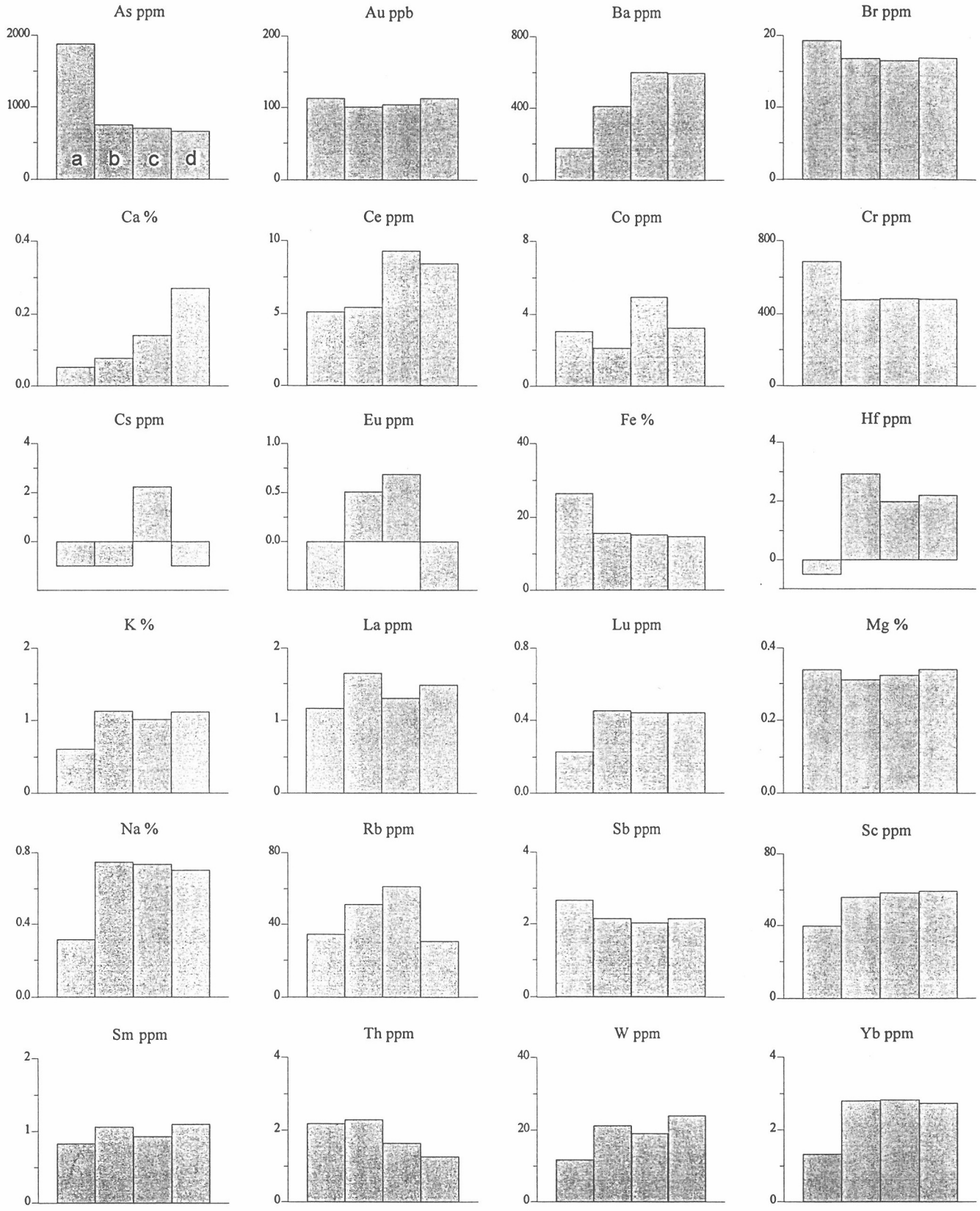

Figure A2.2.1: Elemental abundances for four size fractions from sample 09-3651 from Panglo.
a: +1000 µm; b: + 250 µm -1000 µm; c: - 250 µm +63 µm; d: -63 µm.
Negative data below detection.
For all samples Ag (5), Bi (1), Ir (0.02), Se (5), Ta (1), and U (2) below detection (ppm) indicated in parentheses.

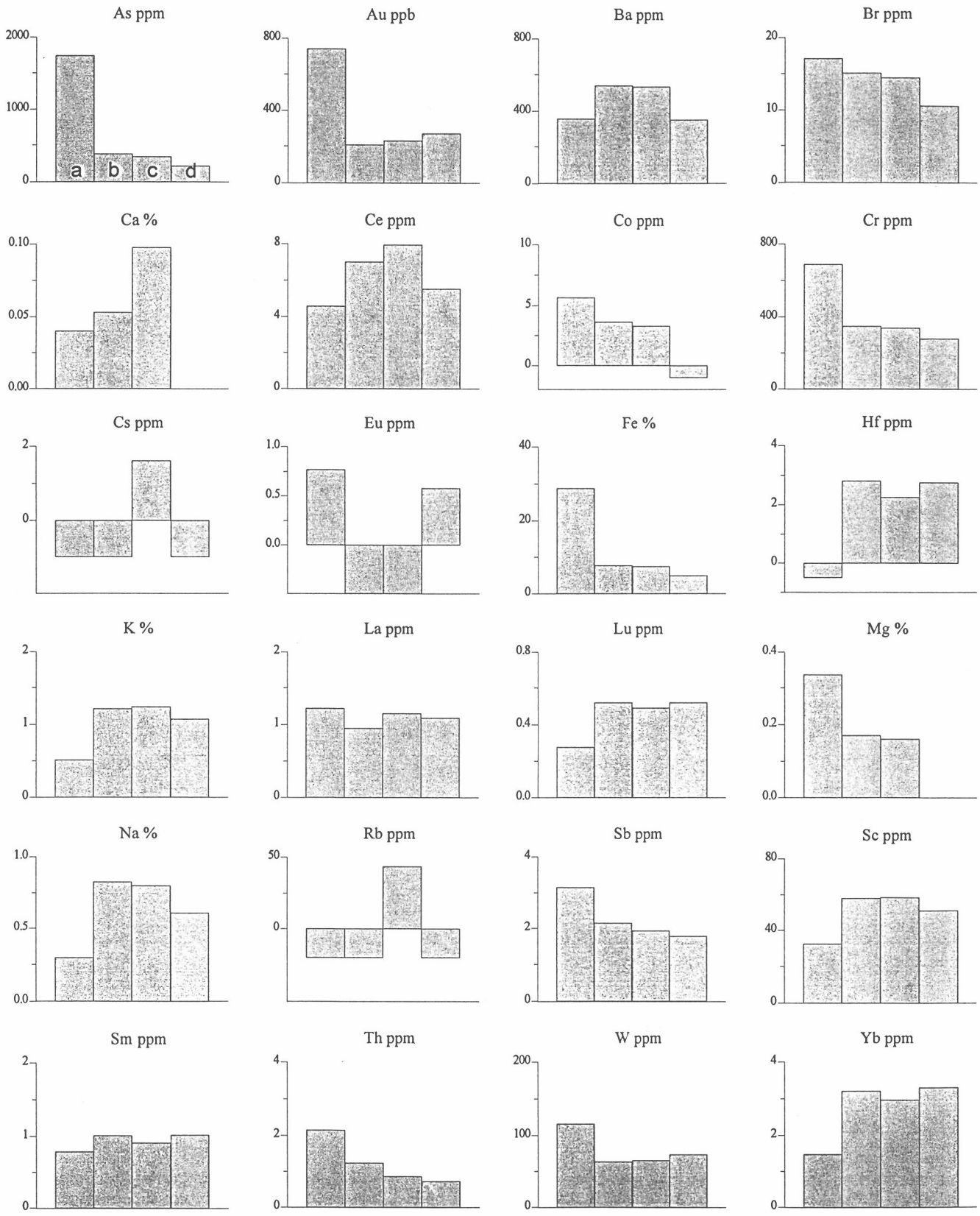

Figure A2.2.2: Elemental abundances for four size fractions from sample 09-3652 from Panglo.
a: +1000 μm; b: + 250 μm -1000 μm; c: - 250 μm +63 μm; d: -63 μm.
Negative data below detection. Insufficient sample for -63 μm Ca and Mg analyses.
For all samples Ag (5), Bi (1), Ir (0.02), Se (5), Ta (1), and U (2) below detection (ppm) indicated in parentheses.

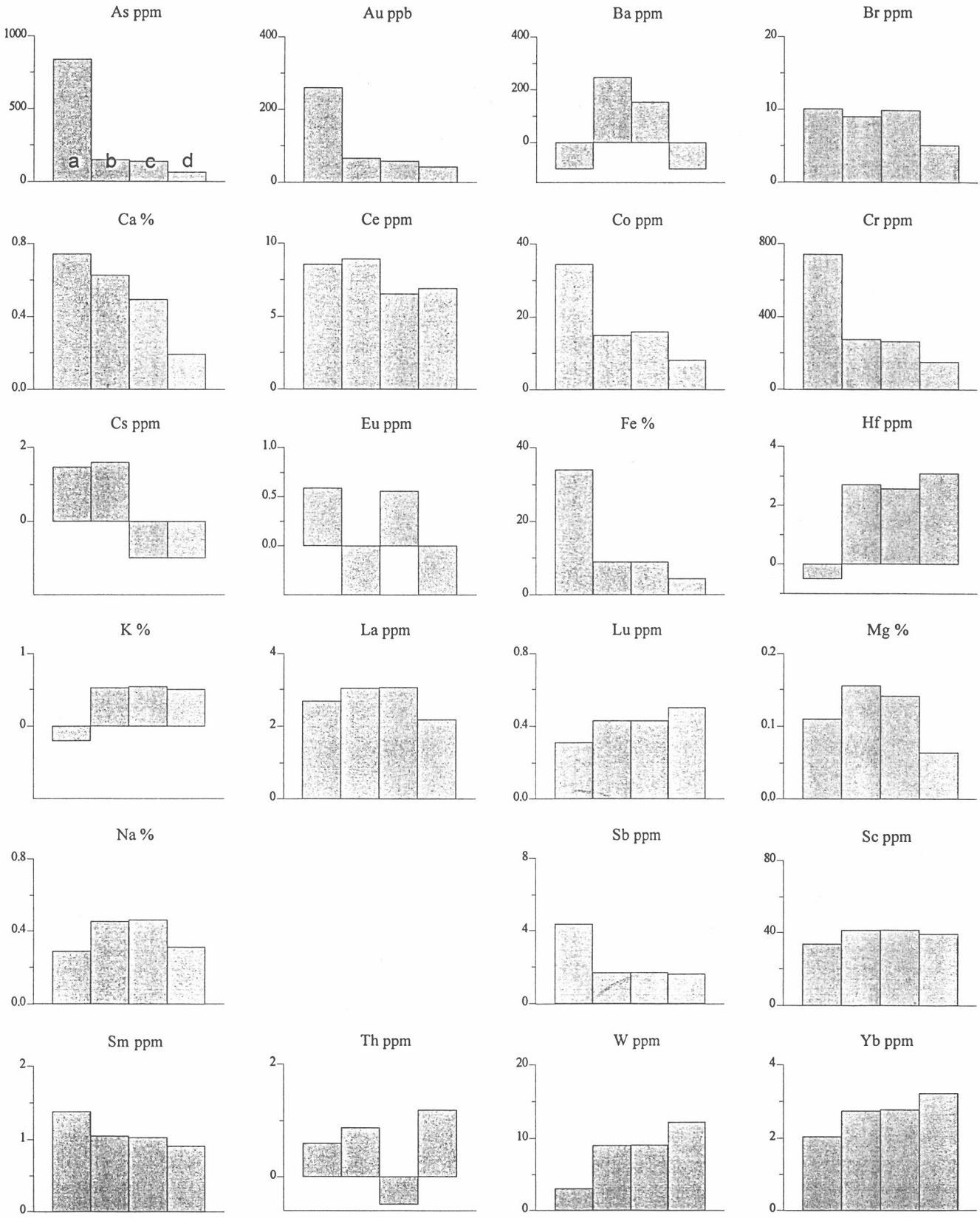

Figure A2.2.3: Elemental abundances for four size fractions from sample 09-3661 from Panglo.
a: +1000 µm; b: + 250 µm -1000 µm; c: - 250 µm +63 µm; d: -63 µm.
Negative data below detection.
For all samples Ag (5), Bi (1), Ir (0.02), Rb (20), Se (5), Ta (1), and U (2) below detection (ppm) indicated in parentheses.

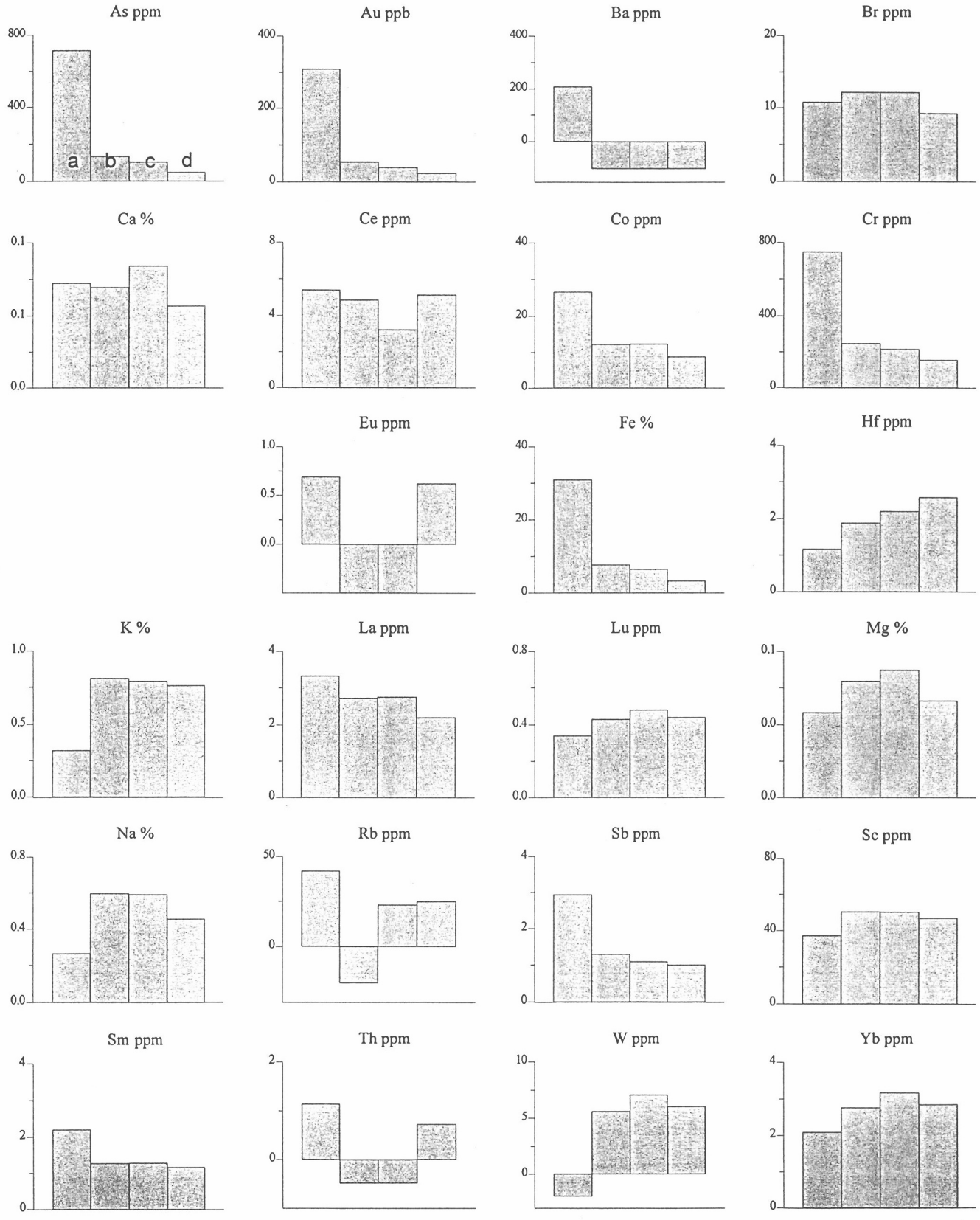

Figure A2.2.4: Elemental abundances for four size fractions from sample 09-3662 from Panglo.
a: +1000 µm; b: + 250 µm -1000 µm; c: - 250 µm +63 µm; d: -63 µm.
Negative data below detection.
For all samples Ag (5), Bi (1), Cs (1), Ir (0.02), Se (5), Ta (1), and U (2) below detection (ppm) indicated in parentheses.

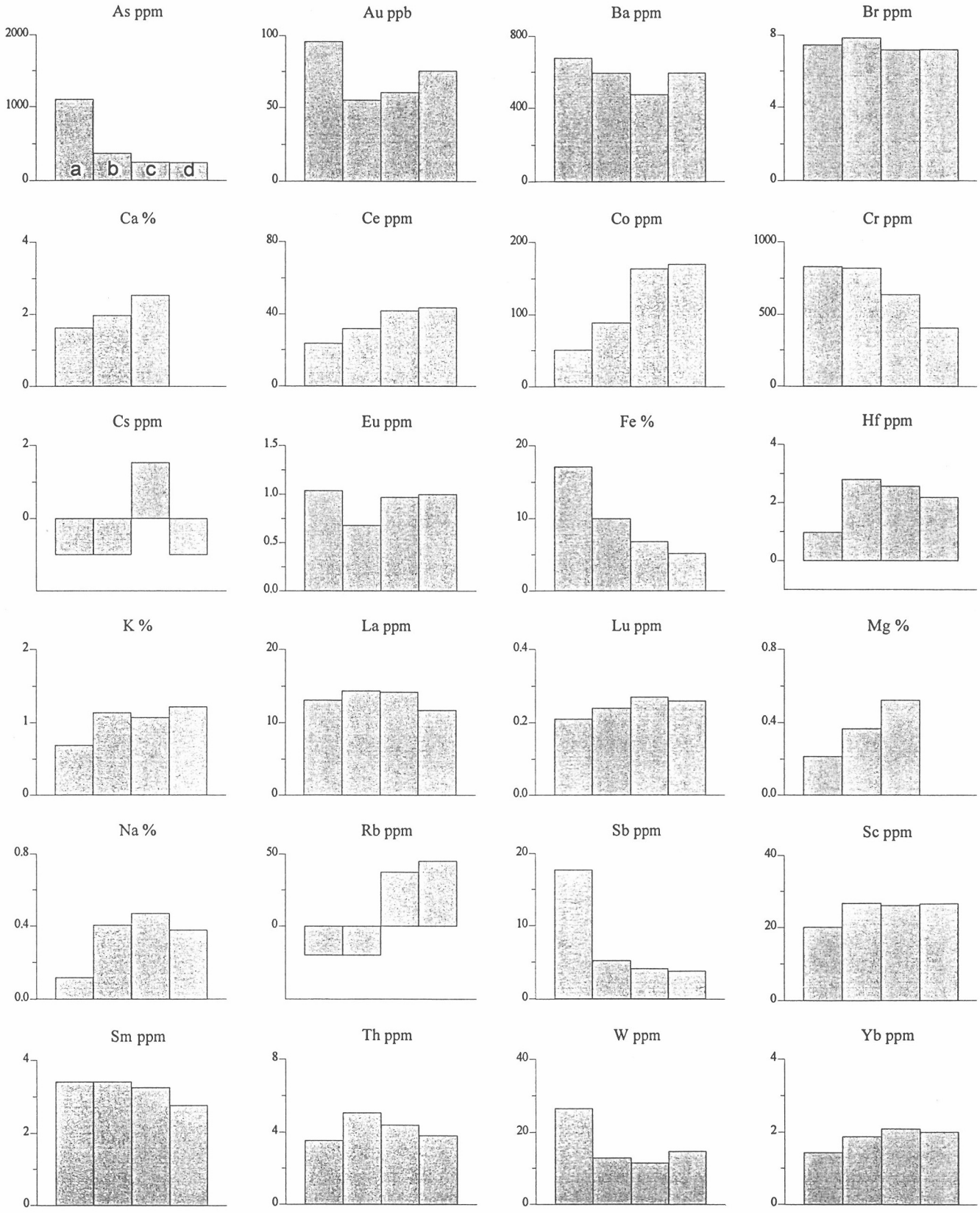

Figure A2.2.5: Elemental abundances for four size fractions from sample 09-3663 from Panglo.
a: +1000 µm; b: + 250 µm -1000 µm; c: - 250 µm +63 µm; d: -63 µm.
Negative data below detection. Insufficient sample for -63 µm Ca and Mg analyses.
For all samples Ag (5), Bi (1), Ir (0.02), Se (5), Ta (1), and U (2) below detection (ppm) indicated in parentheses.

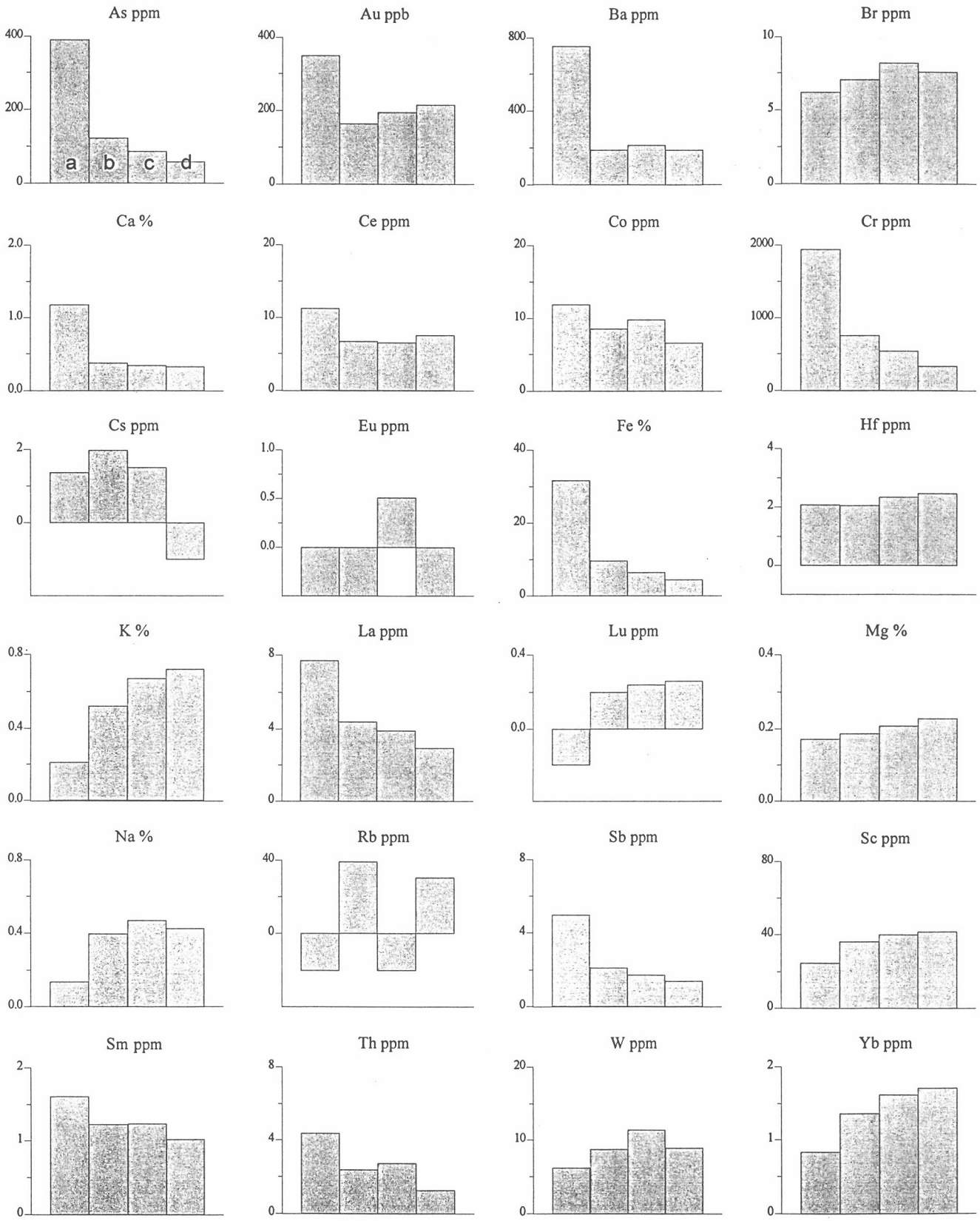

Figure A2.2.6: Elemental abundances for four size fractions from sample 09-3671 from Panglo.
a: +1000 µm; b: + 250 µm -1000 µm; c: - 250 µm +63 µm; d: -63 µm.
Negative data below detection.
For all samples Ag (5), Bi (1), Ir (0.02), Se (5), Ta (1), and U (2) below detection (ppm) indicated in parentheses.

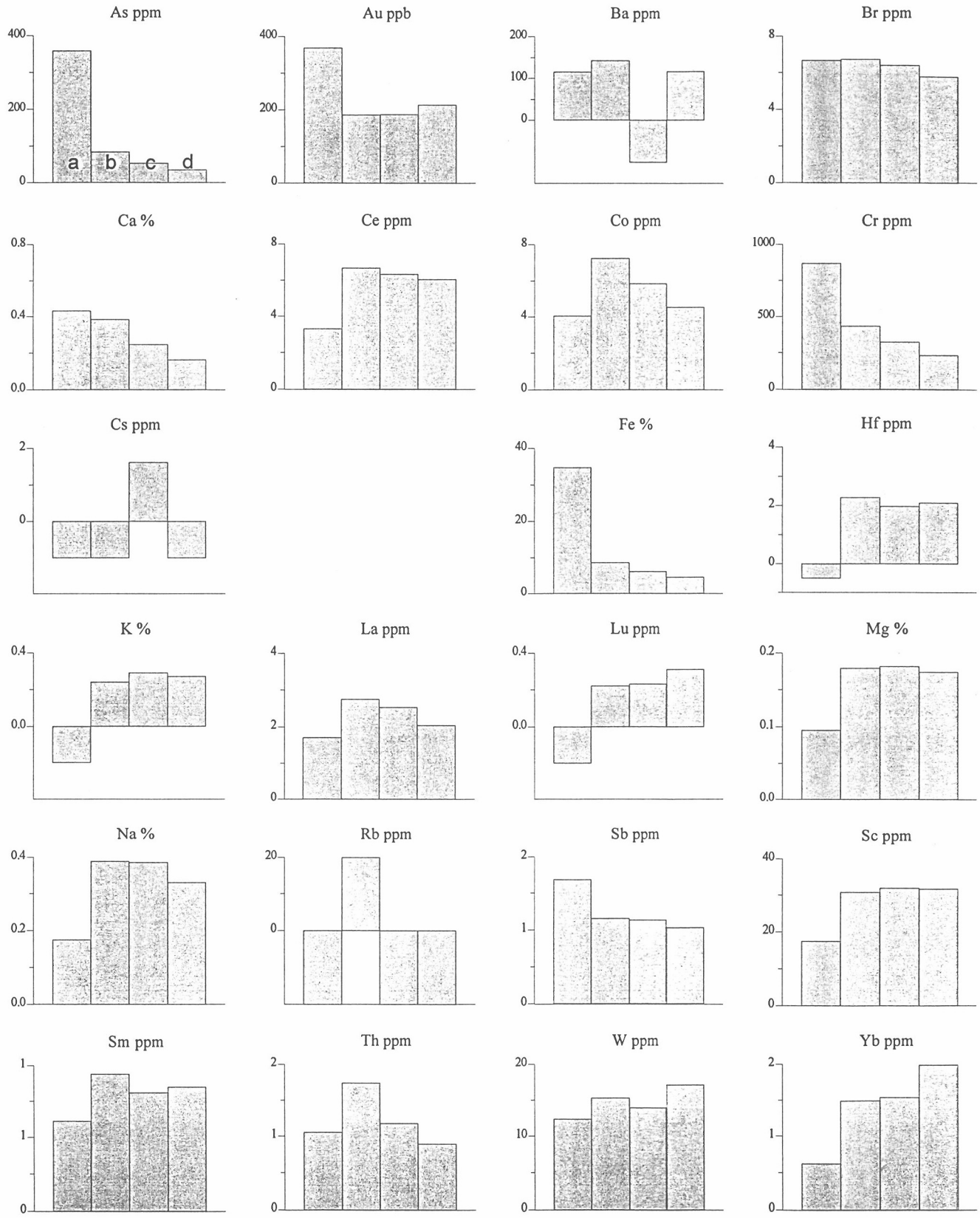

Figure A2.2.7: Elemental abundances for four size fractions from sample 09-3674 from Panglo.
a: +1000 µm; b: + 250 µm -1000 µm; c: - 250 µm +63 µm; d: -63 µm.
Negative data below detection.
For all samples Ag (5), Bi (1), Eu, (0.5), Ir (0.02), Se (5), Ta (1), and U (2) below detection (ppm) indicated in parentheses.

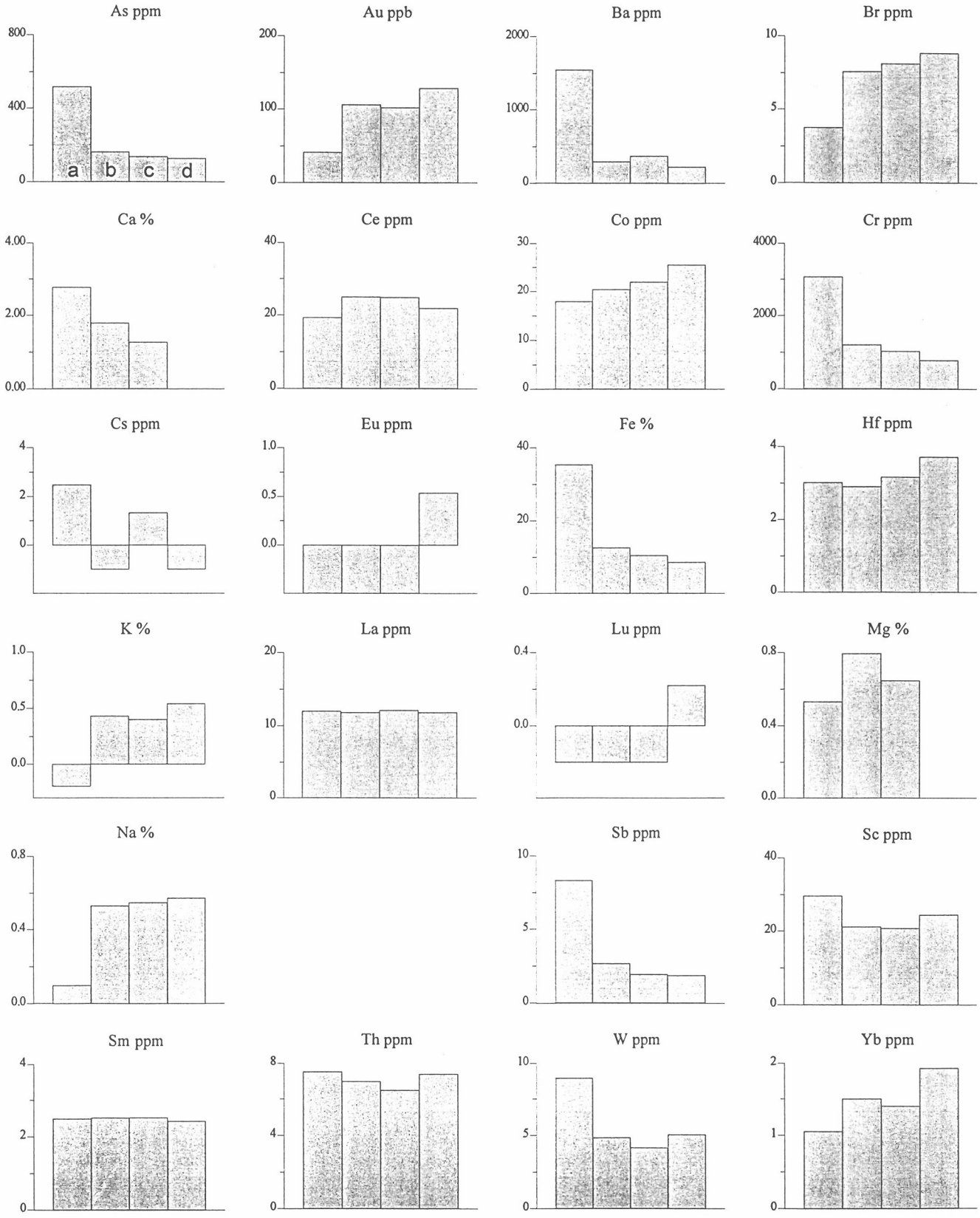

Figure A2.2.8: Elemental abundances for four size fractions from sample 09-3676 from Panglo.
a: +1000 µm; b: + 250 µm -1000 µm; c: - 250 µm +63 µm; d: -63 µm.
Negative data below detection. Insufficient sample for -63 µm Ca and Mg analyses.
For all samples Ag (5), Bi (1), Ir (0.02), Rb (20), Se (5), Ta (1), and U (2) below detection (ppm) indicated in parentheses.

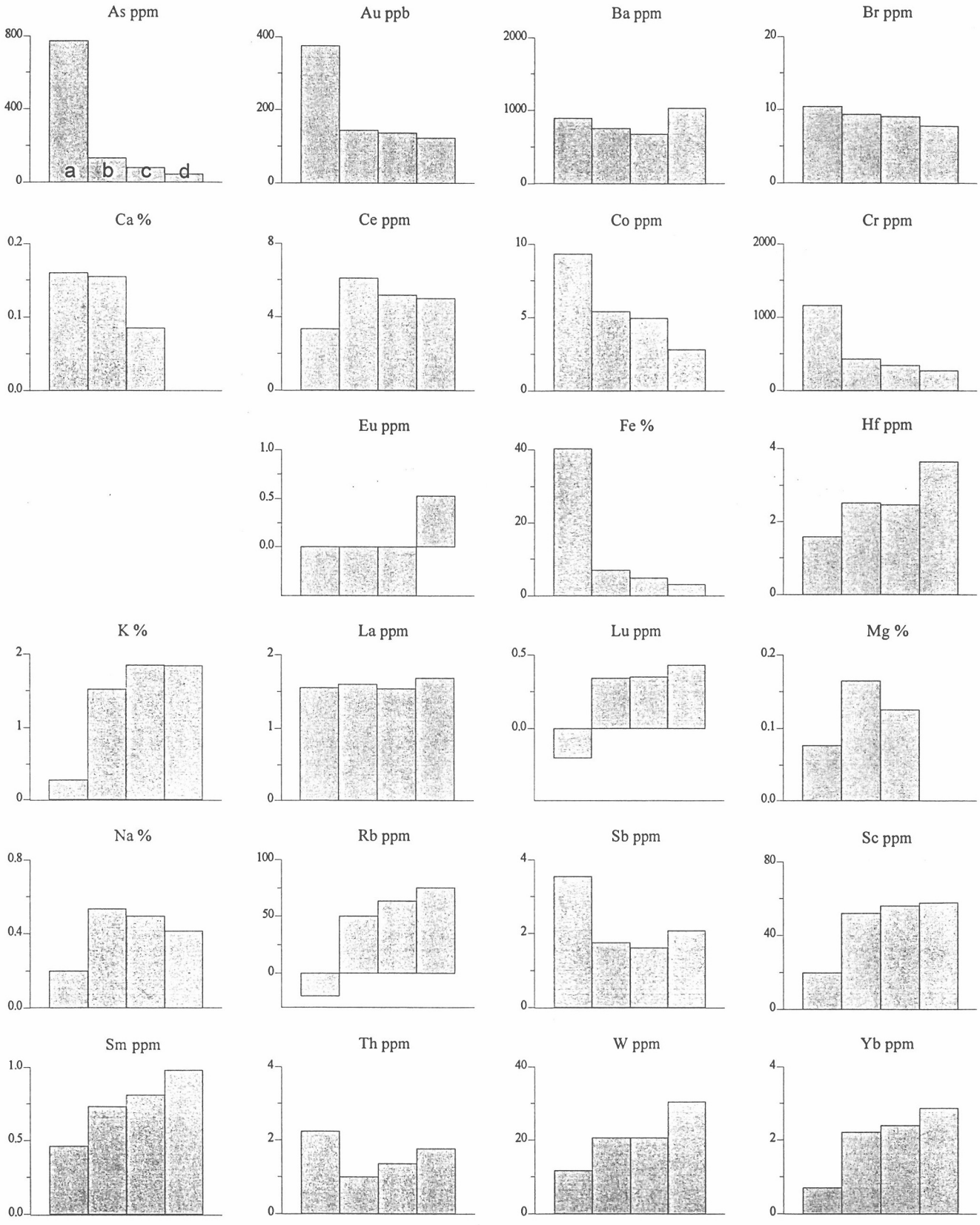

Figure A2.2.9: Elemental abundances for four size fractions from sample 09-3677 from Panglo.
a: +1000 μm; b: + 250 μm -1000 μm; c: - 250 μm +63 μm; d: -63 μm.
Negative data below detection. Insufficient sample for -63 μm Ca and Mg analyses.
For all samples Ag (5), Bi (1),Cs (2), Ir (0.02), Se (5), Ta (1), and U (2) below detection (ppm) indicated in parentheses.

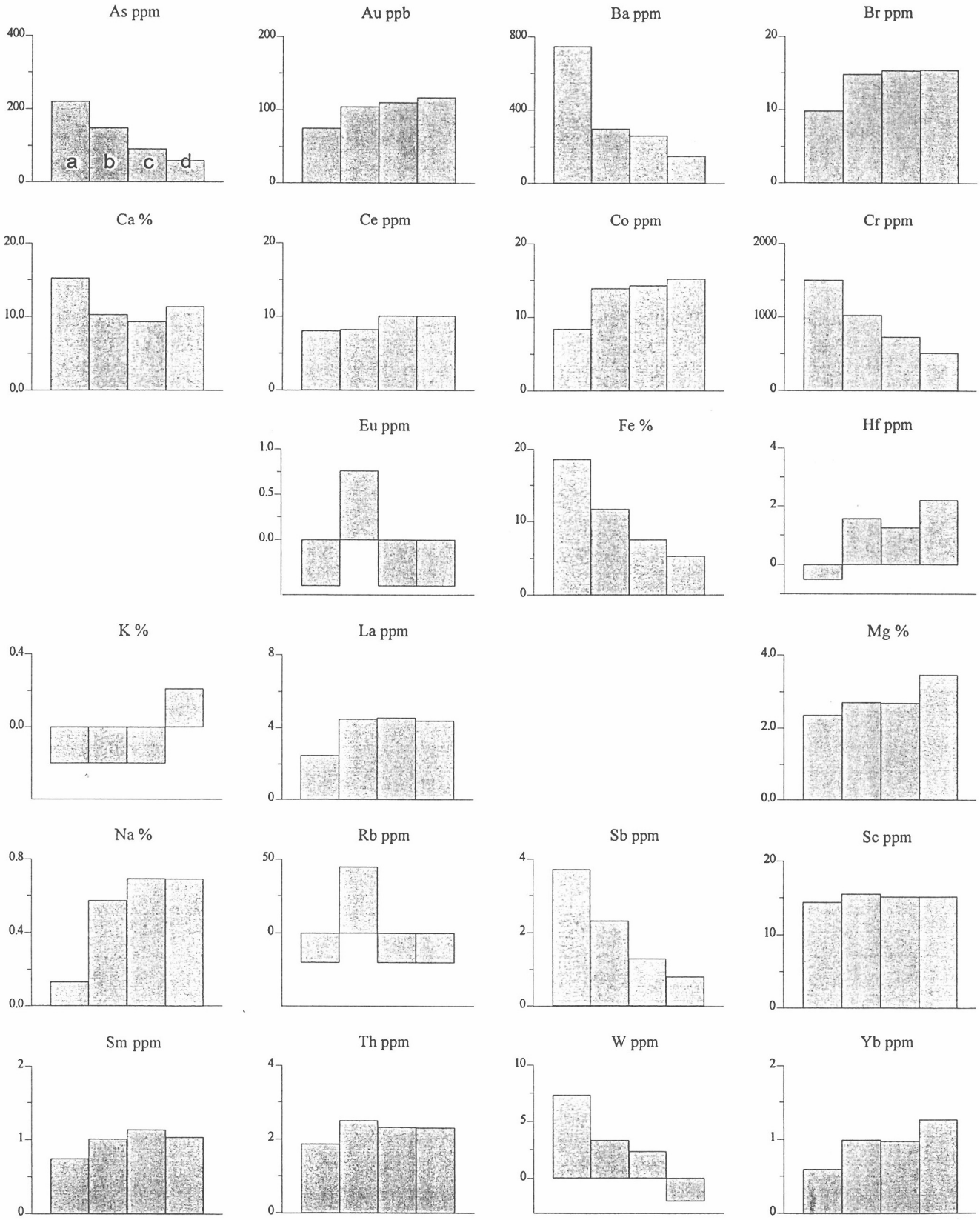

Figure A2.2.10: Elemental abundances for four size fractions from sample 09-3679 from Panglo.
a: +1000 µm; b: + 250 µm -1000 µm; c: - 250 µm +63 µm; d: -63 µm.
Negative data below detection.
For all samples Ag (5), Bi (1), Cs (1), Ir (0.02), Lu (0.2), Se (5), Ta (1), and U (2) below detection (ppm) indicated in parentheses.

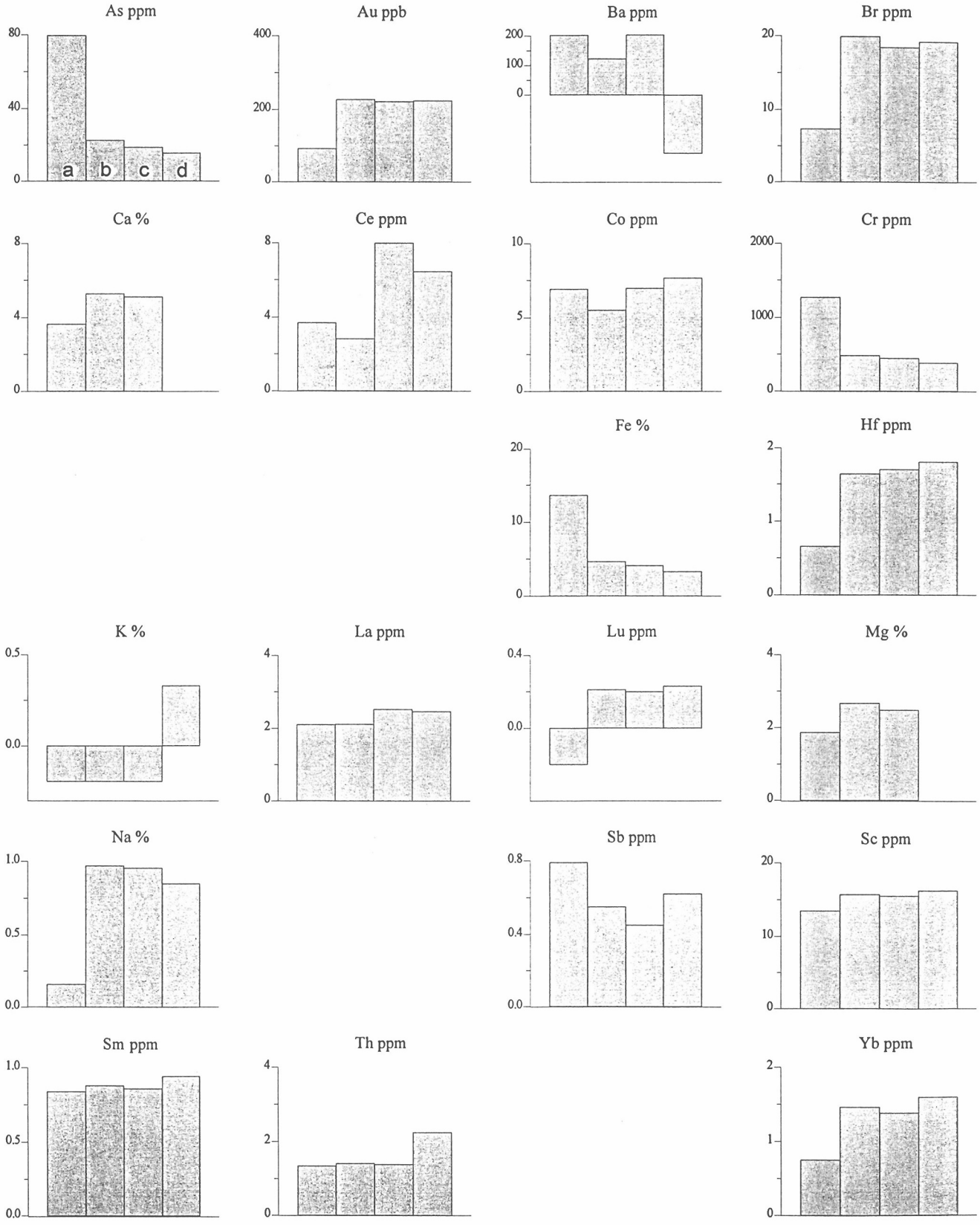

Figure A2.2.11: Elemental abundances for four size fractions from sample 09-3680 from Panglo.
a: +1000 µm; b: + 250 µm -1000 µm; c: - 250 µm +63 µm; d: -63 µm.
Negative data below detection. Insufficient sample for -63 µm Ca and Mg analyses.
For all samples Ag (5), Bi (1), Cs (2), Eu (0.5), Ir (0.02), Rb (20), Se (5), Ta (1), U (2) and W (2) below detection (ppm) indicated in parentheses.

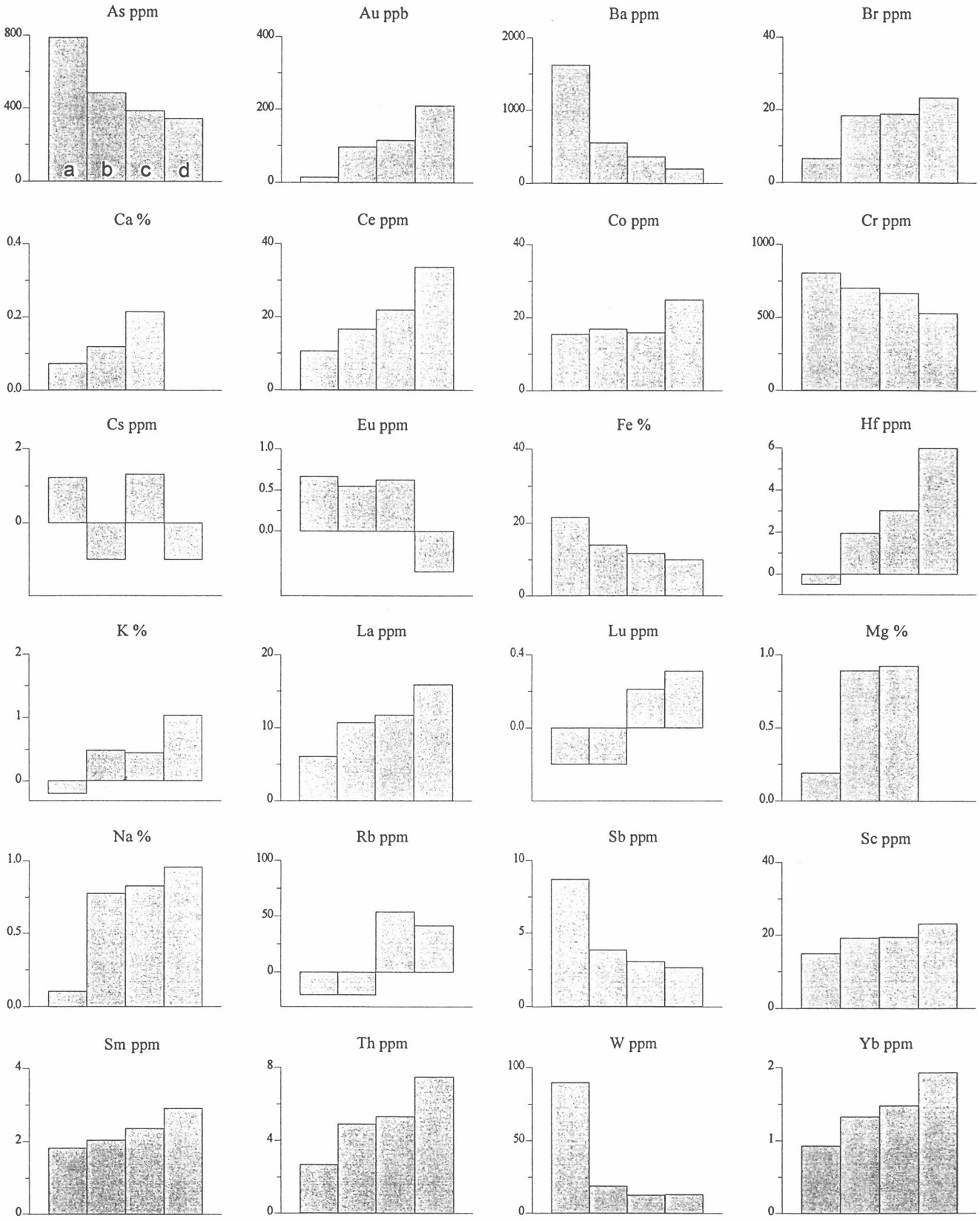

Figure A2.2.12: Elemental abundances for four size fractions from sample 09-3681 from Panglo.
a: +1000 µm; b: + 250 µm -1000 µm; c: - 250 µm +63 µm; d: -63 µm.
Negative data below detection. Insufficient sample for -63 µm Ca and Mg analyses.
For all samples Ag (5), Bi (1), Ir (0.02), Se (5), Ta (1), and U (2) below detection (ppm) indicated in parentheses.

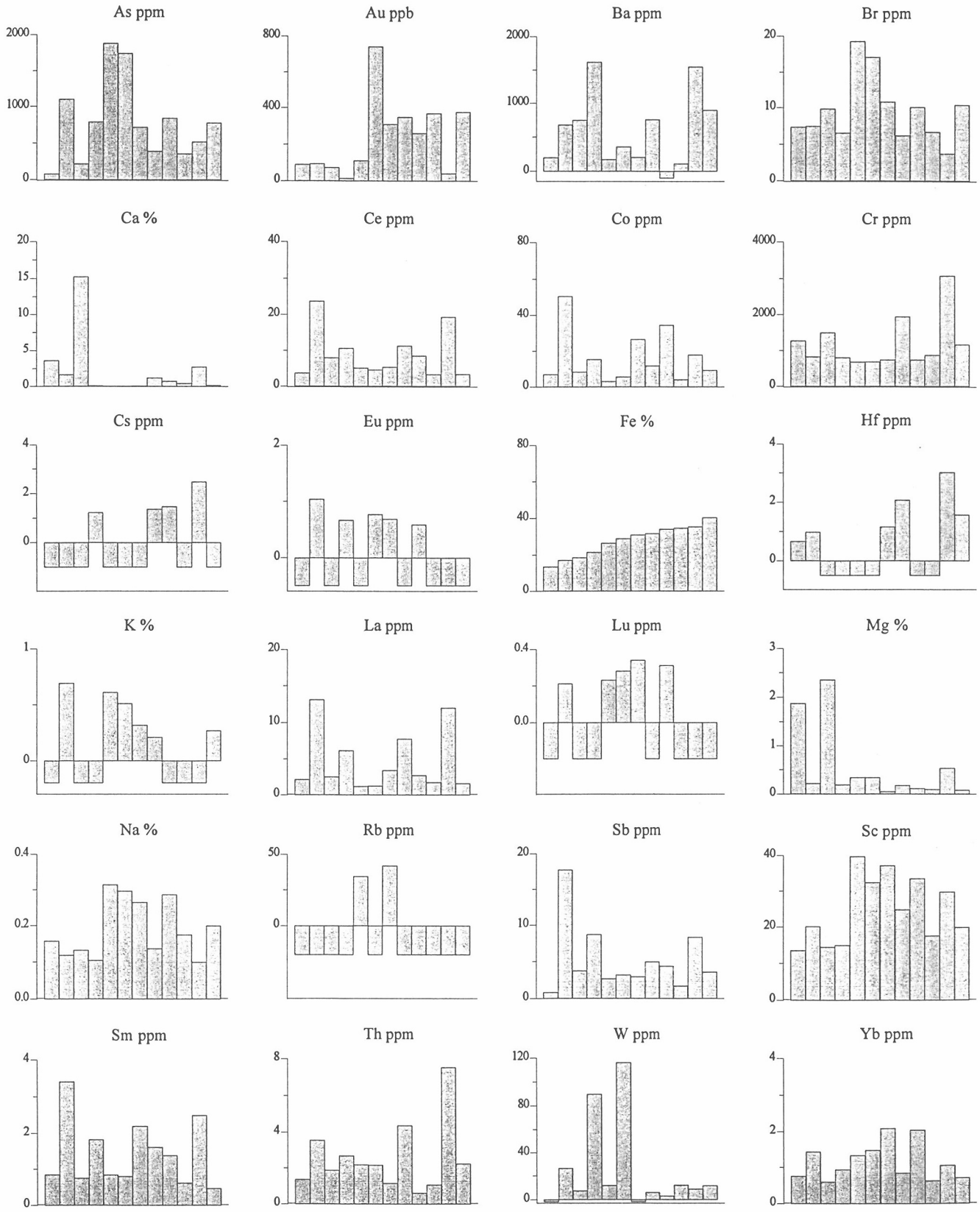

Figure A2.3.1: Elemental abundances for +1000 μm size fraction from Panglo (ranked by Fe concentration).
Negative data below detection.
For all samples Ag (5), Bi (1), Ir (0.02), Se (5), Ta (1) and U (2) below detection (ppm) indicated in parentheses.

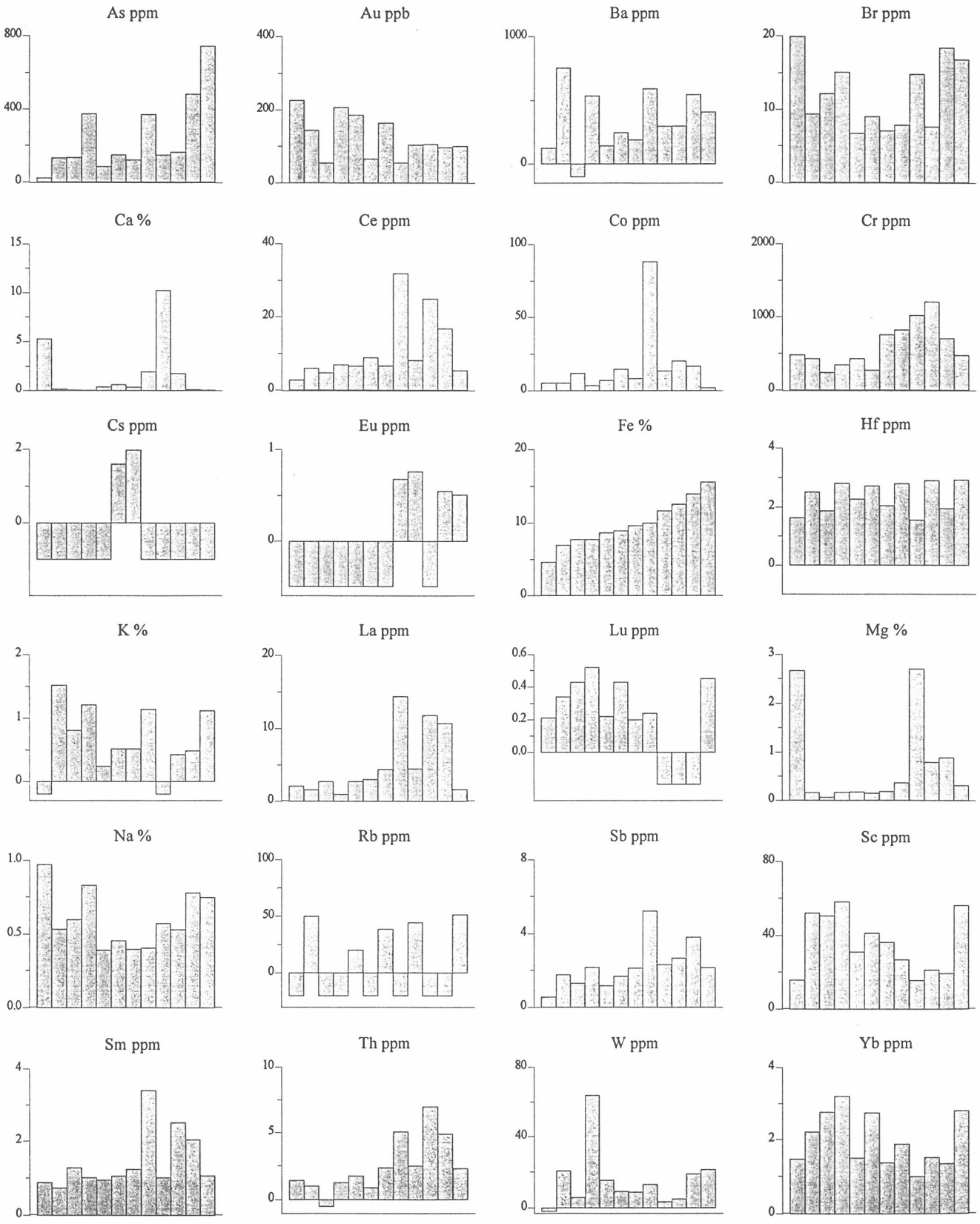

Figure A2.3.2: Elemental abundances for +250 µm -1000 µm size fraction from Panglo (ranked by Fe concentration).
Negative data below detection.
For all samples Ag (5), Bi (1), Ir (0.02), Se (5), Ta (1) and U (2) below detection (ppm) indicated in parentheses.

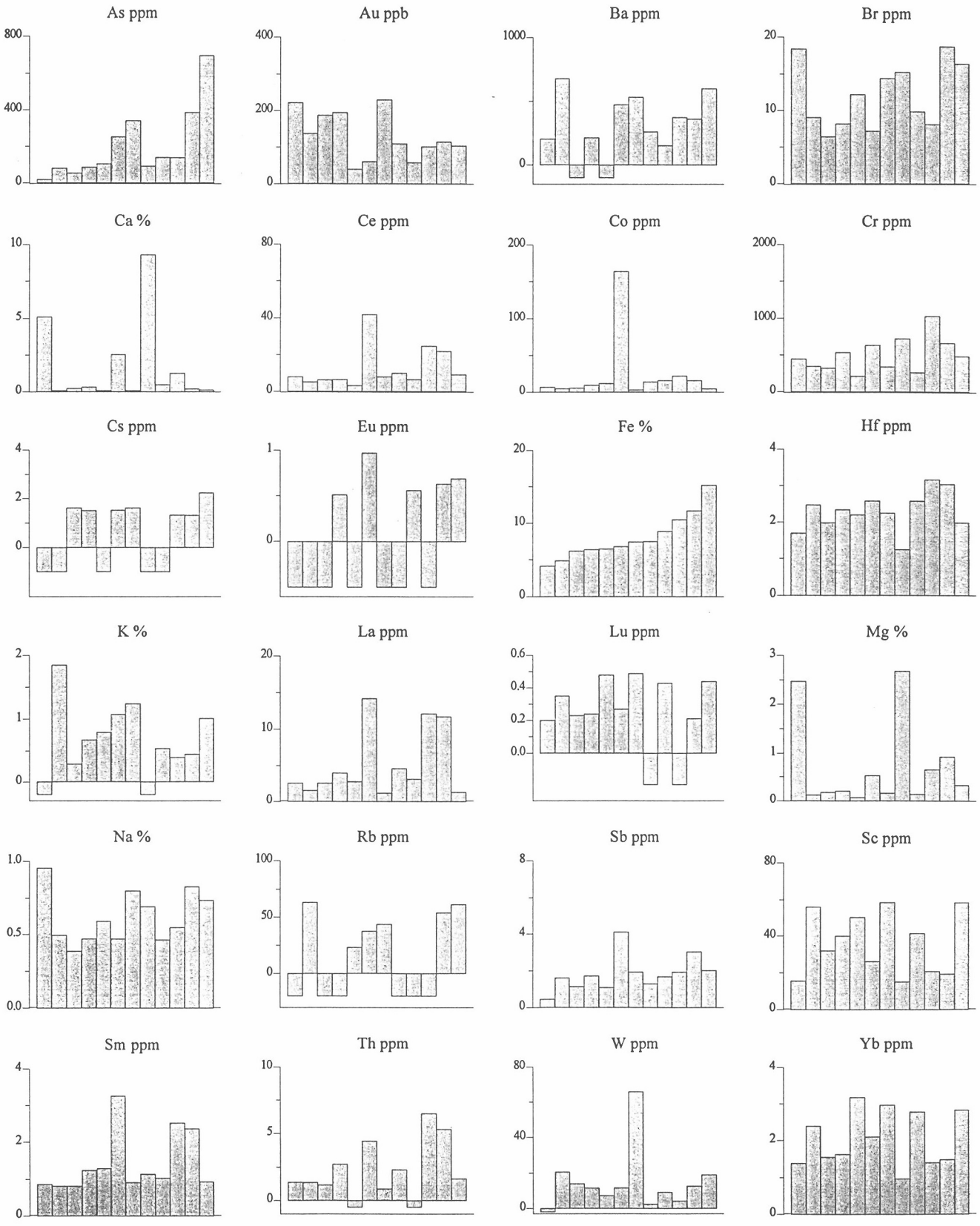

Figure A2.3.3: Elemental abundances for +63 μm -250 μm size fraction from Panglo (ranked by Fe concentration).
Negative data below detection.
For all samples Ag (5), Bi (1), Ir (0.02), Se (5), Ta (1) and U (2) below detection (ppm) indicated in parentheses.

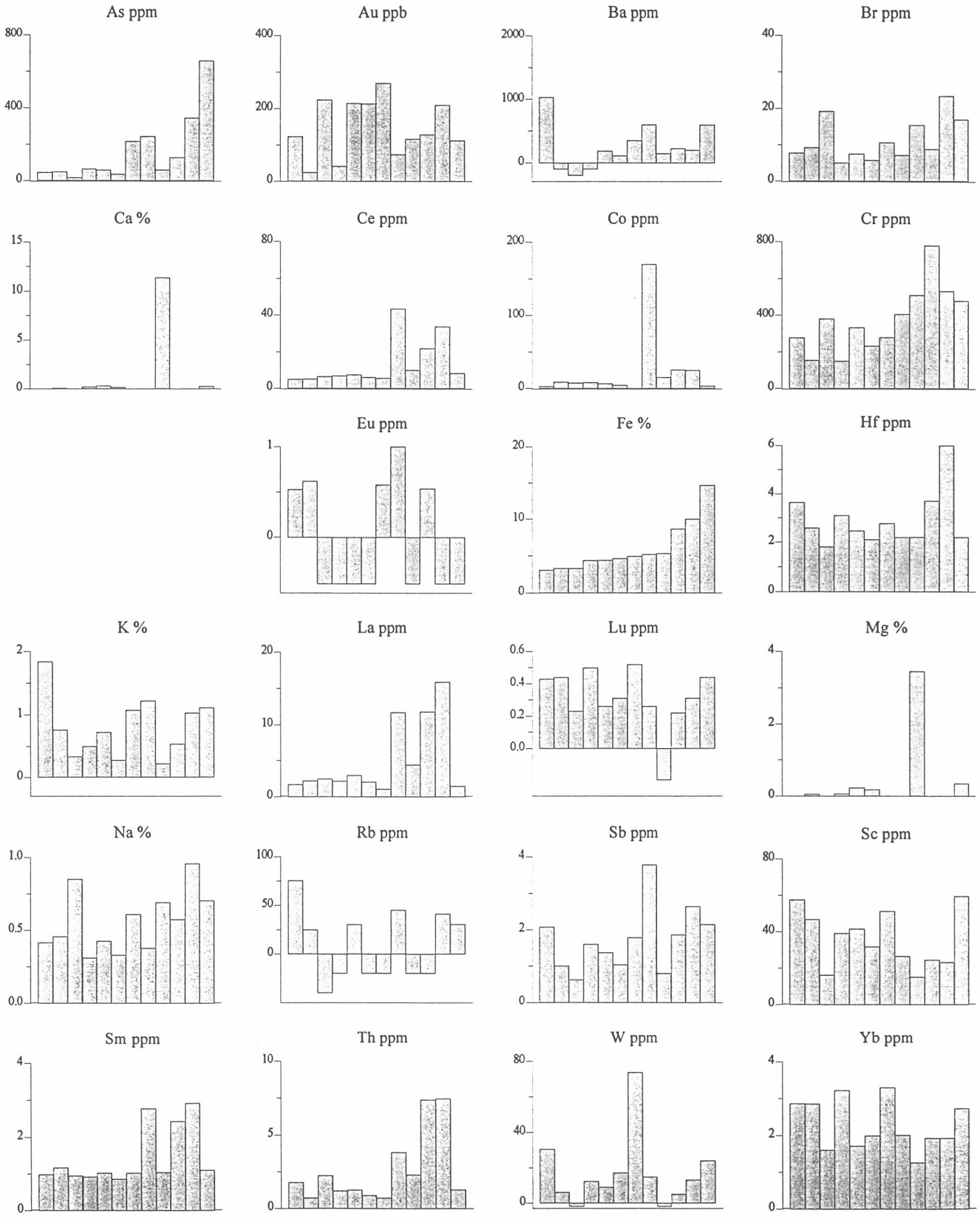

Figure A2.3.4: Elemental abundances for -63 µm size fraction from Panglo (ranked by Fe concentration).
Negative data below detection. Insufficient sample for some Ca and Mg analyses.
For all samples Ag (5), Bi (1), Cs (1), Ir (0.02), Se (5), Ta (1) and U (2) below detection (ppm) indicated in parentheses.

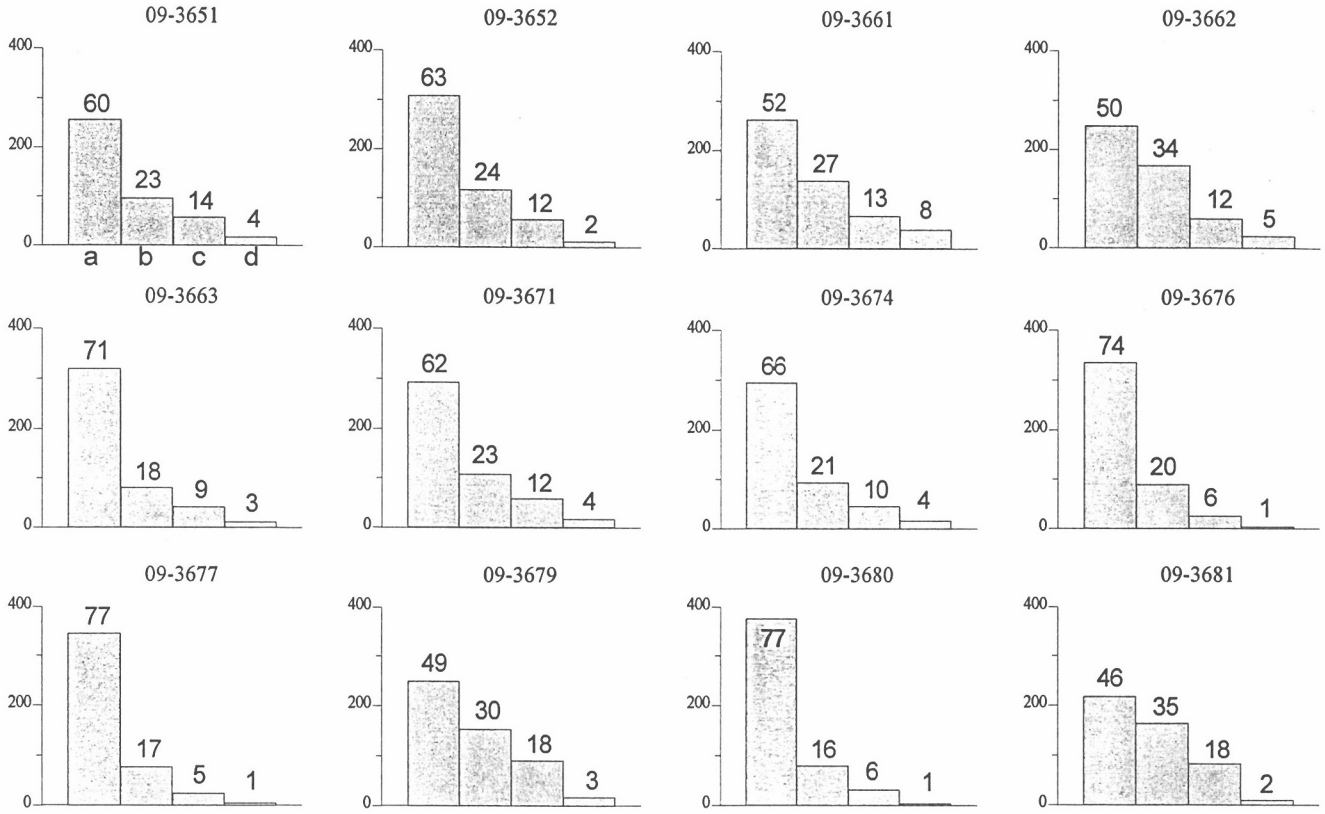

Figure A.2.4: Weights (histograms) and percentage (data) of four size fractions for 12 samples from Panglo a:+1000 µm; b: + 250 µm -1000 µm; c: - 250 µm +63 µm; d: -63 µm

		Table A2.5: Compiled analytical data for size fractions.						
		Negative data below detection.						
Sample	**Size fraction**	**N (AMG)**	**E (AMG)**	**from (m)**	**to (m)**	**Rotap wt(g**	**<1mm wet sieved (g**	**Sb (ppm)**
09-3651	+1mm	6621895	345187	0	1	256.3	185.8	2.66
09-3651	-1mm+250um	6621895	345187	0	1	96		2.14
09-3651	-250um+63um	6621895	345187	0	1	57.6		2.02
09-3651	-63um	6621895	345187	0	1	17.3		2.14
09-3652	+1mm	6621895	345187	1	2	308.6	259.7	3.15
09-3652	-1mm+250um	6621895	345187	1	2	116.8		2.15
09-3652	-250um+63um	6621895	345187	1	2	57.3		1.93
09-3652	-63um	6621895	345187	1	2	11.3		1.78
09-3661	+1mm	6621939	345104	1	2	262.6	83.2	4.35
09-3661	-1mm+250um	6621939	345104	1	2	138		1.67
09-3661	-250um+63um	6621939	345104	1	2	66.4		1.68
09-3661	-63um	6621939	345104	1	2	38.5		1.60
09-3662	+1mm	6621939	345104	2	3	249.1	157.3	2.93
09-3662	-1mm+250um	6621939	345104	2	3	168.2		1.29
09-3662	-250um+63um	6621939	345104	2	3	60.2		1.09
09-3662	-63um	6621939	345104	2	3	24.4		1.00
09-3663	+1mm	6621960	345074	0	1	320.8	178.0	17.70
09-3663	-1mm+250um	6621960	345074	0	1	80.4		5.19
09-3663	-250um+63um	6621960	345074	0	1	41.7		4.10
09-3663	-63um	6621960	345074	0	1	11.4		3.78
09-3671	+1mm	6621983	344989	0	1	292.9	199.7	4.95
09-3671	-1mm+250um	6621983	344989	0	1	107.7		2.12
09-3671	-250um+63um	6621983	344989	0	1	57.9		1.72
09-3671	-63um	6621983	344989	0	1	17		1.37
09-3674	+1mm	6622000	344977	0	1	294.8	193.2	1.68
09-3674	-1mm+250um	6622000	344977	0	1	93.1		1.15
09-3674	-250um+63um	6622000	344977	0	1	45.6		1.13
09-3674	-63um	6622000	344977	0	1	16.6		1.03
09-3676	+1mm	6621992	344947	1	2	336.7	258.2	8.31
09-3676	-1mm+250um	6621992	344947	1	2	89.1		2.66
09-3676	-250um+63um	6621992	344947	1	2	25.3		1.93
09-3676	-63um	6621992	344947	1	2	3.4		1.86
09-3677	+1mm	6621992	344947	2	3	345.7	252.3	3.55
09-3677	-1mm+250um	6621992	344947	2	3	76.2		1.75
09-3677	-250um+63um	6621992	344947	2	3	24.6		1.61
09-3677	-63um	6621992	344947	2	3	4.9		2.07
09-3679	+1mm	6621967	344920	1	2	249.4	103.4	3.70
09-3679	-1mm+250um	6621967	344920	1	2	153.9		2.31
09-3679	-250um+63um	6621967	344920	1	2	90.3		1.29
09-3679	-63um	6621967	344920	1	2	17		0.80
09-3680	+1mm	6621967	344920	1	2	376.5	333.6	0.79
09-3680	-1mm+250um	6621967	344920	1	2	79		0.55
09-3680	-250um+63um	6621967	344920	1	2	31.9		0.45
09-3680	-63um	6621967	344920	1	2	3.4		0.62
09-3681	+1mm	6621920	345228	0	0.6	217.5	174.8	8.69
09-3681	-1mm+250um	6621920	345228	0	0.6	164.1		3.81
09-3681	-250um+63um	6621920	345228	0	0.6	82.7		3.03
09-3681	-63um	6621920	345228	0	0.6	9.5		2.63

		Table A2:5 Compiled analytical data for size fractions (continued).							
Sample	**Size fraction**	**As (ppm)**	**Ba (ppm)**	**Br (ppm)**	**Ca %**	**Ce (ppm)**	**Cs (ppm)**	**Cr (ppm)**	**Co (ppm)**
09-3651	+1mm	1880.0	178.00	19.30	0.05	5.13	-1.0	686.00	3.06
09-3651	-1mm+250um	744.0	410.00	16.80	0.08	5.45	-1.0	478.00	2.11
09-3651	-250um+63um	696.0	601.00	16.50	0.14	9.29	2.2	484.00	4.94
09-3651	-63um	656.0	595.00	16.90	0.27	8.43	-1.0	480.00	3.25
09-3652	+1mm	1740.0	357.00	17.10	0.04	4.60	-1.0	690.00	5.66
09-3652	-1mm+250um	375.0	539.00	15.10	0.05	7.02	-1.0	349.00	3.64
09-3652	-250um+63um	340.0	534.00	14.40	0.10	7.95	1.6	339.00	3.28
09-3652	-63um	216.0	351.00	10.60	nd	5.54	-1.0	279.00	-1.00
09-3661	+1mm	839.0	-100.00	10.10	0.74	8.56	1.5	742.00	34.40
09-3661	-1mm+250um	149.0	247.00	8.99	0.63	8.93	1.6	276.00	15.00
09-3661	-250um+63um	139.0	154.00	9.86	0.50	6.53	-1.0	264.00	16.00
09-3661	-63um	64.2	-100.00	5.08	0.19	6.91	-1.0	150.00	8.11
09-3662	+1mm	715.0	208.00	10.80	0.07	5.39	-1.0	749.00	26.60
09-3662	-1mm+250um	135.0	-100.00	12.20	0.07	4.86	-1.0	246.00	12.20
09-3662	-250um+63um	104.0	-100.00	12.20	0.08	3.22	-1.0	214.00	12.30
09-3662	-63um	48.5	-100.00	9.30	0.06	5.12	-1.0	155.00	8.82
09-3663	+1mm	1100.0	678.00	7.45	1.62	23.70	-1.0	831.00	50.60
09-3663	-1mm+250um	371.0	596.00	7.85	1.97	31.90	-1.0	821.00	88.40
09-3663	-250um+63um	252.0	475.00	7.18	2.54	42.00	1.5	636.00	164.00
09-3663	-63um	244.0	597.00	7.21	nd	43.60	-1.0	405.00	170.00
09-3671	+1mm	390.0	754.00	6.18	1.18	11.30	1.4	1940.00	11.90
09-3671	-1mm+250um	122.0	189.00	7.04	0.38	6.70	2.0	754.00	8.56
09-3671	-250um+63um	85.9	214.00	8.18	0.34	6.52	1.5	538.00	9.81
09-3671	-63um	58.4	189.00	7.57	0.33	7.53	-1.0	332.00	6.59
09-3674	+1mm	359.0	115.00	6.68	0.43	3.30	-1.0	870.00	4.05
09-3674	-1mm+250um	84.7	143.00	6.74	0.38	6.68	-1.0	432.00	7.25
09-3674	-250um+63um	53.6	-100.00	6.41	0.25	6.34	1.6	323.00	5.86
09-3674	-63um	35.0	116.00	5.79	0.16	6.05	-1.0	232.00	4.54
09-3676	+1mm	518.0	1550.00	3.77	2.77	19.30	2.5	3070.00	17.90
09-3676	-1mm+250um	163.0	299.00	7.59	1.79	24.90	-1.0	1210.00	20.40
09-3676	-250um+63um	138.0	374.00	8.12	1.27	24.80	1.3	1030.00	22.00
09-3676	-63um	128.0	227.00	8.84	nd	21.90	-1.0	780.00	25.60
09-3677	+1mm	775.0	895.00	10.40	0.16	3.34	-1.0	1160.00	9.33
09-3677	-1mm+250um	132.0	756.00	9.35	0.16	6.10	-1.0	432.00	5.42
09-3677	-250um+63um	80.0	678.00	9.05	0.09	5.18	-1.0	345.00	4.97
09-3677	-63um	45.4	1030.00	7.83	nd	4.99	-2.0	278.00	2.82
09-3679	+1mm	220.0	746.00	9.85	15.25	8.02	-1.0	1500.00	8.35
09-3679	-1mm+250um	148.0	298.00	14.80	10.27	8.21	-1.0	1020.00	13.90
09-3679	-250um+63um	91.7	261.00	15.30	9.31	10.10	-1.0	729.00	14.30
09-3679	-63um	59.4	151.00	15.40	11.38	10.10	-1.0	510.00	15.20
09-3680	+1mm	79.6	202.00	7.33	3.65	3.70	-1.0	1270.00	6.90
09-3680	-1mm+250um	22.5	123.00	19.90	5.28	2.84	-1.0	483.00	5.52
09-3680	-250um+63um	18.8	204.00	18.40	5.12	8.00	-1.0	446.00	6.98
09-3680	-63um	15.7	-200.00	19.20	nd	6.45	-2.0	380.00	7.67
09-3681	+1mm	788.0	1620.00	6.56	0.07	10.60	1.2	807.00	15.50
09-3681	-1mm+250um	485.0	551.00	18.40	0.12	16.70	-1.0	703.00	17.00
09-3681	-250um+63um	385.0	362.00	18.80	0.22	22.00	1.3	669.00	16.00
09-3681	-63um	344.0	201.00	23.40	nd	33.70	-1.0	532.00	25.00

Table A2:5 Compiled analytical data for size fractions (continued).

Sample	Size fraction	Eu (ppm)	Au (ppb)	Hf (ppm)	Ir (ppb)	Fe (%)	La (ppm)	Lu (ppm)	Mg %
09-3651	+1mm	-0.5	113.00	-0.5	-20.00	26.40	1.16	0.2	0.34
09-3651	-1mm+250um	0.5	101.00	2.9	-20.00	15.60	1.65	0.5	0.31
09-3651	-250um+63um	0.7	104.00	2.0	-20.00	15.20	1.30	0.4	0.32
09-3651	-63um	-0.5	113.00	2.2	-20.00	14.70	1.48	0.4	0.34
09-3652	+1mm	0.8	742.00	-0.5	-20.00	28.80	1.22	0.3	0.34
09-3652	-1mm+250um	-0.5	207.00	2.8	-20.00	7.74	0.95	0.5	0.17
09-3652	-250um+63um	-0.5	230.00	2.3	-20.00	7.44	1.15	0.5	0.16
09-3652	-63um	0.6	270.00	2.8	-20.00	4.93	1.09	0.5	nd
09-3661	+1mm	0.6	260.00	-0.5	-20.00	34.10	2.68	0.3	0.11
09-3661	-1mm+250um	-0.5	66.30	2.7	-20.00	8.93	3.03	0.4	0.16
09-3661	-250um+63um	0.6	58.00	2.6	-20.00	8.89	3.06	0.4	0.14
09-3661	-63um	-0.5	42.30	3.1	-20.00	4.35	2.18	0.5	0.06
09-3662	+1mm	0.7	309.00	1.2	-20.00	30.90	3.33	0.3	0.05
09-3662	-1mm+250um	-0.5	54.20	1.9	-20.00	7.72	2.71	0.4	0.06
09-3662	-250um+63um	-0.5	40.10	2.2	-20.00	6.48	2.74	0.5	0.07
09-3662	-63um	0.6	24.40	2.6	-20.00	3.31	2.20	0.4	0.05
09-3663	+1mm	1.0	95.90	1.0	-20.00	17.10	13.10	0.2	0.22
09-3663	-1mm+250um	0.7	55.10	2.8	-20.00	10.00	14.40	0.2	0.37
09-3663	-250um+63um	1.0	60.50	2.6	-20.00	6.80	14.20	0.3	0.52
09-3663	-63um	1.0	75.60	2.2	-20.00	5.18	11.70	0.3	nd
09-3671	+1mm	-0.5	349.00	2.1	-20.00	31.60	7.71	-0.2	0.17
09-3671	-1mm+250um	-0.5	165.00	2.1	-20.00	9.63	4.39	0.2	0.19
09-3671	-250um+63um	0.5	195.00	2.3	-20.00	6.40	3.91	0.2	0.21
09-3671	-63um	-0.5	215.00	2.5	-20.00	4.41	2.96	0.3	0.23
09-3674	+1mm	-0.5	369.00	-0.5	-20.00	34.70	1.71	-0.2	0.10
09-3674	-1mm+250um	-0.5	186.00	2.3	-20.00	8.67	2.75	0.2	0.18
09-3674	-250um+63um	-0.5	187.00	2.0	-20.00	6.17	2.53	0.2	0.18
09-3674	-63um	-0.5	214.00	2.1	-20.00	4.64	2.04	0.3	0.17
09-3676	+1mm	-0.5	41.60	3.0	-20.00	35.40	12.00	-0.2	0.53
09-3676	-1mm+250um	-0.5	106.00	2.9	-20.00	12.60	11.80	-0.2	0.80
09-3676	-250um+63um	-0.5	102.00	3.2	-20.00	10.50	12.10	-0.2	0.65
09-3676	-63um	0.5	129.00	3.7	-20.00	8.63	11.80	0.2	nd
09-3677	+1mm	-0.5	376.00	1.6	-20.00	40.30	1.55	-0.2	0.08
09-3677	-1mm+250um	-0.5	144.00	2.5	-20.00	6.95	1.60	0.3	0.16
09-3677	-250um+63um	-0.5	137.00	2.5	-20.00	4.84	1.54	0.4	0.13
09-3677	-63um	0.5	123.00	3.7	-30.00	3.06	1.68	0.4	nd
09-3679	+1mm	-0.5	75.20	-0.5	-20.00	18.60	2.48	-0.2	2.35
09-3679	-1mm+250um	0.8	104.00	1.6	-20.00	11.70	4.48	-0.2	2.70
09-3679	-250um+63um	-0.5	110.00	1.3	-20.00	7.52	4.56	-0.2	2.68
09-3679	-63um	-0.5	117.00	2.2	-20.00	5.32	4.38	-0.2	3.46
09-3680	+1mm	-0.5	92.80	0.7	-20.00	13.60	2.10	-0.2	1.87
09-3680	-1mm+250um	-0.5	227.00	1.6	-20.00	4.62	2.11	0.2	2.66
09-3680	-250um+63um	-0.5	222.00	1.7	-20.00	4.11	2.52	0.2	2.47
09-3680	-63um	-0.5	224.00	1.8	-30.00	3.32	2.46	0.2	nd
09-3681	+1mm	0.7	14.40	-0.5	-20.00	21.50	6.14	-0.2	0.19
09-3681	-1mm+250um	0.6	97.10	2.0	-20.00	14.00	10.70	-0.2	0.89
09-3681	-250um+63um	0.6	115.00	3.0	-20.00	11.70	11.70	0.2	0.92
09-3681	-63um	-0.5	210.00	6.0	-20.00	10.00	15.90	0.3	nd

Table A2:5 Compiled analytical data for size fractions (continued).

Sample	Size fraction	Mo (ppm)	K (%)	Rb (ppm)	Sm (ppm)	Sc (ppm)	Se (ppm)	Ag (ppm)	Na (%)
09-3651	+1mm	-5.00	0.6	34.40	0.83	39.7	-5.0	-5.000	0.31
09-3651	-1mm+250um	-5.00	1.1	51.20	1.06	56.0	-5.0	-5.000	0.75
09-3651	-250um+63um	-5.00	1.0	61.30	0.93	58.4	-5.0	-5.000	0.74
09-3651	-63um	-5.00	1.1	30.50	1.10	59.4	-5.0	-5.000	0.70
09-3652	+1mm	-5.00	0.5	-20.00	0.79	32.4	-5.0	-5.000	0.30
09-3652	-1mm+250um	-5.00	1.2	-20.00	1.01	58.0	-5.0	-5.000	0.83
09-3652	-250um+63um	-5.00	1.2	43.60	0.91	58.5	-5.0	-5.000	0.80
09-3652	-63um	-5.00	1.1	-20.00	1.02	51.1	-5.0	-5.000	0.61
09-3661	+1mm	9.40	-0.2	-20.00	1.38	33.5	-5.0	-5.000	0.29
09-3661	-1mm+250um	-5.00	0.5	-20.00	1.05	41.3	-5.0	-5.000	0.45
09-3661	-250um+63um	-5.00	0.5	-20.00	1.03	41.4	-5.0	-5.000	0.46
09-3661	-63um	-5.00	0.5	-20.00	0.91	39.1	-5.0	-5.000	0.31
09-3662	+1mm	-5.00	0.3	41.90	2.20	37.1	-5.0	-5.000	0.26
09-3662	-1mm+250um	-5.00	0.8	-20.00	1.28	50.4	-5.0	-5.000	0.60
09-3662	-250um+63um	-5.00	0.8	23.00	1.29	50.2	-5.0	-5.000	0.59
09-3662	-63um	-5.00	0.8	24.80	1.17	46.7	-5.0	-5.000	0.46
09-3663	+1mm	-5.00	0.7	-20.00	3.41	20.1	-5.0	-5.000	0.12
09-3663	-1mm+250um	-5.00	1.1	-20.00	3.41	26.7	-5.0	-5.000	0.40
09-3663	-250um+63um	-5.00	1.1	37.50	3.25	26.1	-5.0	-5.000	0.47
09-3663	-63um	-5.00	1.2	45.10	2.77	26.5	-5.0	-5.000	0.38
09-3671	+1mm	-5.00	0.2	-20.00	1.61	24.8	-5.0	-5.000	0.14
09-3671	-1mm+250um	-5.00	0.5	39.10	1.23	36.2	-5.0	-5.000	0.40
09-3671	-250um+63um	-5.00	0.7	-20.00	1.24	39.9	-5.0	-5.000	0.47
09-3671	-63um	-5.00	0.7	30.40	1.02	41.5	-5.0	-5.000	0.43
09-3674	+1mm	-5.00	-0.2	-20.00	0.61	17.5	-5.0	-5.000	0.17
09-3674	-1mm+250um	-5.00	0.2	20.00	0.94	30.8	-5.0	-5.000	0.39
09-3674	-250um+63um	-5.00	0.3	-20.00	0.81	31.9	-5.0	-5.000	0.39
09-3674	-63um	-5.00	0.3	-20.00	0.85	31.7	-5.0	-5.000	0.33
09-3676	+1mm	-5.00	-0.2	-20.00	2.49	29.7	-5.0	-5.000	0.10
09-3676	-1mm+250um	-5.00	0.4	-20.00	2.51	21.2	-5.0	-5.000	0.53
09-3676	-250um+63um	-5.00	0.4	-20.00	2.52	20.8	-5.0	-5.000	0.55
09-3676	-63um	-5.00	0.5	-20.00	2.42	24.5	-5.0	-5.000	0.57
09-3677	+1mm	-5.00	0.3	-20.00	0.46	19.8	-5.0	-5.000	0.20
09-3677	-1mm+250um	-5.00	1.5	49.80	0.73	52.0	-5.0	-5.000	0.53
09-3677	-250um+63um	-5.00	1.9	63.20	0.81	55.9	-5.0	-5.000	0.49
09-3677	-63um	-5.00	1.8	75.20	0.98	57.5	-10.0	-10.000	0.41
09-3679	+1mm	-5.00	-0.2	-20.00	0.74	14.4	-5.0	-5.000	0.13
09-3679	-1mm+250um	-5.00	-0.2	44.60	1.01	15.5	-5.0	-5.000	0.57
09-3679	-250um+63um	-5.00	-0.2	-20.00	1.14	15.1	-5.0	-5.000	0.69
09-3679	-63um	-5.00	0.2	-20.00	1.04	15.1	-5.0	-5.000	0.69
09-3680	+1mm	-5.00	-0.2	-20.00	0.84	13.5	-5.0	-5.000	0.16
09-3680	-1mm+250um	-5.00	-0.2	-20.00	0.88	15.7	-5.0	-5.000	0.97
09-3680	-250um+63um	-5.00	-0.2	-20.00	0.86	15.5	-5.0	-5.000	0.95
09-3680	-63um	-5.00	0.3	-40.00	0.94	16.2	-10.0	-10.000	0.85
09-3681	+1mm	-5.00	-0.2	-20.00	1.82	14.9	-5.0	-5.000	0.10
09-3681	-1mm+250um	-5.00	0.5	-20.00	2.04	19.2	-5.0	-5.000	0.78
09-3681	-250um+63um	-5.00	0.5	53.70	2.36	19.4	-5.0	-5.000	0.83
09-3681	-63um	-5.00	1.0	41.30	2.91	23.1	-5.0	-5.000	0.96

		Table A2:5 Compiled analytical data for size fractions (continued).					
Sample	**Size fraction**	**Ta (ppm)**	**Th (ppm)**	**W (ppm)**	**U (ppm)**	**Yb (ppm)**	**Zn (ppm)**
09-3651	+1mm	-1.00	2.18	11.80	-2.00	1.3	197
09-3651	-1mm+250um	1.21	2.29	21.20	-2.00	2.8	246
09-3651	-250um+63um	-1.00	1.64	19.00	-2.00	2.8	210
09-3651	-63um	-1.00	1.27	23.90	-2.00	2.7	234
09-3652	+1mm	-1.00	2.15	116.00	-2.00	1.5	226
09-3652	-1mm+250um	-1.00	1.24	63.90	-2.00	3.2	137
09-3652	-250um+63um	1.14	0.86	65.70	-2.00	3.0	238
09-3652	-63um	1.08	0.72	73.70	-2.00	3.3	222
09-3661	+1mm	1.09	0.60	3.01	-2.00	2.0	149
09-3661	-1mm+250um	-1.00	0.88	9.02	-2.00	2.7	141
09-3661	-250um+63um	-1.00	-0.50	9.07	-2.00	2.8	160
09-3661	-63um	1.08	1.19	12.20	-2.00	3.2	128
09-3662	+1mm	-1.00	1.14	-2.00	-2.00	2.1	147
09-3662	-1mm+250um	-1.00	-0.50	5.60	-2.00	2.8	175
09-3662	-250um+63um	1.21	-0.50	7.07	-2.00	3.2	215
09-3662	-63um	-1.00	0.72	6.02	-2.00	2.9	129
09-3663	+1mm	-1.00	3.53	26.50	-2.00	1.4	104
09-3663	-1mm+250um	-1.00	5.07	12.90	-2.00	1.9	145
09-3663	-250um+63um	-1.00	4.41	11.50	-2.00	2.1	161
09-3663	-63um	-1.00	3.81	14.70	-2.00	2.0	136
09-3671	+1mm	-1.00	4.35	6.16	-2.00	0.8	107
09-3671	-1mm+250um	-1.00	2.37	8.69	-2.00	1.4	121
09-3671	-250um+63um	-1.00	2.72	11.40	-2.00	1.6	170
09-3671	-63um	-1.00	1.25	8.86	-2.00	1.7	153
09-3674	+1mm	-1.00	1.05	12.30	2.54	0.6	-100
09-3674	-1mm+250um	1.10	1.74	15.30	-2.00	1.5	123
09-3674	-250um+63um	-1.00	1.17	13.90	-2.00	1.5	145
09-3674	-63um	-1.00	0.89	17.10	-2.00	2.0	142
09-3676	+1mm	-1.00	7.52	8.95	-2.00	1.1	-100
09-3676	-1mm+250um	-1.00	6.98	4.82	-2.00	1.5	140
09-3676	-250um+63um	-1.00	6.48	4.15	-2.00	1.4	164
09-3676	-63um	2.52	7.39	5.03	-2.00	1.9	302
09-3677	+1mm	-1.00	2.23	11.70	3.35	0.7	-100
09-3677	-1mm+250um	-1.00	0.99	20.60	-2.00	2.2	171
09-3677	-250um+63um	-1.00	1.36	20.60	-2.00	2.4	184
09-3677	-63um	-2.00	1.76	30.40	-2.00	2.9	230
09-3679	+1mm	-1.00	1.86	7.29	2.02	0.6	-100
09-3679	-1mm+250um	-1.00	2.49	3.33	-2.00	1.0	102
09-3679	-250um+63um	1.03	2.32	2.32	-2.00	1.0	130
09-3679	-63um	-1.00	2.30	-2.00	-2.00	1.3	107
09-3680	+1mm	-1.00	1.34	-2.00	-2.00	0.8	-100
09-3680	-1mm+250um	-1.00	1.41	-2.00	-2.00	1.5	-100
09-3680	-250um+63um	1.49	1.38	-2.00	-2.00	1.4	-100
09-3680	-63um	-2.00	2.24	-2.00	-2.00	1.6	170
09-3681	+1mm	-1.00	2.67	89.50	-2.00	0.9	212
09-3681	-1mm+250um	1.00	4.90	18.80	-2.00	1.3	178
09-3681	-250um+63um	-1.00	5.32	12.50	-2.00	1.5	177
09-3681	-63um	2.64	7.46	13.00	-2.00	1.9	220

Table A2.6: Descriptive notes taken during microscopic examination of polished mounts of selected high Au content samples from Panglo.

Sample	Descriptive notes	Au (ppb)
108105A	3 pieces on 3 polished sections.	950
	(i) Complex. Tourmaline crystals (some split). Talc schist structures. Y grains in veinlet. Slugs of Ba and S (barite) in cavities.	
	(ii) ?Mafic. Tourmaline veining of ultramafic which has been ferruginized. Quite complex secondary Fe oxides. Veining by goethite. Dissolution and filling of channels by various Fe oxides (?root structures). > 2 episodes of ferruginization of talcose ultramafic. Pb, Cu and Fe grain. Pb grain.	
	(iii) Fine grained clays. Hematite and goethite stained talc. Ultramafic. ?volcanic. Slugs of Ba and S (barite) in cavities.	
09-3652Fe	5 pieces.	740
	Clay structures larger than for 09-3662Fe. Accordion structures. Quartz and clays. Fe oxides principally goethite. Probably mafic. Zr grain; 3 Y grains;	
09-3662Fe	7 pieces on 2 polished sections.	310
	(B) Mafic to ultramafic. Quartz, clays. Stumpy accordion structures. Goethites. Layer silicates (probably clays). ?Kaolinite. No veining. 2 Au grains in micro-breccia.	
	(A) Mafics. Similar to B. Cu grain; many Y grains.	
09-3671Fe	5 pieces. (Pieces 5 and 3: sediments, granular).	350
	(1) Secondary goethite. 1 has a few remnants of clay.	
	(2) Largely clay. Possibly quartz. Large amounts of layer silicates. Clay and mica set in goethite with irregular voids.	
	(3) Sediments, granular. Clay and goethite. Quite porous (40% void) giving granular appearance. Some vein-like structures of goethite containing layer silicates (after ?talc) - could be schistosity.	
	(4) Secondary goethite. Slightly porous. Massive. No visible clay structures.	
	(5) Sediments, granular. Quartz, clay and goethite. 40% void space giving granular appearance. Some hematite..	
09-3674Fe	4 pieces.	370
	(1-3) Similar, mafic. Clay structures similar to 09-3652Fe. Ferruginous clay. Principally goethitic Fe oxides.	
	(4) Similar structures to 1-3 but has been replaced by Fe oxides. Massive, spongy, some voids. Only small clay structures.	
09-3677Fe	4 pieces.	380
	(1) ?Amphibolite. Fine clay structures (after ?talc) Layer silicates. Chromite grains.	
	(2) ?Amphibolite. Similar to 1). Clays. Ultramafic?	
	(3) ?Amphibolite. Chromite grain?	
	(4) Secondary patches of goethite. Similar to 1-3. Possible chromite. Granular texture Much quartz (angular and rounded), but a lot of clay surrounding it. Mica-clay mixture with goethite. Looks like a sediment.	